Predictive model for estimating nitrogen density in MD2 pineapple crops from multispectral images and sensors integrated in an IoT platform

Jorge Enrique Chaparro Mesa

Tesis para optar al título de Doctor en Ingeniería Electrónica y de Computación

Director
José Edinson Aedo Cobo, Ph.D

Universidad de Antioquia
Facultad de Ingeniería
Doctorado en Ingeniería Electrónica y de Computación
Medellín, Antioquia, Colombia
2024

Cita	(Chaparro Mesa, 2024)
Referencia **Estilo APA 7 (2020)**	Chaparro Mesa, J. (2024) *Predictive model for estimating nitrogen density in MD2 pineapple crops from multispectral images and sensors integrated in an IoT platform* [Tesis doctoral]. Universidad de Antioquia, Medellin, Colombia.

Doctorado en Ingeniería Electrónica y de Computación, Cohorte XXIV.
Grupo de Investigación en Sistemas Embebidos e Inteligencia Computacional (SISTEMIC)
Centro de Documentación de Ingeniería

Centro de documentacion UdeA (A-Z)

Repositorio Institucional: http://bibliotecadigital.udea.edu.co

Universidad de Antioquia - www.udea.edu.co

Rector: John Jairo Arboleda Cespedes.
Decano/Director Dr. Julio César Saldarriaga.
Coordinadora de Posgrados: Natalia Gaviria Gómez.

Advisor
José Edinson Aedo Cobo

Date
November, 2024.

Dedication

I dedicate this achievement with deep gratitude to God, to my family, and to each of the people who in one way or another contributed to this academic formation process. Your support, encouragement, and understanding have been fundamental to reach this goal.

Acknowledgements

I would like to express my deepest gratitude to Dr. José Edison Aedo Cobo for his invaluable management in obtaining equipment and scientific support. I extend my gratitude to the research group in Embedded Systems and Computational Intelligence (SISTEMIC) of the Faculty of Engineering of the University of Antioquia, as well as to the Research Group in Agro-sciences, Biodiversity and Territory - GAMMA, of the Faculty of Agricultural Sciences of the University of Antioquia, especially to Dr. Mario Fernando Cerón Muñoz for his advice and support in the loan of equipment and the construction of the experimental design. I also thank the Universidad Autónoma de Barcelona, the Computer Vision Research Center (CVC), the MSIAU research group (MultiSpectral Image Analysis and Understanding) and PhD Felipe Lumbreras Ruiz for their support and guidance in image processing and the construction of predictive models. I also thank engineer Nelson Barrera Lombana, from the Universidad Pedagógica y Tecnológica de Colombia (UPTC), for his support in the patenting process of the humidity sensor, and the Ministry of Science, Technology and Innovation MINCIENCIAS for the financial support during the Bicentennial Doctoral Excellence Scholarship.

My gratitude is also extended to the Universidad Internacional del Trópico Americano (Unitrópico) for its logistic and economic support during the completion of my doctorate, and to the Empresa Agrícola Santana de los Llanos for allowing me to carry out the experimental design in their crops and for providing qualified labor and guidance during the development of the research process. Finally, I thank my family and friends for their love, patience and for encouraging me to continue with this educational process.

Abstract

Nitrogen is the most important nutritional element during the vegetative growth phase of the pineapple crop; however, its presence in the soil is insufficient to meet plant demands. In this doctoral research, nine machine learning techniques were validated to estimate total nitrogen (TN) content in MD2 pineapple crops from data from multiple sources. These sources included multispectral images captured by an unmanned aerial vehicle (UAV) and in situ sensors that collected information on ecological and environmental factors, such as pH, temperature, solar radiation, relative humidity, soil moisture, and wind speed and direction. In addition, plant information was collected related to SPAD values, which indicate leaf chlorophyll content, and total nitrogen (TN) values, obtained from leaf tissue samples sent to a certified laboratory for analysis. To introduce nitrogen variability, a randomized complete block experimental design was implemented, applying five different treatments in five blocks, each with 12 replications, during a 6-month period in a pineapple crop located in the municipality of Tauramena, Casanare, Colombia. To address the inherent variability of the agricultural and environmental data, dimensionality was reduced using Principal Component Analysis (PCA). Regularization techniques were also applied, including cross-validation, feature selection, boost methods, L1 (Lasso) and L2 (Ridge) regularization, as well as hyperparameter optimization. These strategies generated more robust and accurate models, among which regression, multilayer perceptron (MLP regressor) and extreme gradient boosting (XGBoost) algorithms stood out. On the first sampling date, XGBoost achieved an R^2 of 86.98%, which was the highest during the entire experiment. On subsequent dates, MLP achieved an R^2 of 59.11% on the second date; XGBoost achieved an R^2 of 68.00% on the third date, and on the last date, MLP achieved an R^2 of 69.4%. These results indicate that the integration of data from multiple sources and the use of machine learning models enable nitrogen (N) diagnostics in pineapple crops, especially in real-time applications. These results highlight the promising potential of developing machine learning models that integrate multisensor data fusion for various applications in agriculture. In the implementation of the machine learning models, the total nitrogen content obtained

in the laboratory was considered as the response variable. The predictor variables comprised sensor data, SPAD values, and statistical information derived from 16 vegetation indices calculated from the multispectral images. To reduce the dimensionality of the predictor variable dataset, Principal Component Analysis (PCA) was applied. Following this dimensionality reduction, nine regression algorithms were used to estimate leaf nitrogen content during each of the four study periods. This comprehensive approach yielded close estimates of leaf nitrogen content. The results of the study indicated that the MLP (Multilayer Perceptron) and XGB (XGBoost) regression algorithms stood out for their superior performance, evidenced by the best performance metrics.

Keywords **— Multispectral Imaging, Unmanned Aerial Vehicle (UAV), Internet of Things IoT, Predictive Models, Sensors in the crop, Image processing.**

Contents

List of Figures

List of Tables

Notation

Mathematical notation

Generalities

V	number of views
N_v	Number of objects (observations) in the vth view
D_v	dimensionality of the v-th view
L_v	Dimensionality of the observed features in the vth view
K	Dimensionality of the latent feature vector
J	Number of correspondences (latent vectors) to which objects are assigned

Operators

$\mathbb{E}[\cdot]$	expected value
$\mathrm{tr}(\cdot)$	trace of a matrix

Functions

$k(\cdot,\cdot)$	covariance function for a Gaussian process of $\mathbf{x}_{vn}$
$f_d(t)$	d-th output or response function evaluated at t
$\boldsymbol{\phi}(\cdot)$	nonlinear mapping function

Vectors and matrices

$\mathbf{x}_{vn}$	Observation of the nth object in the vth view, $\mathbf{x}_{vn} \in \mathbb{R}^{D_v}$
$\boldsymbol{\phi}(\mathbf{x}_{vn})$	Observation of the nth feature object in the vth view, $\boldsymbol{\phi}(\mathbf{x}_{vn}) \in \mathbb{R}^{L_d}$
$\boldsymbol{\zeta}_j$	Latent feature vector for the jth correspondence, $\boldsymbol{\zeta}_j \in \mathbb{R}^K$
$\boldsymbol{B}_v$	Projection matrix for the vth view, $\boldsymbol{B}_v \in \mathbb{R}^{L_d \times K}$
θ_j	Mixture weight for the jth cluster, $\theta_j \geq 0$, $\sum_{j=1}^{\infty} \theta_j = 1$
$\mathbf{K}_v$	covariance matrix with entries $k(\mathbf{x}_{vn}, \mathbf{x}'_{vn})$
$\mathbf{f}_d$	$f_d(t)$ evaluated at $\mathbf{f}_d = [f_d(t_{d,1}), \ldots, f_d(t_{d,N_d})]^\top$
$\mathbf{f}$	vectors $\{\mathbf{f}_d\}_{d=1}^D$, stacked in one column vector
$\mathbf{I}_N$	identity matrix of size N

Abbreviations

AI	Artificial Intelligence
ANN	Artificial Neural Network
CNN	Convolutional Neural Network
DL	Deep Learning
EC	Electrical Conductivity
ELM	Extreme Learning Machines
ET	Evapo-Transpiration
ETc	Estimation of evapotranspiration
GBM	Gradient Boosting Model
GPS	Global Positioning System
IoT	Internet of Things
LAI	Leaf-Area Index
LASSO	Least Absolute Shrinkage and Selection Operator Regression
LS-SVM	Least square support vector machine
MAE	Mean Absolute Error
ML	Machine Learning
MLP	Multi-Layer Perceptron
NDVI	Normalized Difference Vegetation Index
(N)	Nitrogen
NIR	Near-Infrared
NN	Neural Network
PCA	Principal Component Analysis
R	Correlation Coefficient
RF	Random Forest
RGB	Red Green Blue
Red Edge	Red Edge
RIDGE	Ridge Regression
RMSE	Root Mean Square Error
RT	Regression Tree
R^2	Coefficient of Determination
SVM	Support Vector Machines
SVR	Support Vector Regression
TN	Total Nitrogen
UAV	Unmanned Aerial Vehicle
VI	Vegetation Index
XGBoost	Extreme Gradient Boosting

Introduction

Nitrogen (N) is one of the most sought after nutrients in crops and is essential to ensure optimal yield (Liang et al., 2022; Yao et al., 2024). It is considered a primary macroelement and its content in the soil is not sufficient to cover the plant needs despite its abundance in the form of N_2 in the air, since it is only usable in its assimilable forms of ammonium (Mello Prado, 2021). Pineapple is the second most produced tropical fruit worldwide after mango, with an average annual growth rate of 4.6% in recent years, sold and consumed worldwide (Mohd Ali et al., 2023). According to DANE figures (Colombia Department of National Administrative Statistics), between January and July 2022, Colombia exported more than 3 million net kilos of pineapple. Pineapples grow in warm and humid tropical climates, generally in warm environments with temperatures ranging from 20°C to 36°C (Maia et al., 2020). The average rainfall required is between 1,500 and 3,500 mm. If this value is too low, growth is affected and the size of the fruit is reduced; on the other hand, if there is excess water, root diseases occur. Within nutritional requirements, potassium (K) and nitrogen (N) are the two most important elements for plant growth. The amount of nitrogen used in pineapple varies between 5 and 8 g/plant (330-630 kg/ha with 80,000 plants/ha) (Mohsin et al., 2020). Previous studies have shown that pineapple fruit yields increase significantly with high levels of N under irrigated and rainfed conditions (Oliveira et al., 2022). Balanced nutrition in pineapple can be considered one of the main determinants of improving fruit quality and weight (Maia et al., 2020). In this sense, monitoring nutrient levels is essential to reduce economic costs and reduce environmental impacts; therefore, matching nitrogen supply with actual crop demand is one of the strategic objectives of site-specific nutrient management (Wang et al., 2022a).

Non-destructive technologies for assessing nutrients in pineapple crops are gaining popularity over conventional methods (Mohd Ali et al., 2023). The introduction of the concept of digital agriculture has transformed traditional agriculture, improving agricultural productivity and environmental sustainability (Pathmudi et al., 2023). In the

last decade, the combination of digital imaging, IoT platforms, and machine learning techniques has gained relevance for the development of interdisciplinary tools that facilitate the understanding of agroecological and environmental systems (Boursianis et al., 2020). These three instruments, when combined, become a powerful interdisciplinary tool that helps improve agricultural planning and optimize resources in crop production. In this context, the Internet of Things (IoT) provides tools for real-time monitoring of environmental, soil, or plant variables, such as temperature, humidity, pH, wind speed, solar radiation, and rainfall, among others (Mathi et al., 2023).

Spectral imaging methods such as near-infrared (NIR) and mid-infrared (MIR) have been widely used to measure nutrients in different fruit crops such as banana, avocado, blackberry, blueberry, cherry, mandarin, and others (Cozzolino et al., 2020; Kljusurić et al., 2020). These methods commonly use image-derived vegetation indices (VI) for the estimation of nutrients (Mouazen et al., 2023).

Machine learning (ML), in this context of precision agriculture, together with internet of things (IoT) devices and multispectral cameras superimposed on unmanned aerial vehicles (UAVs), have been making significant contributions to the concept of smart agriculture (Akkem et al., 2023). Various research studies have evaluated different machine learning algorithms to predict nitrogen (N) in traditional crops, such as rice, palm, sugar, wheat, among others (Liao et al., 2023; Mouazen et al., 2023). Algorithms such as artificial neural networks (ANN) have been used to predict vegetation and crop yield parameters, presenting better performance metrics than some supervised learning algorithms (Sakthipriya and Naresh, 2022). However, algorithms such as Random Forest (RF), Support Vector Machines (SVM), and XGBoost have demonstrated robustness and high accuracy in predicting plant N status (Chen et al., 2023; Sakthipriya and Naresh, 2022). The combination of IoT, multispectral imagery, and predictive modeling results in intelligent fertilization systems that improve accuracy in the amount of fertilizer needed (Berger et al., 2020b; Saranya et al., 2023).

In this doctoral thesis, different machine learning algorithms were validated to estimate the nitrogen content in the MD2 variety of pineapple plants from multispectral images, IoT sensors, and SPAD values of leaf chlorophyll content. To obtain the variability of nitrogen, a complete randomized block experimental design was carried out, applying five different nitrogen treatments (0, 3.3, 6.7, 9.3 and 12.0 g N / plant) in five blocks. Twelve replications were carried out over a period of six months, based on the methodology proposed by (Shendryk et al., 2020). In this case, the experimental application of blocks is not used to estimate the effect of treatment on the biomass or

yield of the crop; instead, it is used as a source of variability to obtain different samples of nitrogen content.

This doctoral thesis represents a significant contribution to scientific and technological knowledge in the field of precision agriculture and agricultural sustainability. The document is divided into 8 chapters which are detailed below:

- **Chapter 1. Statement of the Problem, Justification and Objectives**. In this chapter, the specific objectives of the research are established, the problem to be addressed is presented, and the relevance of this study is justified.
- **Chapter 2. Systematic Literature Review and Key Factor Analysis**. Presents a systematic review of the literature and a detailed analysis of the factors that will provide crucial input for the following stages of the research.
- **Chapter 3. Theoretical framework**. Develops a theoretical framework that supports the research methodology, addressing aspects such as pineapple crop ecophysiology, techniques for nitrogen estimation in fruit crops, the use of multispectral images and sensor networks in agriculture, as well as the concepts associated with artificial intelligence applied in this sector.
- **Chapter 4. Materials and Methods.** Details the methodology used to achieve the general objective, including materials and methods, the description of the study area, and the experimental design implemented.
- **Chapter 5. Data Acquisition**. The purpose of this chapter is to show the development of the data acquisition methodology, providing details on the capture of multispectral images, the acquisition of data on soil and environmental variables, and the acquisition of chlorophyll level data using SPAD values.
- **Chapter 6. Predictive Models**. This chapter presents data processing and analysis, the calculation of vegetation indices, the reduction of dimensions, and the development of predictive models for the estimation of nitrogen in the pineapple crop.
- **Chapter 7. Discussion**. This chapter presents an analysis and interpretation of the data obtained in this research, contrasting these results with previous studies that have used similar methodologies and objectives in other crops. Since the systematic review of the literature did not identify comparable studies on pineapple

crops, studies on other crops will be used as a reference for the discussion and comparison of findings.

- **Chapter 8. Conclusions and Future Lines of Research.** Finally, this chapter summarizes the general conclusions of the study, offers recommendations, and points out possible lines of future research.

Chapter 1

Problem, Justification and Objectives

1.1 Problem Statement

Pineapple cultivation accounts for almost 20% of the world's tropical fruit production, after mango and banana. Globally, 27.81 million tons of pineapple are produced on 1.07 million hectares under cultivation, with the Philippines, Costa Rica and Brazil being the three main pineapple producers in the world (Lakho et al., 2023). Colombia is a strategic country for the establishment of this type of crop, due to its location in the tropical zone. According to figures for 2022, the average annual pineapple production in Colombia reached 432 thousand tons. Santander stands out as the main contributor, accounting for 39.9% of the total, followed by the departments of Valle del Cauca (17.2%), Cauca (11.1%), Quindío (5.1%), Meta (4.7%), Casanare (4.1%) and other departments that contribute on a smaller scale (Olaya et al., 2022). Currently, the most requested variety by both pineapple producers and consumers is MD2, a hybrid from Hawaii. This variety stands out for its high Brix content compared to other varieties, as well as for reaching maturity earlier. These attributes have made it one of the most commercialized options worldwide (Hasni and Ahmad, 2022). The dynamics of pineapple production in Colombia, measured in tons per hectare, varies between 41 and 60 t/ha, with production costs close to US$11,400 per hectare and harvest times of 14 to 15 months. In contrast, countries such as Indonesia and Costa Rica, the main exporters of fresh pineapple in the world, achieve yields ranging between 83 and 120 t/ha, which motivates Colombian farmers to improve their yields (Cerón, 2022). However, increasing the planting density requires more efficient crop management, as plant spacing significantly influences fruit

size and quality. Higher density implies increased nutrient consumption per unit area, integrated pest and disease management, as well as the implementation of better flower induction methods and more efficient irrigation and drainage systems.

In this context, adequate nutrient intake is revealed to be one of the most significant factors to increase productivity, given its crucial impact on fruit growth and development. Maintaining a nutritional balance in pineapple cultivation is positioned as one of the main determinants of improving both fruit quality and weight (Maia et al., 2020). Among the essential nutrients for pineapple cultivation, nitrogen (N), phosphorus (P) and potassium (K) stand out, followed by calcium (Ca), magnesium (Mg), iron (Fe), and zinc (Zn). It is important to note that nitrogen (N) stands out as one of the most requested macronutrients by pineapple and is closely related to the weight and productivity of the fruit (Maia et al., 2020). Adequate nitrogen nutrition leads to the production of larger and higher quality fruit, thanks to an optimal ratio between acidity and soluble solids. On the other hand, nitrogen deficiency causes generalized chlorosis, initially manifested in older leaves, since nitrogen is considered a mobile element in the plant. This deficit directly impacts growth, resulting in plants of smaller stature and yellowish coloration (Liang et al., 2022). Nitrogen shortages can arise from various biotic and abiotic factors, linked to crop management, climatic conditions, soil properties, and the specific nutritional needs of each variety.

On the contrary, excess nitrogen application not only implies unnecessary costs in inputs and fertilizers, but also leads to the release of anthropogenic nitrogen into the air, water, and soil. This generates a series of environmental and human health problems that highlight the importance of managing the application of this nutrient in a balanced way. The application of fertilization that exceeds the recommended dose causes nutritional imbalances, generating negative effects on the environment, and contributing to greenhouse gas emissions (Demir et al., 2024). Additionally, the cultivation and fertilization practices adopted by farmers are based mainly on their individual experience, which is one of the key reasons for the remarkable yield disparities between different farms. In this regard, site-specific nutrient management (SSNM) presents itself as a solution to address this problem. The implementation of SSNM not only improves fertilizer efficiency, decreases environmental pollution, but also increases profits, and reduces yield disparities between farms within the same region (Demir et al., 2024).

Efficient water management is another crucial factor that directly affects crop yield. Pineapple differs from most commercial crops due to its photosynthetic adaptation through crassulacean acid metabolism (CAM), which facilitates the absorption of carbon

dioxide at night, thus improving its efficiency of water use, especially under dry conditions (Carr, 2012). Inappropriate water management leads to liquid losses and favors the proliferation of diseases and pests, directly affecting the farmer and the environment (Ricson L Ines et al., 2023).

The water requirements of the pineapple crop are related to the phenological stage, the type of soil, and the altitude (de Azevedo et al., 2007). It is advisable to irrigate preferably during the phenological stage of the greatest plant growth activity, which is from planting to flower induction. This avoids water stress and prevents possible effects on plant growth (Ricson L Ines et al., 2023). Consequently, continuous crop monitoring, including environmental variables and soil conditions, is imperative as an integral part of efficient crop management. Within this approach, monitoring can be integrated into management strategies that incorporate Decision Support Systems (DSS), which allow, for example, determining crop nitrogen requirements and assessing soil water status. The use of these strategies, when combined with practices such as fertigation and drip irrigation, is essential for efficient nitrogen management, reducing losses and minimizing environmental impacts (Padilla et al., 2020).

Agriculture 4.0 is generating a significant transformation in traditional agriculture, contributing to improving both agricultural productivity and environmental sustainability. In this context, the concept of precision agriculture, based on information technologies, is consolidating as an attractive technique for modern and sustainable agricultural development (Bui et al., 2024). During the last decade, the combination of digital images, the (IoT) platforms, and machine learning techniques has gained relevance in the development of interdisciplinary tools that facilitate understanding of the complexity characterizing agroecological and environmental systems (Kumar Kasera et al., 2024). To monitor and manage agricultural operations, this cutting-edge technology combines networks, devices, AI (AI), and big data analytics from the (IoT). Through the use of various electronic, biochemical and electrical sensors and actuators, various crop data can be collected, and environmental, soil or plant variables such as temperature, soil moisture, relative humidity, pH, wind speed, solar radiation and rainfall, among others, can be monitored in real time; and from these data it is possible to develop various operations for specific agricultural applications (Kumar Kasera et al., 2024). On the other hand, multispectral photogrammetry has gradually displaced traditional soil monitoring and mapping methods. This technology offers faster, more accurate, informative and professional assessment techniques in a cost-effective manner, making it one of the most valuable resources for precision agriculture. Multispectral imagery provides key

information for computing vegetation indices, such as the (NDVI) and the Crop Water Stress Index (CWSI). These indices facilitate the evaluation of crop vegetative state, evapotranspiration and biomass, among other aspects. They also allow for more efficient nutrient management, adequate irrigation and early detection of crop diseases and pests (Hareesh, 2024). The combination of images, sensors and AI, used together, becomes a powerful interdisciplinary tool to develop models that optimize agricultural planning through research. Although this approach has recently been implemented in several crops such as rice, soybeans, corn, citrus, vegetables, and coffee, its application in pineapple cultivation has been little explored, showing a limited presence in the scientific literature. This gap offers an opportunity to carry out research that contributes to the advancement of knowledge in this area, facilitating the optimization of nutritional systems. This process, in turn, will result in increased yield per hectare, reduced costs, and reduced environmental impacts (Devia et al., 2019; Kumar Kasera et al., 2024; Mej and Narvaez, 2020). This thesis evaluates the effectiveness of several regression algorithms to estimate the amount of nitrogen needed in a pineapple crop of the MD2 variety. For this purpose, multispectral images captured by a drone, agrometeorological information provided by a network of sensors, and plant chlorophyll data obtained through SPAD values are analyzed. This agricultural planning tool seeks to help pineapple growers manage their crops more efficiently, improving yields. Information on the amount of nitrogen present in the plant will allow better dosing of nutrient application, avoiding waste, and reducing input and fertilizer costs. In addition, it will be possible to trace agro-meteorological information on the crop and mitigate the environmental impacts associated with excessive nitrogen use.

1.1.1 Research question

¿Is it possible to estimate the optimal nitrogen demand in pineapple crops using non-invasive techniques, integrating machine learning, from multispectral images and data from field sensors integrated in an IoT platform?

1.2 Justification

Traditional agriculture is highly vulnerable to climate change and to the presence of diseases and pests, which are increasingly harmful and resilient to common agrochemicals. This type of agriculture is characterized by the use of rudimentary techniques

that minimize the productive capacity of soils and cause negative impacts on the environment and human and animal health (Saikanth et al., 2023). Although Colombia is a vocation agricultural country and has become a strategic country for pineapple cultivation, due to its location in the tropical zone, yields are below international standards, especially compared to leading export countries such as Indonesia and Costa Rica (Olaya et al., 2022). The Strategic Plan for Science, Technology and Innovation in the Colombian Agricultural Sector, PECTIA - Pineapple Chain, highlights the urgent need to strengthen research processes, focusing especially on two critical areas: plant physiology and nutrition, as well as soil and water management. According to established priorities, plant physiology and nutrition is the essential core, addressing fundamental aspects such as "diagnostics for the identification of physiological and edaphoclimatic causes that affect fruit quality" and "studies of nutritional requirements in relation to the phenological stage of the crop" (Minagricultura, 2022).

A crucial strategy to improve productivity in pineapple cultivation involves the precise definition of nutritional requirements adapted to the specific environmental conditions of each plantation. This approach requires detailed analyses, such as growth studies and foliar analysis, to understand the nutritional needs of plants (Mohsin et al., 2020). It is important to note that this topic has been scarcely addressed in the country, and growers base their nutritional recommendations on research conducted in countries such as Brazil, Costa Rica, and Mexico (Rúa et al., 2016). Efficient determination of nutrient use in the crop is essential to achieve maximum yields, prevent fertiliser loss, and understand the nutrient absorption capacity of the plant. The balanced nutrition of pineapple is one of the main factors in improving fruit quality and weight, with nitrogen (N) being one of the most requested macronutrients, closely related to fruit weight and productivity.

However, fertilisation is one of the most expensive activities for the farmer when establishing a production system, where agricultural inputs represent between 30-40 % of total production costs (FAO, 2016). In this context, nitrogen emerges as the most expensive element in pineapple production. The timely assessment of nitrogen content in the crop canopy becomes a fundamental aspect for the diagnosis of growth and accurate crop management. This approach not only seeks to maximise crop yield and quality, but also aims to minimise adverse environmental impacts, thus contributing to more sustainable and efficient agricultural production (Liu et al., 2023a). Precision agriculture offers solutions for efficient nitrogen management through noninvasive techniques that combine technologies such as IoT, multispectral imaging, and AI. These technologies

allow real-time monitoring of environmental and crop variables and the generation of vegetation indices such as NDVI and CWSI, which help to assess crop condition and nitrogen need.

Despite the potential offered by precision agriculture, its implementation in pineapple cultivation has not been explored sufficiently, and the lack of existing information prevents definitive conclusions on the effectiveness of these technologies in accurately predicting nitrogen requirements. This knowledge gap presents a clear opportunity to develop predictive models that address the specific nitrogen demand in pineapple cultivation, enabling more efficient management of this nutrient. The fundamental purpose of this research is to contribute to the advancement of knowledge in the application of precision agriculture in pineapple cultivation. It aims to fill the existing gap in the scientific literature, providing valuable information that not only benefits the academic community, but also translates into practical tools for farmers. Successful implementation of predictive nitrogen demand models would not only improve farmer competitiveness, but also strengthen the sustainability of the sector by optimising input use and potentially reducing environmental impacts associated with overfertilization.

1.3 General Objective

To develop a predictive model to estimate the amount of nitrogen required for the efficient management of an MD2 pineapple crop, based on non-invasive techniques that combine the analysis of multispectral images and agrometeorological information transmitted by sensors.

1.3.1 Specific objectives

- Determine the main parameters, variables and information required for the construction of the model, based on the multispectral images and data obtained with the sensors.
- Define the modeling technique, structure and methodology for the construction of the predictive model according to the hypothesis and available data.
- Implement a prototype prediction system, where the selected model is integrated, in order to carry out the process of controlled experimental verification and effectiveness estimation, in a regional agricultural context..

- To carry out a systematic verification process of the proposed model, based on simulation and/or experimental tests in controlled environments.

Chapter 2

Systematic Literature Review and Key Factor Analysis

This chapter presents a comprehensive and systematic search of the literature applying predefined methods and inclusion and exclusion criteria. Given the significant progress in the field of AI in the last two years, this systematic review of the literature identifies articles published in scientific journals indexed in the Scimago Journal Rank (SJR) portal of Scopus during the period 2022-2024. The primary purpose of this review is to provide an objective summary of the existing evidence regarding nondestructive techniques for nutrient estimation, involving predictive models, multispectral imaging, and IoT sensors installed in the crop. It seeks to identify possible knowledge gaps and point out areas that require further research, thus contributing to the advancement of knowledge in this specific field.

In the last decade, agriculture has witnessed a radical transformation, called Agriculture 4.0, characterized by the integration of Information and Communication Technologies (ICT) into traditional agricultural methods (Li et al., 2023a). Emerging technologies such as remote sensing, the (IoT), (UAV), Big Data Analytics (BDA) and Machine Learning (ML) stand out for their great potential. These innovations represent a milestone in the progress of agricultural practices, ushering in a new era in the sector (Boursianis et al., 2020). The use of satellite and aerial imagery has been implemented to monitor crops, detect diseases, assess plant health, estimate nutrients, and forecast yields. However, (IoT) technologies use sensors connected in real time to monitor environmental conditions such as humidity, temperature, and soil pH. Machine learning (ML) makes use of the information generated by images and sensors to predict yields, identify diseases, and optimize agricultural practices, providing personalized recommendations

based on the specific conditions of each crop (Istiak et al., 2023). Accurate nutrient estimation plays a crucial role in efficient crop management. Various techniques have been developed in applied AI to agriculture to improve this task. Methods such as spectral analysis, remote sensing, and machine learning algorithms enable a more accurate assessment of crop nutritional requirements, thus optimizing yields (Ennaji et al., 2023).

One of the most demanded macronutrients in fruit crops, and at the same time the most important for fruit growth, weight and quality, is nitrogen (N) (Fu et al., 2022). This element is directly related to the photosynthetic capacity of crops. Over- or under-application of nitrogen fertilizers not only limits crop productivity, but also causes negative environmental impacts. Excess nitrogen can cause eutrophication in water bodies, a process that refers to the increase of inorganic nutrients, such as nitrogen and phosphorus, often resulting from runoff from human activities. On the other hand, lack of nitrogen can reduce crop yields. In addition, excessive use of nitrogen fertilizers can release nitrogen oxides into the atmosphere, contributing significantly to global warming (Fu et al., 2022).

Accurate estimation of nitrogen (N) in crops is essential to optimize productivity, reduce costs, and minimize environmental impact. There are several methods for (N) estimation, which fall into two categories: destructive and non-destructive (Liao et al., 2023). Destructive methods, such as soil and plant tissue analysis, are accurate but require time and effort to process. Additionally, laboratories are generally not located near crops, implying higher costs and time to obtain results (Liang et al., 2022). Non-destructive methods, on the other hand, are becoming increasingly popular due to their speed, ease of use, and lower cost. Some examples of these methods are sensors, which allow measurement of the reflectance of light at different wavelengths, which can be related to the N content of the plant. Multispectral imaging, which captures images of the plant in different bands of the electromagnetic spectrum, allowing the estimation of N content through image analysis techniques, and predictive models that use information such as crop phenological stage, climatic conditions, and soil properties to estimate N demand (Ruan et al., 2023).

The use of canopy spectral measurements in crop nutrient estimation has attracted considerable interest in the scientific community. These measurements are more effective in determining growing conditions compared to foliar spectral measurements, which are limited to predicting information about individual leaves. This approach offers a more holistic and accurate perspective for assessing the nutritional status of crops, supporting more efficient decision making in agriculture (Fu et al., 2022).

In this doctoral research, a systematic review of the literature (SLR) is conducted with the objective of establishing the state of the art in the use of multispectral imagery, IoT technologies, and machine learning methods for the estimation of nutrient content, especially nitrogen, in crops. The systematic review of the literature is approached as a comprehensive and methodical approach that seeks to identify, evaluate, and synthesize the available research in this area of knowledge (Bandara and Syed, 2023).

According to the search criteria established in the methodology described in this chapter for systematic review of the literature (SLR), 523 relevant studies were identified and analyzed in five electronic databases: ScienceDirect, Scopus, Springer, IEEE Xplore, and Google Scholar. From this broad selection, 87 articles were examined in detail, applying inclusion and exclusion criteria. These research papers were carefully selected and organized by topic using the Mendeley tool, which facilitated the management and selection of these documents by specific topics. This tool not only enables the organization and sharing of research material, but also the referencing of documents, participation in academic social networks, and the stimulation of debate around a specific topic.

The analysis of the 87 selected papers focused on answering four carefully formulated research questions detailed in section 2.2.1 of this thesis. These questions were designed to address various aspects related to the predictive models reported in the literature for the estimation of nitrogen content in crops. The predictive models analyzed are based on machine learning techniques, such as neural networks, decision tree learning, Support Vector Machines and linear regression, among others. These models use information derived from multispectral images and IoT platforms for the measurement of various crop parameters, with special emphasis on nitrogen.

This literature review explores the most recent advances in the use of machine learning to support crop yield prediction, with a particular focus on nitrogen estimation by analyzing multispectral images and relevant variables captured by soil and plant sensors. Given the significant progress in the field of AI in the last two years, this systematic review covers the period from the year 2022 to the papers identified up to the first quarter of the year 2024. It starts by providing an account of related works, i.e., similar literature reviews, with the purpose of establishing a general context and guiding the subsequent analysis towards the identified knowledge gaps.

Before analyzing the 87 research articles, a search for review articles was conducted to contrast their results with those obtained from the analysis of the 87 studies, in order to guide the research. The results of the analysis of the review articles are presented

below, followed by the methodology used and the analysis of the 87 articles.

2.1 Review articles analyzed

In this section, several literature reviews published between 2022 and 2024 in the field of Machine Learning, multispectral imaging, vegetation indices and IoT sensors applied to agriculture are examined. Priority is given to works focused on the prediction of nutrients and crop yields from agricultural 4.0 technologies, covering the most commonly employed algorithms in these areas of study. This specific period addressed in the review allows obtaining an updated view of the most recent advances and approaches in the integration of these technologies to improve agricultural management. The review of related works was structured by topic to facilitate the understanding of the papers reviewed.

2.1.1 Estimation of nutrients (nitrogen) and crop yields through UAV imagery

(Ennaji et al., 2023), present a review of machine learning-based techniques for estimating fertilizer and nutrient status developed in the last decade. The authors make a comparison of the advantages and disadvantages of machine learning approaches, and future prospects for ML adaptation in crop nutrient management are discussed. In the study carried out by (Rivera et al., 2023), a literature review was conducted on the use of machine learning as a support tool to predict yields in various types of crops. On the other hand (Saikanth et al., 2023), they present results that show the positive impact of combining machine learning and IoT in improving crop yields. The authors highlight the effectiveness of the combined use of machine learning and IoT in smart agriculture in increasing crop productivity. (Zhou et al., 2022), they conducted a review on determining fruit maturity to decide the optimal harvesting time and yield prediction. Non-destructive methods, including colorimetry, visible imaging, spectroscopy, as well as machine learning and regression models used to assess maturity, were also analyzed. (Goffart et al., 2023) investigated advances in the use of optical sensors to monitor nitrogen (N) status in potato crops. They concluded that traditional methods are accurate but laborious, and that developing a more generic reference method would allow rapid assessment of N status using biophysical variables derived from optical sensors, with promising real-time monitoring capabilities. In the review by (Patil et al., 2023), the estimation of nitrogen content in sorghum crops using (UAVs) was addressed. Five dif-

ferent RGB-spectrum vegetation indices were evaluated and correlated with current crop nitrogen content values using simple linear regression and stepwise backward regression. (Bazzo et al., 2023), conducted a comprehensive review of recent studies using (UAVs) to estimate aerial biomass in grasslands. They analyzed 64 articles, considering key aspects such as, species composition, drone platforms, flight parameters, sensors, field measurements, biomass indices, data processing and analytical methods. This review established a comprehensive workflow, from data collection to data processing. In the work done by (Istiak et al., 2023), the authors examined several critical dimensions facing (UAVs) in precision agriculture. They also conducted an assessment of the impact of imaging modalities and datasets in agricultural applications, as well as a categorization of UAV configuration and a detailed analysis of currently used AI (AI) methods. (Zheng et al., 2022), they conducted a study to identify current research trends and key issues related to nitrogen (N) monitoring. They began with a comprehensive statistical analysis of the literature on remotely sensed N monitoring in rice and wheat over the past two decades. Subsequently, they elucidated the physiological mechanisms and spectral response characteristics of canopy N remote sensing monitoring. (Wong, 2023) discussed the potential of optical remote sensing for phenotyping, monitoring and evaluation of vegetation. Optical properties, vegetation index applications, sun-induced fluorescence, and machine learning approaches were addressed, highlighting how covariance can empirically approximate plant traits and functions.

(Montero et al., 2023), present "Awesome Spectral Indices" (ASI), a standardized catalog of spectral indices for terrestrial research. ASI provides a complete, machine-readable catalog of indices linked to a Python library. It includes a variety of attributes for each index, such as names, formulas and references, making it easy to use and understand in a variety of scientific contexts. On the other hand (Radočaj et al., 2023), they reviewed the most relevant plant indexes, considering their frequency in scientific papers indexed in the Web of Science Core Collection (WoSCC) since 2000. By examining articles related to "precision agriculture" and vegetation index (VI), it became evident that the United States and China stand out in global research on precision agriculture and the use of vegetation indices.

2.1.2 Analysis of Articles on Machine learning techniques for nutrient and crop yield estimation

The article published by (Kganyago et al., 2024), provides an overview of recent advances in remote sensing technology and machine learning algorithms for estimating key parameters in precision agriculture. It aims to highlight advances in obtaining these parameters by remote sensing and advances in sensing technologies and machine learning algorithms. Likewise (Wakchaure et al., 2023), they conducted a comprehensive review of recent studies using AI and robots for agricultural applications. This work performs a comparative analysis in three essential phases of agriculture: Cultivation, Tracking and Harvesting, detailing in each of these the applicability of machine learning techniques and agricultural robotics. (Wang and Yao, 2023), carried out a review on machine learning techniques in the field of crop yield, highlighting the use of artificial neural networks, fuzzy systems, decision trees, regression-based analysis and Bayesian networks. In addition, they considered time series analysis, Markov chain models and clustering techniques such as k-means, k-nearest neighbor and support vector machines applied to agriculture. Similarly (Pandey et al., 2022), conducted a comprehensive review of nearly 170 papers applying the latest methodologies in image processing, machine learning, deep learning, (IoT), data mining and wireless sensor networks in the agricultural sector. (Wang et al., 2023b), they highlighted advances in optical sensors and machine learning algorithms to develop multi-organic nitrogen estimation models for rice. The authors conducted rice field trials over three years, using manual sampling along with digital and hyperspectral imagery captured by UAVs. (Petso and Jamisola, 2023; Silva et al., 2023), conducted a literature review in which monitoring systems with drones and deep learning algorithms are addressed, focusing on optimizing plant agricultural production and improving yields. Different models and their effectiveness under various environmental conditions and drone types are evaluated.

2.1.3 IoT and UAV technology in agriculture

In the work aimed at (Boursianis et al., 2020), the authors conducted a survey of the most recent research on the application of IoT and UAV technology in agriculture. The fundamental principles of IoT technology are described, addressing aspects such as smart sensors, types of IoT sensors, networks, and protocols used in agriculture, as well as the various IoT applications and solutions in smart agriculture. (Chander et al., 2023), discusses advances in smart agriculture technologies, providing information on the current

state and future possibilities. The authors comprehensively review the integration of IoT, wireless communication, sensors and hardware in smart agriculture, highlighting the transformative potential of integrating IoT and advanced technologies in agriculture to improve efficiency and automation. The paper presented by (Boursianis et al., 2020) reviews the fundamental principles of IoT technology, considering smart sensors, types of sensors, networks and protocols used in agriculture, as well as IoT applications and solutions in smart agriculture. Along the same lines, (Majumdar et al., 2021), conducted an analysis of contemporary IoT-oriented agricultural automation methods using weather monitoring. Within this analysis, they reviewed IoT components, communication protocols, prediction methods, security vulnerabilities of communication protocols, cost of IoT hardware, comparison of data repositories, and dependency analysis of weather parameters. (Prakash et al., 2023), the authors of this article thoroughly analyze the key components of smart agriculture, such as IoT, wireless communication technology, sensors, and hardware. The authors present a systematic review of the implications of agricultural automation and how operations can benefit from technological advances. Challenges and future applications for crop, human, and machine health are discussed. In the paper by (Abbasi et al., 2022), a systematic review of the literature related to precision agriculture published in the last decade is carried out. The results showed that digital technologies such as autonomous robotic systems, the (IoT), and machine learning are significantly explored; also, it is found that these technologies are more frequently applied in open field crops (69%), as opposed to indoor crops (31%). (Alahmad et al., 2023), this review analyzes the potential advantages of using Information and Communication Technologies (ICT) in precision agriculture to promote sustainable agricultural development. Highlights the relevance of incorporating modern technologies such as the (IoT) and AI (AI) in the agricultural industry to ensure long-term productivity. The authors (Alexopoulos et al., 2023), reviewed the challenges and advantages of UAVs, satellites, and ground-based sensors (IoT) in agriculture, highlighting their joint use to drive Precision Agriculture and the transition to Agriculture 4.0. The article concludes that by combining technologies such as terrestrial IoT sensing and remote sensing via satellite and UAV, along with data analytics, agriculture is moving towards a more efficient, productive and sustainable approach.

2.2 Methodology used in this review

The methodology carried out for this systematic review of the literature was divided into three phases which, in turn, were organized into 10 steps, as detailed in Figure. 2.1.

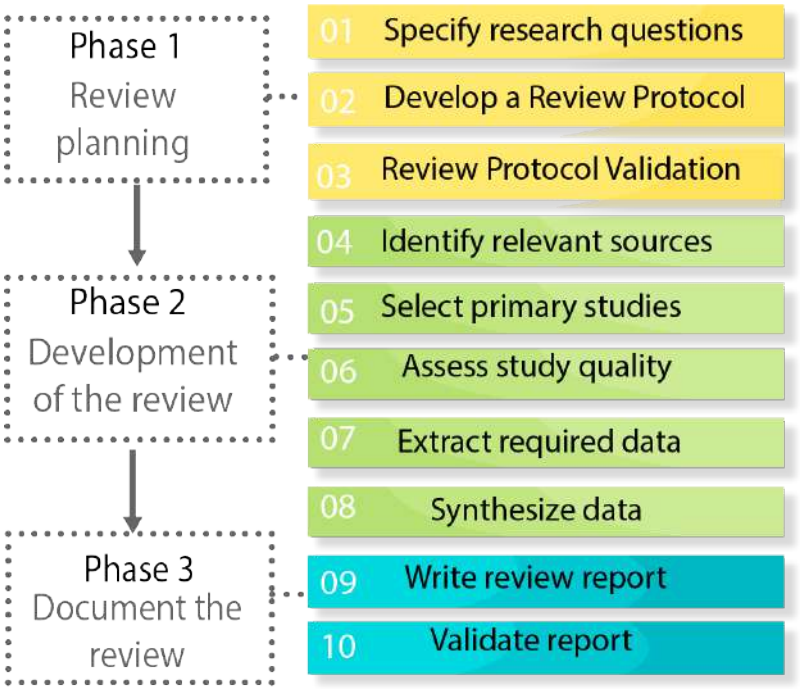

Figure 2.1: Description of the phases of the review protocol. Source: Own elaboration.

- Phase 1: In this phase, research questions are defined, and a document selection protocol is developed and validated. Additionally, publication sources, search equations, and selection criteria are established.
- Phase 2: The review is conducted by selecting publications that meet the inclusion and exclusion criteria from the chosen databases. Bibliographic data are automatically extracted using Mendeley, and key information is summarized in the "notes" section to address the research questions.
- Phase 3. This phase ends with the analysis of the papers, taking into account the formulated research questions. Figure. 2.1 illustrates the steps to follow in each of the phases.

2.2.1 Research Questions

This section formulates the general objective of the review, which is structured around four research questions.

Objective: Critically evaluate the current scientific evidence on the use of machine learning techniques to estimate the amount of nutrients, especially nitrogen, in crops, from the information provided by spectral images and sensors integrated in IoT platforms.

Based on this general objective, the following research questions are raised:

1. Q1- What are the most commonly used machine learning algorithms for nutrient and crop yield estimation from spectral imagery and IoT sensors

2. Q2- How do IoT technologies and (UAVs) integrate with machine learning algorithms to create comprehensive agricultural management systems

3. Q3- On what types of crops have machine learning techniques been implemented for nutrient and yield estimation, and what evaluation parameters have been used to measure their effectiveness

4. Q4- What is the current scientific evidence on the accuracy and reliability of machine learning techniques for crop nitrogen estimation from machine learning, spectral imaging and IoT systems and what are the challenges and future prospects

2.3 Results

2.3.1 Extraction of required data

This section presents the results of the extraction of information from the 87 studies analyzed. To answer the research questions, the information was organized in different tables. Table. 2.1 details the name and acronym of the algorithms used in the analyzed articles to estimate crop nitrogen. Table A.1 and Table A.2 describe the machine learning algorithms used for crop nitrogen estimation from spectral images and sensors. Tables A.3 and A.4 detail the variables and types of UAV and satellite spectral images used for the estimation of nitrogen and other crop parameters. Table. A.5 presents the vegetation indices used for this estimate. Finally, Table. A.6 describes the work carried out with IoT systems and images, which were used in the analyzed articles to estimate nitrogen and other variables in crops.

Table 2.1: Name and acronym of algorithms used in the articles analyzed for the estimation of Nitrogen in crops.

Abbreviation	Algorithm name
PLSR	Partial Least Squares Regression
MLR	Multiple Linear Regression
SVR	Support Vector Regression
GPR	Gaussian Process Regression
ANN	Artificial Neural Networks
MLP	Multilayer Perceptron
CNN	Convolutional Neural Networks
BPNN	Backpropagation Neural Networks
ResNet	Residual Neural Network
RegNet	Regularized Neural Network
EfficientNet	Efficient Neural Network
EfficientNetV2	Efficient Neural Network Version 2
RF	Random Forest
DNN	Deep Neural Networks
LSTM	Long Short-Term Memory
Lasso	L1 Regularized Linear Regression
K-NN	K-Nearest Neighbors
ELM	Extreme Learning Machine
NNA	Neural Network Architecture (unspecified)
SMLR	Stepwise Multiple Linear Regression
QRF	Quadratic Random Forest

2.3.2 Analysis and synthesis of information to answer research questions

The results corresponding to the 4 research questions, based on the previously mentioned tables, are presented below.

Q1- What are the most commonly used machine learning algorithms for nutrient and crop yield estimation from spectral images and IoT sensors?

Most used algorithms and explanatory variables

The most commonly used machine learning algorithms for estimating crop and nutrient yields from spectral imagery and IoT sensors comprise several advanced techniques. To address this question, a literature review was conducted on 37 articles, the results of which were compiled in Table A.1 and Table A.2. In these, the algorithms used for crop nitrogen estimation using spectral imagery and sensors are detailed.

The analysis of the articles reveals that the most commonly used algorithms for crop nitrogen estimation are Random Forest (RF) and Support Vector Regression (SVR), with 19 and 5 occurrences respectively (Fan et al., 2022a; Liang et al., 2023; Wang et al., 2023b; Zhou et al., 2023). Other common algorithms include Partial Least Squares Regression (PLSR) and combinations such as random forest and gradient boost machines

(RF, GBM) (Bossung et al., 2022; Fan et al., 2022a; Jiang et al., 2023; Li et al., 2023b; Liu et al., 2023a; Shu et al., 2022; Singha et al., 2023; Zhou et al., 2023). Other prominent algorithms are Artificial Neural Networks (ANN), which employ various algorithms such as Decision Neural Network (DNN), Long Short-Term Memory (LSTM), multi-layer perceptron (MLP) and, evidencing a diversity in the approaches used for this task in agricultural research (Jiang et al., 2023; Putra et al., 2022; Ruan et al., 2023; Sahoo et al., 2023). The Machine Learning Algorithms used in the reviewed articles to estimate nitrogen from remote sensing are described in Figure. 2.2. The Table. 2.1 shows the machine learning algorithms used in the first column the acronym and in the second column the definition of the algorithm.

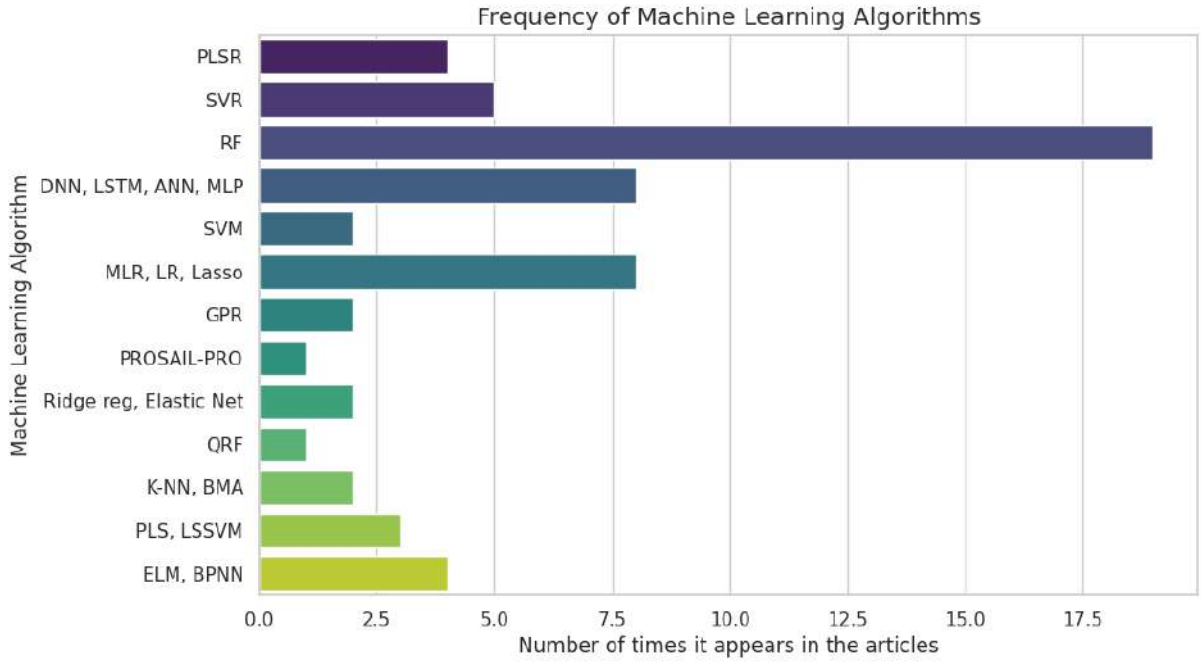

Figure 2.2: Machine Learning articles used in the analyzed articles.

The estimation of nitrogen in soil and crops is carried out using a set of explanatory variables that include soil properties, the characteristics of the crop itself, information obtained from remote sensors and, in some cases, additional data such as meteorology and genetics. The choice of the most appropriate variables depends on the specific objective of the study and the estimation technique used. Based on the types of explanatory variables used for crop nitrogen estimation, the following conclusions can be drawn from the articles reviewed:

Soil variables: many studies use variables related to soil properties, such as pH,

electrical conductivity (EC), organic matter (OC) content, nitrogen (N), phosphorus (P), zinc (Zn), and soil particle composition (clay, sand, silt). These soil variables provide important information on plant nutrient availability and growing conditions (Liu et al., 2023a; Ruan et al., 2023; Singha et al., 2023; Venkatesh and Naik, 2024; Wang et al., 2023b).

Plant variables: The vast majority of studies relate variables such as plant biomass, leaf chlorophyll content, leaf area index (LAI) and nitrogen concentration in leaves (LNC) and stems (SNC), which provide information on the health status and photosynthetic capacity of the plant. These variables are related to plant health and nutritional status, which can influence nitrogen uptake and utilization (Bossung et al., 2022; Fu et al., 2022; Liu et al., 2023b; Lu et al., 2022a; Patel et al., 2024; Patil et al., 2023; Wang et al., 2023b; Zhou et al., 2023).

Phenotypic and morphological variables: Some studies incorporate phenotypic and morphological variables of plants, such as leaf and stem shape, as well as leaf area and chlorophyll density. These variables can provide information on plant development and growth, which may be related to their ability to absorb and utilize nitrogen (Fan et al., 2022b).

Meteorological variables: It is noted that some studies include meteorological variables, such as temperature, precipitation and solar radiation data. These variables can influence the availability and uptake of nutrients by plants, and are therefore important for the estimation of nitrogen content (Li et al., 2023a; Singha et al., 2023).

Table 2.2 details the explanatory variables used by machine learning models to predict nitrogen content in crops according to the articles analyzed in this review.

Analysis with respect to R^2 and RMSE performance metrics

The analysis of performance metrics in models for crop nutrient estimation, especially in the application of spectral imaging for nitrogen prediction, reveals a diversity of approaches and results. A wide range of coefficients of determination R^2 and root mean square errors (RMSE) is observed, which evidences the variability in the accuracy and predictive ability of the models evaluated. To compare their performance, an analysis is performed using the R^2, considering that the value of the RMSE varies significantly according to the type of crop.

In this context, models based on machine learning (ML) techniques such as Random Forests (RF), Support Vector Machines (SVM), Artificial Neural Networks (ANN) and Multilayer Neural Networks (MLP) have shown outstanding performance, reaching (R^2)

Table 2.2: Explanatory variables used in machine learning models

Explanatory variables used in ML models
Soil properties
pH
Electrical conductivity (EC)
Organic matter (OC)
Nitrogen (N)
Phosphorus (P)
Zinc (Zn)
Texture (clay, sand, silt)
Plant variables
Leaf chlorophyll content (LCC)
Leaf area index (LAI)
Leaf nitrogen concentration (LNC)
Stem nitrogen content (Zn)
Stem nitrogen content (SNC)
Meteorological variables
Temperature
Precipitation
Solar radiation
Wind speed and direction
Remote sensing data
Vegetation indices
Canopy images
Other data
Crop growth stage
Weather data
Genetic information
Management practices

values between 0.64 and 0.99. However, the vast majority of related studies converge to a mean R^2 of 0.75. This consistent trend is attributed to the intrinsic complexity of agroecological and environmental systems, where multiple variables interact in different compartments (Dong et al., 2022; Fan et al., 2022a; Jiang et al., 2023; Wang et al., 2023b). Figure 2.3 shows the results of the analysis of the R^2 performance metric.

These models have the ability to capture nonlinear and complex relationships between spectral variables and nutrient levels in crops. Among them, RFs stand out for their remarkable ability to estimate the nutritional status of nitrogen in crops, with coefficients of determination ranging from 0.63 to 0.93 (Jiang et al., 2022, 2023; Li et al., 2022b; Lu et al., 2022a; Ruan et al., 2023; Wang et al., 2023b). However, it has been observed that in advanced phenological stages, problems of saturation of spectral variables can arise, affecting the accuracy of the estimates. Despite this complexity, the significant advance in the performance of ML models for nitrogen prediction represents an important step towards more accurate and sustainable agriculture. The ability of these models to analyze and process large data sets efficiently allows researchers and producers to optimize nitrogen fertilizer application, improve crop yields and manage

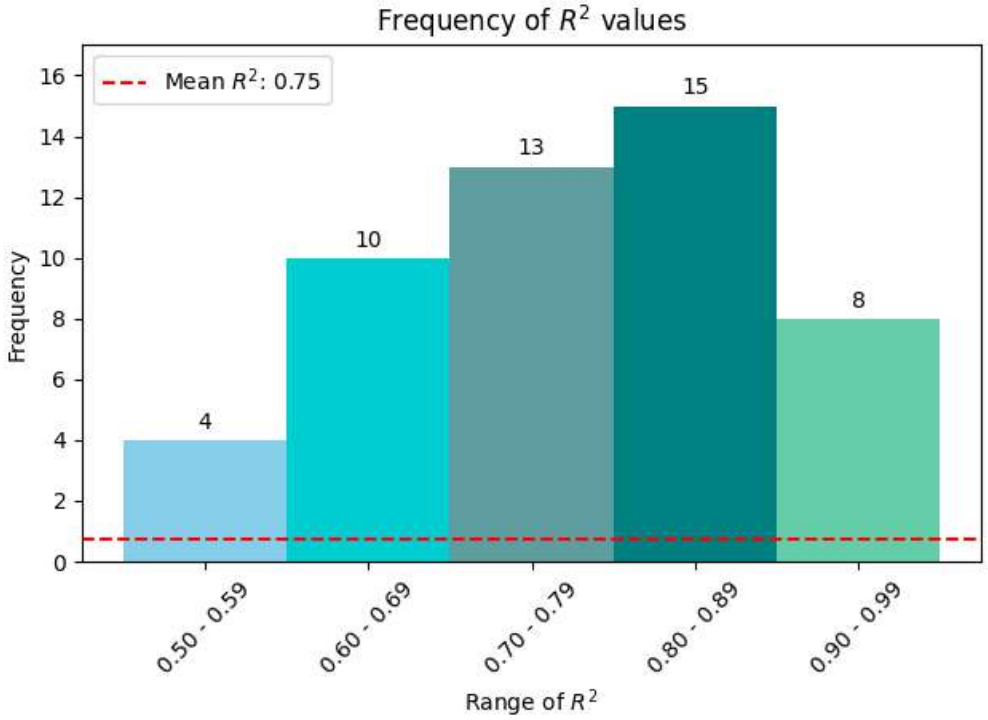

Figure 2.3: Frequency of R^2 values found in the reviewed articles.

water resources efficiently, since nitrogen is a crucial element in the water cycle, so its accurate prediction allows better irrigation management and conservation of this vital resource (Peng et al., 2022; Tian et al., 2022; Zhang et al., 2023).

Q2- How do IoT technologies and (UAVs) integrate with machine learning algorithms to create comprehensive fertilizer management systems especially Nitrogen?

The integration of IoT technologies and (UAVs) with machine learning algorithms enables the creation of highly efficient and accurate integrated agricultural management systems. UAVs equipped with remote sensors can collect detailed data on crop condition and environmental conditions in real time, providing a complete and up-to-date overview of the crop (Shu et al., 2022). This data, along with information collected by IoT devices such as soil sensors and weather stations, can be processed using machine learning algorithms such as neural networks and support vector machines for advanced analysis and accurate predictions (Patil et al., 2023).

In order to answer question 2, a comprehensive analysis of the literature related to the application of spectral imagery and IoT systems in agriculture was carried out. The analysis focused on two main aspects: crop yield estimation and fertilizer management,

with special emphasis on nitrogen. The information gathered was synthesized in Tables A.3 and A.4, which detail studies employing spectral imagery for yield estimation and fertilizer requirement. As for IoT systems in agriculture, several approaches were identified, described in Table A.6. In the area of multispectral imagery for fertilizer and crop yield estimation, the extensive use of vegetation indices (VI) derived from multispectral imagery obtained using drones or satellites has been observed. Among the most commonly employed indices are the (NDVI), enhanced vegetation index (EVI), and near-infrared vegetation reflectance (NIR). The vegetation indices mentioned above are described in Table. A.5 with their respective formulae.

Types of sensors used

In this research, several studies were reviewed that employed sensors of different nature to estimate the foliar and soil nitrogen content in crops. In order to facilitate their understanding, they were classified into two main categories: contact sensors, which require direct access to the crop for data acquisition, and remote sensors, which do not require physical contact with the plant and use nondestructive techniques to capture information.

Remote sensors

Among the sensors employed, those that capture multispectral or hyperspectral images, both from satellites (such as Sentinel-2) and from (UAVs), stood out. These sensors provide detailed spectral information of the soil and vegetation canopy in various bands of the electromagnetic spectrum, facilitating the calculation of vegetation indices related to nitrogen content. Among the most widely used are the MicaSense sensors, which combine MicaSense technology with UAV platforms (e.g. MicaSense RedEdge-M, MicaSense Altum)(Li et al., 2023a; Liu et al., 2023a; Mathi et al., 2023; Mouazen et al., 2023; Narmilan et al., 2022; Nikos Tsoulias, 2023; PEI et al., 2023; Pereira et al., 2022; Salazar-Reque et al., 2023; Shu et al., 2022; Su et al., 2023; Wang et al., 2023c; Zhu et al., 2022). UAVs equipped with RGB cameras, multispectral or hyperspectral sensors represent a valuable tool for nitrogen estimation at local scales, as they allow obtaining high resolution aerial images with great spatial detail (Kou et al., 2022; Lukáš et al., 2023; Song et al., 2022).

Contact sensors

GreenSeeker and Crop Circle ACS-430: These sensors attach to tractors or other agricultural equipment and measure canopy reflectance across the field. SPAD-502: This portable meter measures light transmittance in the leaf to estimate chlorophyll content,

indirectly related to nitrogen (Dong et al., 2022; Farid et al., 2022; Wang et al., 2023e; Zsebő et al., 2024). Leaf fluorescence sensor Dualex: Measures leaf fluorescence, another indicator of nitrogen status in the plant (Dong et al., 2022; Song et al., 2022). ASD HandHeld-2 Spectroradiometer: This portable device allows high-resolution spectral measurements to be obtained in the field (Patel et al., 2023; Wang et al., 2023b; Yin et al., 2023). Figure. 3.4 details the types of sensors used to acquire data on foliar nitrogen content in crops.

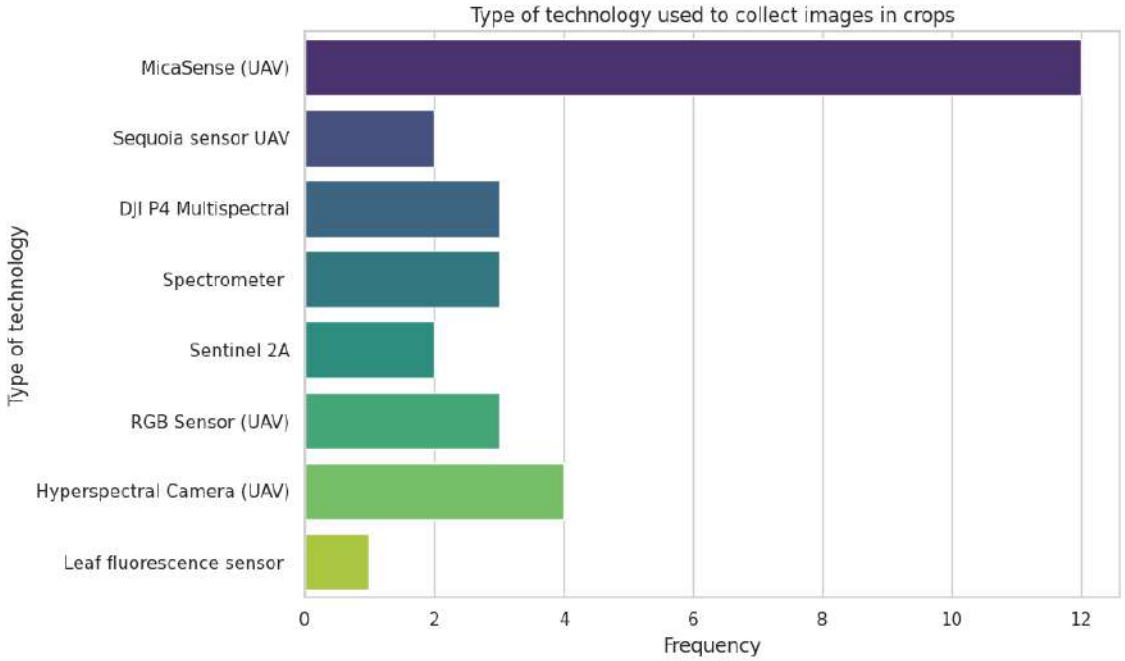

Figure 2.4: Type of sensors used to acquire data on foliar nitrogen content.

2.3.3 Vegetation Indices

The use of vegetation indices (VI) derived from multispectral images, either taken with drones or from satellites, is fundamental for fertilizer and crop yield estimation. Among the most commonly used is the (NDVI), which assesses vegetation health and density (Chen et al., 2022; Li et al., 2022c; Wang et al., 2023e; Zhou et al., 2023). Another common index is the Enhanced Vegetation Index (EVI), which corrects for atmospheric and soil distortions of the NDVI. In addition, the Near Infrared Vegetation Reflectance (NIR) provides valuable information on plant health and chlorophyll content. These indices, along with others derived from multispectral imagery, allow researchers and farmers

to more effectively monitor and manage crops, optimizing fertilizer use and improving yields (Chen et al., 2022). In addition to the aforementioned indices, specific others can be found in related articles, such as Modified Soil Vegetation Index (MSAVI), Modified Enhanced Chlorophyll Reflectance Index (MCARI), Leaf Area Index (LAI), among others, which offer a variety of insights into crop health and development, improving the assessment of fertilizer needs and yield potential(Kayet et al., 2023; Liu et al., 2024; Salazar-Reque et al., 2023; Thinley et al., 2024; Wang et al., 2023f). The above mentioned vegetation indices with their respective formulae are listed in Appendix A.5.

IoT and sensor applications in crops

Agriculture 4.0 represents a cutting-edge technological innovation aimed at optimizing agricultural production and management at all stages. This revolution seeks to improve control, monitoring and efficiency through modern, scalable and automated solutions. Key enablers include the (IoT), big data analytics, AI (AI), cloud computing, remote sensing, (UAVs) and the fifth-generation (5G) network, which enable automated predictive services and smarter, more reliable agricultural decisions (Morchid et al., 2024b). The (IoT) and (UAVs) are revolutionizing agriculture by enabling comprehensive monitoring of soil conditions, including moisture, temperature and pest presence, through interconnected sensor networks (Majumdar et al., 2023; Morchid et al., 2024a,b; Prasanna Lakshmi et al., 2023). This technology enables accurate and efficient management of resources, allowing a timely response to any problems that may arise. UAVs, meanwhile, offer the ability to survey large areas of crops quickly and in detail, facilitating the timely application of pesticides and detailed monitoring of crop growth (Hundal et al., 2023; Javaid, 2023; Kumar Kasera et al., 2024; Kumar Singh and Sobti, 2022; Prasanna Lakshmi et al., 2023; Saba et al., 2023). Table. 2.3 and Table. A.6, describes the technologies and relevant aspects of the articles that include sensor and IoT information to estimate nutrients and water in crops. From the information analyzed, it can be concluded that there is a wide variety of devices and systems used to monitor and collect data in the agricultural field.

Wireless sensor networks (WSNs) play a key role in the collection and management of data crucial for informed decision making. The WSN architectures proposed in the different papers are based on heterogeneous sensor networks that collect a wide range of parameters, including light irradiance, soil characteristics such as temperature, pH, salinity, moisture and nutrients, as well as foliar variables such as leaf wetness and leaf thickness, and atmospheric aspects such as humidity, carbon dioxide content and air

temperature. The quality of data acquisition, along with the efficient processing and transfer of data through the WSN infrastructure, are critical to ensure the efficiency of predictive models. Some of these architectures found include communication modules such as DHT22 and water level and humidity sensors, connected to embedded systems such as ESP32 and using the ThingSpeak cloud (Irwanto et al., 2024; Morchid et al., 2024a; Phasinam et al., 2022). In addition, microcontrollers, positioning modules such as the Beidou/GPS ATK-1218-BD, and wireless sensor networks such as PotatoNet are used. Common controllers such as Raspberry Pi 3 (RPI3) are used to control various sensors, and specific technologies such as LoRa and LoRaWAN are used for long distance wireless communication (Hasan et al., 2022; Karaman et al., 2023; Ting and Chan, 2024).

Table 2.3: IoT technologies and supporting sensors for nutrient and crop yield estimation.

IoT technologies and supporting sensors for nutrient and crop yield estimation
Sensors for Environmental and Crop Monitoring: Main sensors: humidity, temperature, pH, NPK (nitrogen, phosphorus, potassium). Additional sensors: Light (visible and infrared), RGB sensors. Function: Collection of data on the crop environment (humidity, temperature, illumination) and its condition (nutrients in the soil).
Microcontrollers and Development Boards: Examples: Raspberry Pi 3, Arduino, NodeMCU. Function: Process information from sensors and send it to other devices or the cloud.
Wireless Sensor Networks (WSN): High-Level WSN Architecture Heterogeneous Environmental Sensors Protocols and Topologies Function: connect sensors to each other and to other devices to transmit data wirelessly.
Communication Technologies: LoRaWAN, LoRa and NB-IoT: Long-range, low-power communication protocols for wireless sensor networks. WiFi: For local communication between devices. Function: Enable data transmission from sensors to the cloud or mobile devices.
Remote Sensors: Mentioned together with: Technologies such as LoRa and NB-IoT, suggesting their use to collect data remotely. Function: Capture crop information from satellites or other aerial devices (complementing sensors in the field).

In terms of specific applications, according to the review it was found that these technologies have a wide range of uses in modern agriculture. They are applied in smart irrigation systems to optimize water use, as well as in the detection of diseases in crops

such as potatoes, fruits and vegetables, which contributes to the effective management of pests and diseases. In addition, they are used to monitor water quality and create optimal conditions in greenhouses and mushroom crops. They are also used to assess and monitor ecological factors and environmental conditions, helping to improve efficiency and sustainability in agricultural production (Jabbar et al., 2024; Kumar Kasera et al., 2024; Prakash et al., 2023).

Q3 - On what types of crops have machine learning techniques been implemented for nutrient and yield estimation, and what evaluation parameters have been used to measure their effectiveness?

Spectral imaging techniques combined with sensor data have become a valuable tool for nitrogen (N) estimation in various crops. This technology offers a non-invasive and efficient alternative to monitor crop nutritional status and optimize N management, which is crucial for sustainable agricultural production. When analyzing the results of studies on non-invasive techniques for estimating nitrogen in different types of crops using spectral imaging and IoT sensors, interesting trends are observed that reveal the effectiveness of these methodologies. These trends are reflected in Figure. 2.5, showing how these technologies are being successfully applied in various crops to estimate nitrogen content effectively and non-invasively.

-**Cereals (rice, maize, winter wheat)**: Cereals represent the category most studied, with a total of 16 occurrences. This reflects the importance of these crops as a food source and their high (N) demand.

-**Industrial crops (sugar cane, cotton, sugar beet)**: These crops also stand out for their frequency, with 5 occurrences. Accurate estimation of N in these crops is crucial to optimize yield and quality of the final product.

-**Other crops**: A variety of other less frequent crops are observed, including grasses, vegetables, fruit trees and root vegetables. This indicates that spectral imaging and sensor techniques are being explored for a wide range of crops.

On the other hand, analyzing the variables used in the machine learning models to estimate nitrogen, the following can be stated:

- **Emphasis on soil properties**: frequent use is observed of variables related to soil properties, such as pH, electrical conductivity (EC), organic matter (OC), clay, sand and silt content. These variables provide information on the soil's capacity to retain and release nitrogen.

- **Remote sensing data**: Multispectral images and derived vegetation indices (NDVI, RVI, NDRE, RERVI) are used to estimate plant nitrogen content from foliage

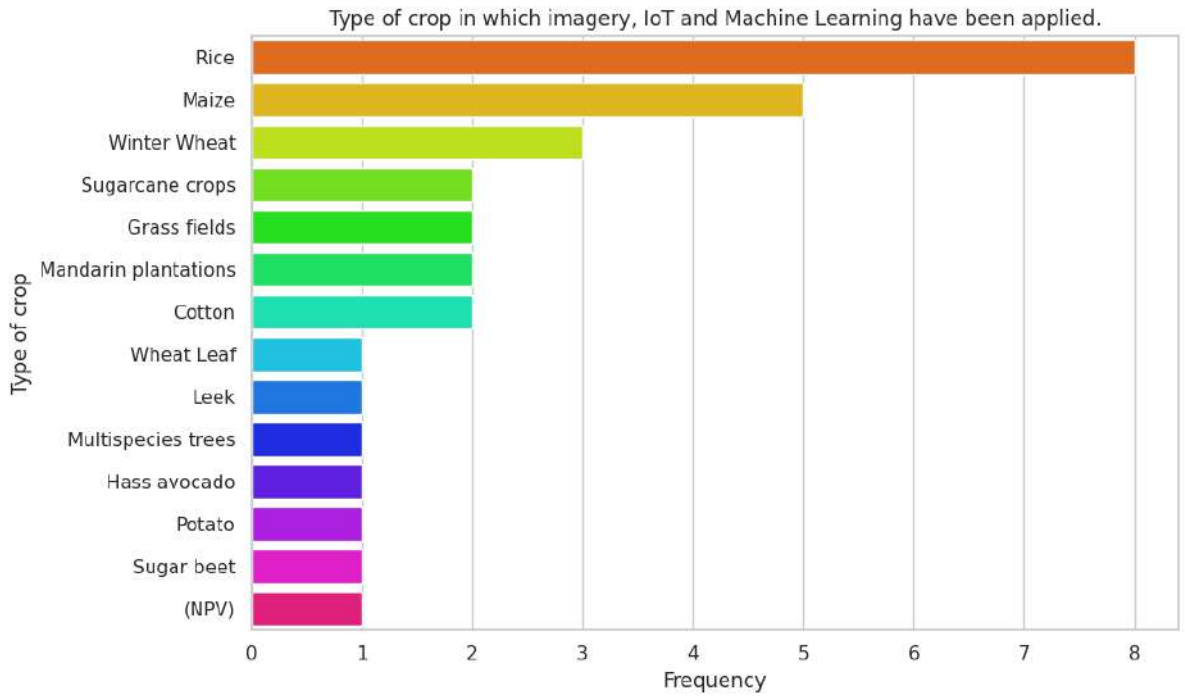

Figure 2.5: Types of crops in which nitrogen estimation techniques from images, sensors and Machine Learning have been implemented.

reflectance. - Plant variables: variables directly related to the plant are used, such as leaf chlorophyll content, leaf area index (LAI) and leaf nitrogen concentration (LNC).

- **Other relevant data**: Additional variables such as crop growth stage, meteorological data, genetic information and management practices (nitrogen rate applied, irrigation, previous crop) are included.

Q4 - What is the current scientific evidence on the accuracy and reliability of machine learning techniques for crop nitrogen estimation from machine learning, spectral imaging and IoT systems and what are the challenges and future prospects?

Accuracy: Several studies have demonstrated the high accuracy of machine learning techniques for estimating nitrogen (N) content in crops. As detailed in Figure 2.3. the mean R^2 of all reviewed articles is found to be 0.75, this value is very interesting considering the complexity of agricultural and environmental systems.

Reliability: The reliability of machine learning techniques depends on several factors, such as the quality of the training data, the selection of algorithms and the parameters used.

Machine learning and crops: Machine learning algorithms can process and ana-

lyze large datasets of spectral images and IoT sensor data to extract relevant information about crop N status. Spectral imaging: Spectral imaging captures the reflectance of light at different wavelengths, providing information on chemical composition and plant health. IoT systems: IoT systems collect real-time data on environmental variables such as temperature, humidity and solar radiation, which can be used by machine learning models to improve the accuracy of N estimates.

Challenges and future prospects

There are some challenges and difficulties encountered in the articles analyzed. First, the lack of inclusion of the impact of environmental factors in many studies is highlighted, which may affect the generalization of the models and make it difficult to accurately estimate certain parameters. In addition, an unclear relationship between chlorophyll density (CCD) and characteristics at different growth stages is noted, as well as the difficulty in estimating CCD due to the complexity of canopy structure and planting density. The limitation in the number of observations for training and testing is also highlighted as a factor that may affect the stability and accuracy of the models. Other challenges include difficulty in accurately converting DN values to reflectance, loss of information by not fully utilizing multiple view images, and difficulty in extracting textural features from images with multiple views. Lack of consideration of additional factors, such as soil properties and integration of more factors for crop growth and nitrogen status, is also identified as a major limitation. In addition, specific technical challenges are mentioned, such as the difficulty in differentiating objects with similar spectral characteristics using sensors such as HSI and LiDAR, and the need for accurate sensor calibration to ensure the reliability of field-scale remote sensing applications. The importance of addressing these limitations to improve the accuracy and applicability of machine learning models in precision agriculture is highlighted. There are other challenges and limitations such as data availability and model interpretability. The "black box" of machine learning models can make it difficult to understand their predictions and limit their adoption by farmers. Another challenge encountered is the lack of validation under real conditions. More research is needed to validate the accuracy and reliability of machine learning techniques in different growing conditions and on a large scale.

2.4 Discussion

Optical remote sensing of nitrogen (N) status in plants is based on the nondestructive analysis of the spectral reflectance of the plant canopy in the visible and near infrared (NIR; 400-900 nm) wavelength range. This technique is carried out directly in the field, which significantly reduces the number of samples required, thus optimizing the time and costs associated with sample collection, preparation and analysis in the laboratory. Additionally, the estimation of N content is performed at the level of the entire crop, thanks to the ability of multispectral images to generate georeferenced orthophotomosaics of the entire cultivated area. This feature represents a great advantage over traditional methods based on point field samples.

Regarding research question P1- What are the most widely used machine learning algorithms for crop nutrient estimation it can be analyzed that accurate estimation of nitrogen (N) content and crop yield is crucial for sustainable agriculture. Traditional laboratory analysis techniques are costly, time-consuming and destructive. In this context, machine learning (ML) coupled with spectral imaging and IoT sensors offer a promising alternative for non-invasive and efficient estimation of nutrients and crop yields.

The machine learning algorithms evaluated include Random Forest (RF), Artificial Neural Networks (ANN), Support Vector Machines (SVM) and Linear Regression (LR) Models. The RF stands out for its robustness and versatility in estimating nutrients and crop yields, demonstrating high precision in predicting the nitrogen nutrition index (NNI) and grain yield in corn. ANNs, especially convolutional neural networks (CNN) and recurrent neural networks (RNN), are preferred for their ability to identify complex patterns in multispectral and temporal data, as observed in the CNN-based SSVT model for estimating nitrogen status in wheat. SVMs are noted for their efficiency in classification and regression, being effective even in small or noisy data sets, as evidenced by recognition of the irrigation level in wheat. Finally, LR models, although simple and transparent, show good accuracy in estimating variables such as the nitrogen content of the leaf in rice, which makes them useful as reference models or for the interpretation of more complex models.

Regarding the effectiveness of models in predicting the foliar nitrogen content in crops, it is observed that metrics, such as the coefficient of determination R^2, in the vast majority of reviewed articles oscillate around 0.75, as detailed in Figure 2.3. This consistent trend is attributed to the inherent complexity of agroecological and environmental systems, which involve an interaction of multiple variables with distinct behaviors.

2.4.1 Factors influencing the choice of algorithm.

The choice of algorithm depends on several factors, such as the size and quality of the data set, the complexity of the relationship between the variables, and the specific objective of the estimation. Moreover, it is important to evaluate different algorithms and select the one that is best suited to the problem at hand.

With respect to the type of crop, estimation of N using spectral imaging and sensor techniques has received considerable attention in various types of crops. Cereals and industrial crops are the most studied, reflecting their economic importance and the challenges associated with N management. There is growing interest in applying these techniques to a wider range of crops, including grasses, vegetables, fruit trees, and root vegetables.

Regarding Question 2 concerning the integration of IoT technologies, (UAVs) and machine learning algorithms for nitrogen management, it is important to note that the integration of spectral image data and IoT sensors with machine learning algorithms will further improve the accuracy and robustness of estimates.

In addition, the importance of the interpretability of machine learning models is highlighted to better understand the relationships between variables and facilitate agronomic decision making. Although the methods described share a common structure of image acquisition, processing and classification, the selection of specific algorithms must be tailored to the individual characteristics of each crop and application.

The reviewed studies highlight the combined use of IoT technologies and sensor networks in the context of precision agriculture. The integration of sensors for environmental and crop monitoring, in conjunction with microcontrollers, wireless networks, and machine learning models, has been shown to significantly improve yields, optimizing efficiency in farm management.

Chapter 3

Theoretical Framework

This chapter describes the theoretical framework that supports the process of estimating crop nutrient from spectral images. The paper discusses the most relevant aspects related to sensors and how they are used to estimate nutrients, as well as the most relevant characteristics of the pineapple crop.

3.1 Ecophysiology of Pineapple Cultivation

Pineapple (Ananas comosus) is one of the most important tropical fruits worldwide, known both for its commercial value and its nutritional benefits (Martins et al., 2020). Originally from South America, pineapple has spread to various tropical and subtropical regions, where it is cultivated mainly for its flavor, vitamin and mineral content, and its use in various food and cosmetic industries. Its cultivation has grown significantly in recent decades due to global demand, which has led to the implementation of precision agriculture techniques to improve its yield and quality. However, the success of this crop depends largely on maintaining optimal growing conditions, which vary according to specific climatic and edaphic factors (Liu et al., 2023c).

Pineapple is a tropical, perennial, herbaceous plant belonging to the monocotyledons (Liu et al., 2023c). Optimal conditions for its cultivation require a precise combination of environmental factors. The ideal altitude ranges from 300 to 900 meters above sea level, and the temperature should be maintained between 23 and 30 ℃, with an optimum of 27 ℃ being optimal. If the temperature drops below 23 ℃, flowering is accelerated, resulting in smaller, acidic and perishable fruits. Conversely, temperatures above 30 ℃ can burn the epidermis and underlying tissues, favoring the appearance of diseases (Martins et al., 2020).

Annual precipitation should be between 1,500 and 3,500 mm. When water is insufficient, with rainfall less than 1,000 mm, plant growth is affected and fruit size decreases; excess water, on the other hand, favors root diseases. Soil water availability should average between 1.3 and 5.0 mm per day.

Optimum luminosity is 1,500 hours of light per year. Excessive exposure will result in scorching of the fruit surface, while low light reduces sugar content and increases fruit acidity. Soil pH also plays a crucial role: it should be maintained between 5.5 and 6.2. A high pH causes iron chlorosis (iron deficiency), while a pH below 5.5 affects root growth and decreases the availability of key nutrients such as potassium and calcium (Martins et al., 2020).

Nutritional requirements, nutritional demands, and mineral or organic supplementation with macro and micronutrients is required during its growth cycle to obtain high productivity and fruit quality. The nutrients considered essential for the crop are N, P, K, Ca, Mg, S, Fe, Mn, Zn, Cu, B and Mo. Nitrogen is one of the macronutrients most demanded by pineapple and the one most related to fruit weight and productivity (Martins et al., 2020). Diseases, mainly Phytophthora, which causes root rot and is favored by poor drainage, waterlogging, wounds and pH $>$ 6 (S. R et al., 2022; Wali, 2019). However, in order to reach harvest maturity, which is usually achieved through floral induction, induced plants should have the same phenotypic characteristics in terms of size, weight, and health (Mohsin et al., 2020).

Figure. 3.1, depicts a crop system, visualizing the interactions between soil and plant in relation to the influences of several explanatory variables, such as environment, water, soil properties and crop management. This last aspect refers to the decisions taken to ensure the adequate development of planting and harvesting.

3.2 Nitrogen estimation in pineapple crops

Nitrogen (N) stands out as the most prevalent nutrient in fruit trees, significantly influencing the quality and development of the stem, root and fruit (Martins et al., 2020; Mohsin et al., 2020). Pineapple is considered a plant that demands nutrients, requiring both mineral and organic supplementation with macronutrients and micronutrients to ensure high productivity and fruit quality. Among the essential nutrients, Nitrogen (N), Phosphorus (P), Potassium (K), Calcium (Ca), Magnesium (Mg), Sulfur (S), Iron (Fe), Manganese (Mn), Zinc (Zn), Copper (Cu), Boron (B) and Molybdenum (Mo) stand out. Nitrogen is one of the most demanded macronutrients for pineapple and is closely related

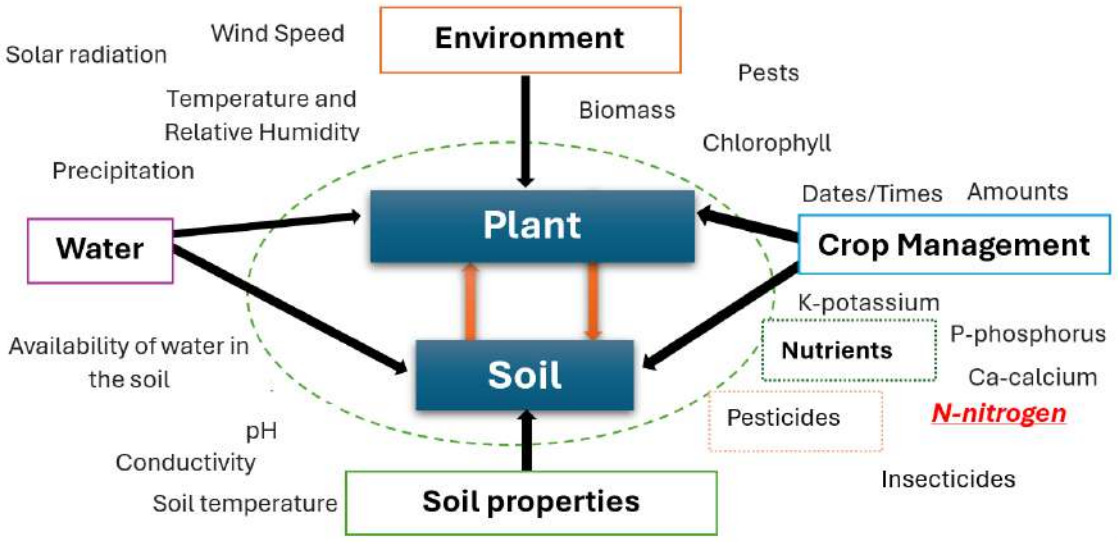

Figure 3.1: Interactions between soil-plant components, crop management, water, response variable (N-Nitrogen) and explanatory variables. Source: Own elaboration.

to the weight and productivity of the fruit (Martins et al., 2020; Wali, 2019). For optimum yields, nitrogen (N) uptake at the end of the crop cycle has been observed to range from 452 to 764 kg/ha, depending on the variety and growing conditions. N deficiency in cash crops is usually associated with factors such as soil quality, inadequate management practices and adverse weather conditions (Sanyal and Sarkar, 2021). Pineapple cultivation in sandy soils is common, but these soils are often poor in nutrients and organic matter, requiring careful nutritional management. Organic or green fertilization is a common strategy to increase N availability under these conditions, which contributes to larger and higher quality fruit. N deficiency is manifested in plants by symptoms such as generalized chlorosis, especially in older leaves, due to the mobility of N in the plant (Mohsin et al., 2020).

The omission of N in the nutrient solution can cause severe symptoms of deficiency, such as yellowing of the leaves and reduced fruit size and quality, as can be seen in Figure. 3.2. It is crucial to maintain an adequate N supply to ensure vigorous plant growth and high-quality fruit production. Nitrogen deficiency leads to a reduction in amino acid and thus protein synthesis, resulting in reduced plant growth and accumulation of non-nitrogen metabolites. This, in turn, favors a greater availability of photoassimilates for the synthesis of compounds of secondary metabolism, such as ascorbic acid and other organic acids (Martins et al., 2020). However, it is important to remember that the visual diagnosis of symptoms of deficiency serves only as an initial guide to identify potential

nutritional problems, as several nutrients, such as iron and magnesium, also influence leaf color formation because they are responsible for chlorophyll synthesis. Therefore, an accurate interpretation of leaf color as an indicator of nitrogen deficiency depends on consideration of other nutritional factors that may also affect leaf appearance (Martins et al., 2020).

Figure 3.2: Symptoms of nitrogen deficiency in pineapple. (A) Plants without nitrogen deficiency. (B, C y D) Nitrogen-deficient plants. Source: image taken from (Martins et al., 2020)

3.3 Techniques to diagnose the nutrient status of pineapple crop

Accurate estimation of nitrogen (N) in crops is essential to optimize productivity, reduce costs, and minimize environmental impact. There are several methods for (N) estimation, which fall into two categories: destructive and nondestructive (Liao et al., 2023).

Destructive methods, such as soil and plant tissue analysis, are accurate but require time and effort to process. In addition, laboratories are often not located near crops, which means higher costs and time to obtain results (Liang et al., 2022). Nondestructive methods are becoming increasingly popular due to their speed, ease of use, and lower cost.

3.3.1 Destructive methods for nitrogen estimation in pineapple crops

Techniques based on soil monitoring

- **Soil analysis**: this is the most common technique and consists of extracting a representative sample of the crop soil to analyze its nutrient content. This technique allows determining the levels of macronutrients (N, P, K, Ca, Mg, S) and micronutrients (Fe, Mn, Zn, Cu, B, Mo) in the soil (Martins et al., 2020). Proper nitrogen fertilization is based on the measurement of mineralized nitrogen, the total amount of nitrate and ammonium, in the soil. Soil sampling with auger and subsequent chemical analysis in a laboratory is state of the art. However, this process is time-consuming and often delayed by the logistics involved.

- **Soil sensors**: These devices allow real-time or high-frequency measurement of various soil parameters, such as moisture, electrical conductivity, pH and the concentration of some nutrients (Haddon et al., 2023; Vikuk et al., 2024).

Techniques based on plant monitoring

- **Foliar analysis**: this technique involves the extraction of a representative sample of crop leaves to analyze their nutrient content. it is a chemical analysis of leaves and other plant organs used to diagnose the nutrient status of fruit crops. Plant nutrient levels can vary according to growth stage as well as from one part of the plant to another. Samples are usually taken from the fully developed upper leaf before the reproductive stage or mid-season. This method samples the upper leaves, washes them and then dries them to be crushed and analyzed through chemical processes (Llanderal et al., 2020).

- **Sap analysis**: This technique involves extracting a sample of plant sap to analyze its nutrient content. This technique is less common than foliar analysis, but can be

useful for detecting acute nutrient deficiencies. This technique has been used since 1920 and is carried out on fresh material, giving a semi-quantitative assessment of extractable nutrients that are present in soluble inorganic forms in the plant just at the time of sampling (Llanderal et al., 2020). Generally this method selects samples of fully developed young leaves. Petiole sap extraction is usually performed using a hydraulic press, according to the methodology described by (Esteves et al., 2021).

Integrated diagnosis

The combination of different diagnostic techniques, such as soil analysis, foliar analysis and sensor monitoring, can provide a more complete picture of the nutritional status of the pineapple crop and allow more accurate fertilization decisions to be made. It is important to note that the choice of the most appropriate diagnostic technique(s) will depend on a number of factors, such as crop age, soil conditions, fertilization history and plant symptoms (Esteves et al., 2021).

3.3.2 Non-destructive methods

Optical sensors

Optical sensors, especially those based on canopy reflectance, represent one of the most promising non-destructive techniques to monitor crop nutritional status. In this process, plant canopies with adequate levels of nitrogen and chlorophyll absorb photosynthetically active radiation (PAR), comprising red and blue light, while reflecting green and infrared light, generating a characteristic pattern. These methods have been widely applied in various fruit crops, such as bananas, avocados, blackberries, blueberries, cherries, and tangerines, using spectral imaging, such as near-infrared (NIR) and mid-infrared (MIR).

The estimation of nutrients from remote sensing is based on the spectral reflectance properties of plants, which vary according to the absorption, reflection, and transmission of electromagnetic waves of different wavelengths. These spectral characteristics depend not only on the morphological structure of the plant, but also on its growth environment and development conditions (Wang et al., 2023d). Factors such as soil moisture, nutrient content, as well as the presence of pests and diseases, affect the growth and biochemical composition of the plant, which is reflected in different spectral reflectance patterns related to chlorophyll, nutrient, and water content (Zhang et al., 2023). The Figure 3.3 illustrates the relationship between color and vegetative state of the crop as a function of

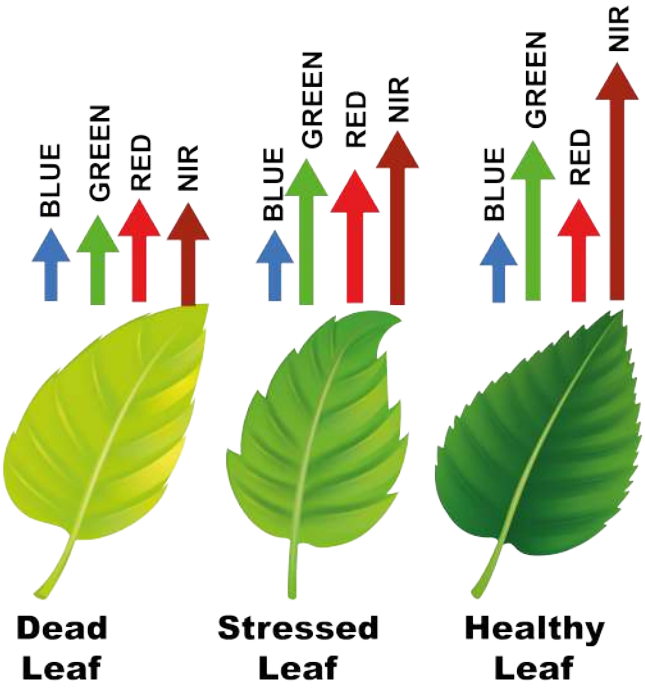

Figure 3.3: Relationship between color and vegetative state of the crop as a function of spectral bands. Source: Own elaboration.

the spectral bands used. For example, if the NIR level is = 50% and a RED level = 8% on a leaf, one can calculate whether this leaf is healthy, stressed, or dead by calculating the NDVI as follows:

$$NDVI = \frac{(\text{ NIR - RED})}{(\text{ NIR + RED})} = \frac{(\text{ 50 - 8})}{(\text{ 50 + 8})} = \mathbf{0.72} \ = \mathbf{Healthy\ leaf}$$

On the other hand, if you have an NIR level = 40% and a RED level = 30%

$$NDVI = \frac{(\text{ NIR - RED})}{(\text{ NIR + RED})} = \frac{(\text{ 40 - 30})}{(\text{ 40 + 30})} = \ \mathbf{0.14} = \mathbf{Stressed\ leaf}$$

Spectroscopy for crop analysis

Spectroscopy has become a key tool for crop analysis within the field of precision agriculture, allowing detailed and non-invasive monitoring of plant health, water stress, nutrient content and other parameters essential for agricultural management (Cozzolino et al., 2020). Vibrational spectroscopy methods, both near-infrared (NIR) and mid-infrared (MIR), are widely used to measure nutrients in crops and plants. These methods measure the vibrations of chemical bonds present in samples, which occur at specific fre-

quencies related to the mass of atoms and molecular structure. Molecules absorb these vibrations in the infrared (IR) region, where the bonds can stretch or compress, changing the distance between atoms (Cozzolino et al., 2020).

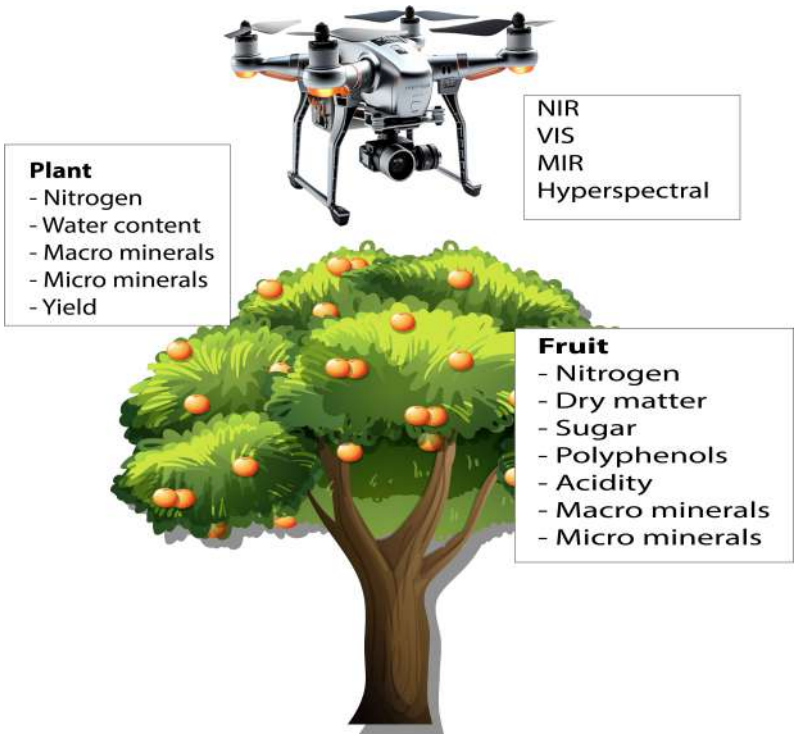

Figure 3.4: Applications of optical sensors (vibrational spectroscopy) in fruit and plant analysis. Source: Own elaboration.

Depending on the capacity of the spectra handled by the optical sensor, it is possible to obtain a large amount of crop data, and for this reason, multivariate techniques are used to extract significant information that relates the different parameters (Li et al., 2019). For example, correlations between leaf nitrogen and leaf chlorophyll content (Cab) have been empirically demonstrated, which led to the (Cab) content being used as an approximation of the N content of the crop (Berger et al., 2020a). The Figure 3.4 describes applications of optical sensors (vibrational spectroscopy) in the analysis of fruits and plants.

3.4 Vegetation Index used in this doctoral thesis

The Table 3.1, shows the bands of the MicaSense RedEdge M multispectral camera used in this Ph.D. thesis with their respective wavelengths in (mm). These bands were used

to calculate the vegetation indices mentioned below.

Table 3.1: MicaSense RedEdge M multispectral camera band and wavelength information in (mm)

Spectral Band	**Band**	**Wavelength (nm)**
Blue	1	475
Green	2	560
Red	3	668
Red Edge	4	717
NIR	5	840

3.4.1 NDVI - Normalized Difference Vegetation Index

The most common index in agriculture, characterizes the density of vegetation and allows farmers to assess germination, growth, the presence of weeds or diseases, as well as predict the productivity of the fields. Index indicators are generated through satellite images of green mass, which absorbs electromagnetic waves in the visible red range and reflects them in the near-infrared range. The red region of the spectrum (0.62 - 0.75 μm) accounts for the maximum absorption of solar radiation by chlorophyll, and the near infrared zone (0.75 - 1.3 μm) has the maximum energy reflection by the leaf cell structure. High photosynthetic activity leads to lower values of the reflection coefficients in the red region of the spectrum and large values in the near-infrared region of the spectrum. The ratio of these indicators allows for clear separation of vegetation from other natural objects (Amarasingam et al., 2022; Chen et al., 2023; Tsoulias et al., 2023; Zhu et al., 2023).

$$NDVI = \frac{NIR - R}{NIR + R}$$

3.4.2 NDRE - Normalized Difference Red Edge Index

This index is used in remote sensing to measure the chlorophyll content in plants. It is calculated using a combination of a near-infra-red (NIR) band and the RedEdge range between visible Red and NIR (Amarasingam et al., 2022).

$$NDRE = \frac{NIR - RE}{NIR + RE}$$

3.4.3 GNDVI - Green Normalized Difference Vegetation Index

This index is used to estimate photosynthetic activity and determine the water and nitrogen consumption of vegetation cover (Amarasingam et al., 2022).

$$GNDVI = \frac{NIR - Green}{NIR + Green}$$

3.4.4 EVI - Enhanced Vegetation Index

An optimized (VI) invented by Liu and Huete to improve the vegetation signal with better sensitivity in areas of high biomass. Corrects NDVI results for atmospheric changes as well as soil background signals in dense canopy zones (Amarasingam et al., 2022; Chen et al., 2023).

$$EVI = 2.5 \times \frac{NIR - R}{NIR + 6 \times R - 7.5 \times B + 1}$$

3.4.5 CVI - Chlorophyll Vegetation Index

This index has increased sensitivity to the chlorophyll content in deciduous cover and is used from the beginning to the middle of the crop growth cycle (Shendryk et al., 2020).

$$CVI = \frac{NIR}{G} \times \frac{Red}{G}$$

3.4.6 SAVI - Soil-Adjusted Vegetation Index

This index minimizes soil brightness influences using a soil brightness correction factor, especially useful in arid regions with low vegetative cover (Chen et al., 2023).

$$SAVI = \frac{NIR - R}{NIR + R + L} \times (1 + L)$$

3.4.7 OSAVI - Optimized Soil Adjusted Vegetation Index

Developed by Rondeaux et al., this index uses the reflectance in the near-infrared (NIR) and red (R) bands with an optimized soil adjustment coefficient (Shendryk et al., 2020).

$$OSAVI = \frac{NIR - R}{NIR + R + 0.16}$$

3.4.8 SCCCI - Simplified Canopy Chlorophyll Content Index

This index avoids the use of bounds and is simply the ratio of the computed NDRE over NDVI (Shendryk et al., 2020).

$$SCCCI = \frac{NDRE}{NDVI}$$

3.4.9 MACI - Modified Anthocyanin Content Index

This index estimates the anthocyanin content using the ratio of reflectances in the near-infrared (NIR) and the green spectral bands (Shendryk et al., 2020).

$$MACI = \frac{NIR}{Green}$$

3.4.10 VARI - Visible Atmospherically Resistant Index

Designed to emphasize vegetation in the visible portion of the spectrum, while mitigating illumination differences and atmospheric effects, it is ideal for RGB or color images (Zhu et al., 2023).

$$VARI = \frac{G - R}{G + R - B}$$

3.4.11 TCARI - Transformed Chlorophyll Absorption and Reflectance Index

Indicates the relative abundance of chlorophyll and is affected by the underlying soil reflectance, particularly in vegetation with a low LAI (Shendryk et al., 2020).

$$TCARI = 3[(RE - R) - 0.2(RE - G)(RE/R)]$$

3.4.12 IPVI - Infrared Percentage Vegetation Index

This index is functionally and linearly equivalent to the normalized difference vegetation index, and is computationally faster and never negative (Liu et al., 2023a).

$$IPVI = \frac{NIR}{NIR + R}$$

3.5 Multispectral imaging applied to agriculture

Multispectral imaging, fundamental in precision agriculture, provides valuable information on crop health status. Mostly, the near-infrared (NIR) band is used due to the high reflectance of vegetation in this region of the electromagnetic spectrum (Goffart et al., 2023). These images are captured by sensors located on artificial satellites or drones that transform the radiance of the Earth's surface into numerical values that represent specific wavelength ranges. Although satellites offer accuracy, low resolution, high cost, and weather conditions limit their usefulness. In contrast, drones equipped with multispectral cameras allow for more frequent monitoring and higher spatial resolution (Patil et al., 2023). These sensors typically capture information in several bands, including green, red, red-edge, and NIR. From multispectral images, especially in visible and near-infrared (VIS-NIR) bands, spectral indices such as NDVI and CWSI can be calculated, providing crucial information on the vegetative state of the crop and the evapotranspiration, which facilitates the prediction of diseases or pests (Bazzo et al., 2023). This technology promises to significantly improve agricultural management by allowing a detailed and timely assessment of crop condition (Istiak et al., 2023).

3.5.1 Calibration process in multispectral sensors

To ensure the accuracy of the collected information and minimize errors, image calibration and correction procedures are required. In the field of remote sensing, sensors play a key role in capturing specific physical parameters (Teixeira Crusiol et al., 2020). These sensors can be active, such as radar and LiDAR, which generate and receive their own radiation, or passive, which collect electromagnetic energy from land surfaces. Passive sensors include photographic systems, multispectral and hyperspectral radiometers, and imaging spectrometers. Upon receiving radiance, sensitive detectors convert wavelengths into electrical signals which are then transformed into digital levels (DLs). Each ND represents a pixel in the image and is based on the light reflected or emitted by the Earth's surface in a specific band of the spectrum. This information, essential for crop analysis, provides a numerical representation of the characteristics of the land in particular locations, facilitating interpretation and decision making in precision agriculture (Teixeira Crusiol et al., 2020).

Data quality in multispectral sensors

The quality of multispectral sensors is largely determined by their resolution, which covers spatial, spectral, radiometric, and temporal aspects. This ability to record and discriminate information in detail is essential to obtain accurate crop data. However, multispectral images captured by UAV can face challenges such as sensor noise, irregular illumination, and atmospheric disturbances. These problems can be mitigated by radiometric calibration and atmospheric correction techniques, which improve the sensitivity of canopy reflectance and facilitate the determination of nitrogen status in the crop. In addition, hyperspectral images can be altered as a result of interaction with the atmosphere, caused by various factors such as aerosol scattering and absorption of gaseous substances. The application of appropriate techniques to address these challenges is essential to ensure the reliability of the data collected and its usefulness in precision agriculture. Figure 3.5 shows the main confounding factors, the methods for minimizing these factors, and the corresponding application cases.

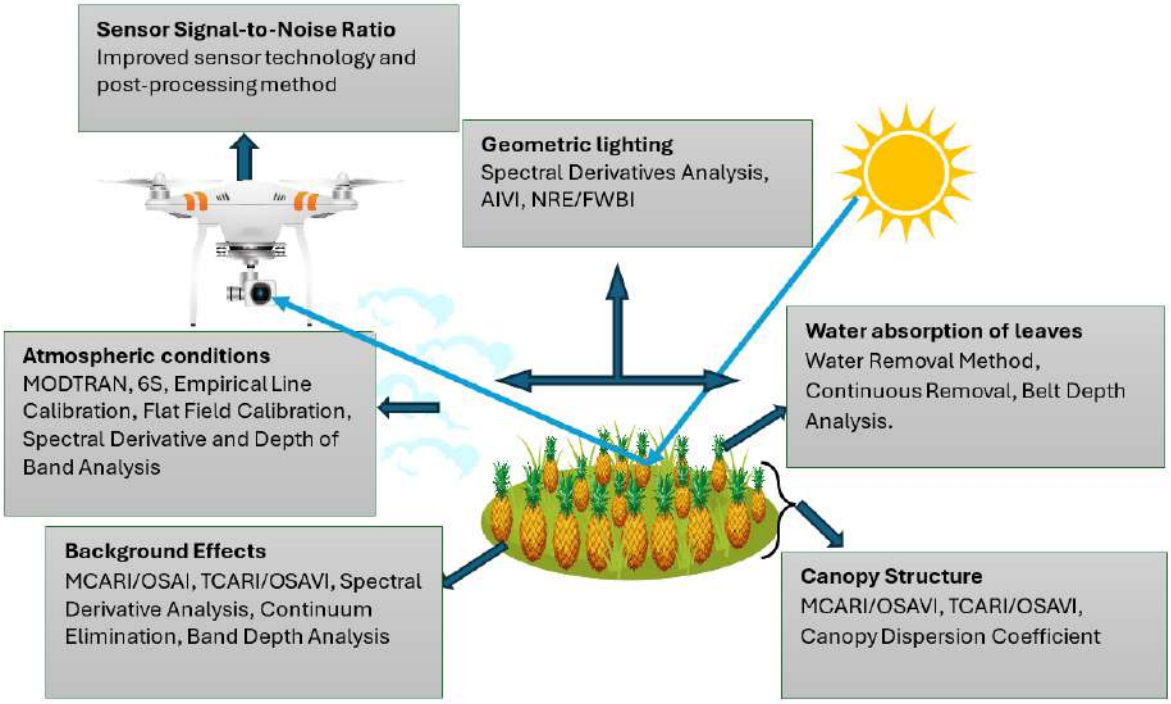

Figure 3.5: Summary of the main confounding factors, methods to minimize these factors and corresponding application cases. Source: Own elaboration.

3.5.2 Geometric and radiometric errors in multispectral images

The process of converting raw images to radiance and reflectance in multispectral images, such as those captured by cameras like the MicaSense RedEdge, involves a series of correction and calibration steps that ensure that the digital data are interpretable for analysis of biological or physical variables. During this process, errors may arise in the images due to a variety of sources, such as instrument failures, atmospheric conditions, or terrain characteristics. These errors are divided into geometric and radiometric errors. Radiometric errors occur when the mean of the pixel intensity or digital number (ND) values is irregular, which may be due to the behavior of the recording instruments, wavelength variability of solar radiation or atmospheric effects. On the other hand, geometric errors can be both systematic and non-systematic, and affect the correct alignment and spatial representation of the images (Bourgeon et al., 2016).

Conversion of digital numbers (ND) to radiancy

Radiance is the amount of energy emitted or reflected by a surface, measured over a specific area, at a solid angle, and at a specific wavelength. In the context of multispectral imaging, the camera captures digital values that do not directly represent radiance. The basic formula for converting from digital numbers (ND) to radiance (L) is as follows.

The basic formula to convert digital numbers (DN) to radiance (L) is:

$$L = \frac{DN \cdot a_1}{\text{exposure time} \cdot \text{gain} \cdot 2^{\text{bit depth}}}, \tag{3.1}$$

Where:

- DN: is the digital number or raw value captured by the sensor.
- a_1: is the radiometric calibration coefficient that converts the digital numbers to physical units of radiance.
- Exposure time: the camera's exposure time.
- Gain: the gain factor, usually represented by the image's ISO value.
- $2^{\text{bit depth}}$: is the sensor's bit depth, which indicates how many possible values the sensor can record.

This process also includes camera corrections related to vignetting (darkening towards the corners of the image) and black level compensation (correction for dark levels or dark pixels present in the camera).

Geometric calibration

Geometric calibration is used to correct for the effects of pitch, roll, lateral rotation, trajectory, height, and platform velocity. The optical device creates geometric distortions in the images: lengths, shapes, and surfaces are modified, which will prevent the future calculation of morphometric indicators such as leaf area. Moreover, as the luminous flux is directed through a prism to separate visible and NIR light, the geometric distortions of both types of images are different. The NIR and visible images could not overlap without this correction step. Consequently, to characterize vegetation zones, we need to correct the images for the geometric distortions produced by the wide-angle lens and the prism of the imaging system (Bourgeon et al., 2016).

To correct errors in georeferenced images, parametric and nonparametric methods are used. Non-parametric methods adjust the image using X and Y coordinates, being useful in flat terrain. On the other hand, parametric methods perform inverse transformations based on orbital and sensor characteristics, highlighting orthorectification that uses terrain elevation to eliminate scale and offset variations. This approach is recommended for remote sensing from aerial platforms.

Radiometric Calibration

Direct and reflected solar radiation interact with atmospheric factors, causing errors in sensor data capture, known as the "atmosphere effect". These factors include gases, aerosols, and clouds, which scatter and absorb radiation. This can result in the radiation measured by the sensor being less than the current radiation or the capture of a pixel being contaminated by scattering from other areas outside the intended target. This type of contamination depends on the wavelength, the reflectivity of the surface, the camera used, and the object of study. In addition, changes in time and date also affect radiation (Cao et al., 2019). Figure 3.5 illustrates how the atmosphere influences the measurement errors of the energy captured by a sensor.

The solar spectral radiance before entering the atmosphere is defined as $E(\lambda)$, if the solar zenith angle is taken as θ_S, it will result that the spectral irradiance incident on the ground is the product of $E(\lambda)\cos\theta_S$. If one also takes into account the log per spectral

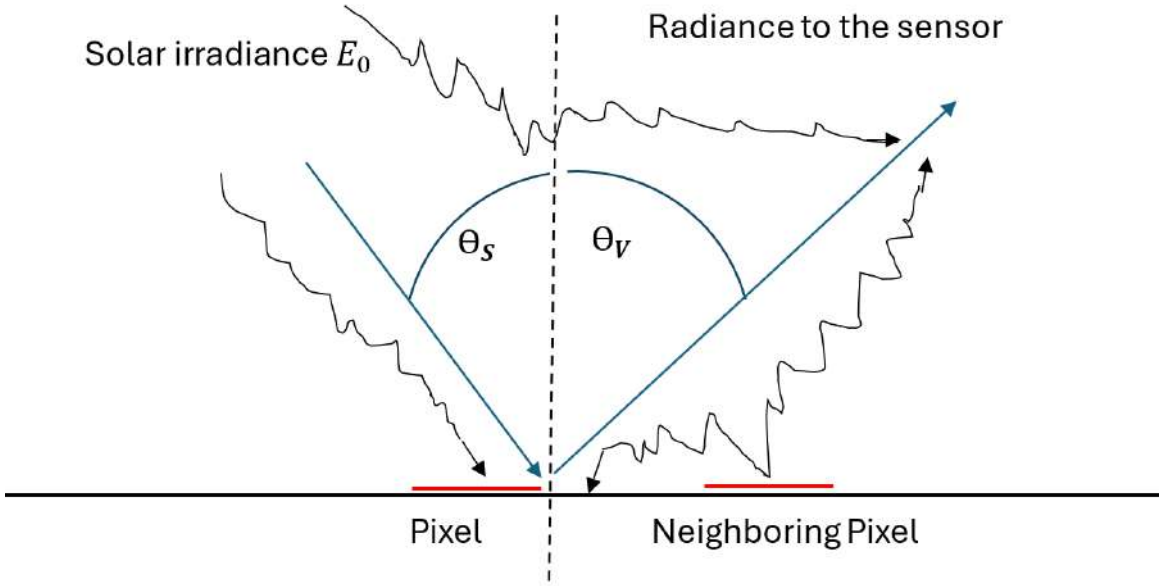

Figure 3.6: Effect of atmosphere on single pixel radiance. Source. Figure Adapted from (Cao et al., 2019).

range captured by a certain filter in the sensor indicating $(\lambda)_1$ and $(\lambda)_2$ (wavelength range in which a filter can capture), then it is expressed as:

$$E(\lambda) = \int_{(\lambda)_1}^{(\lambda)_2} E(\lambda) \cos\theta_S d\lambda, \tag{3.2}$$

If the difference between $(\lambda)_1$ and $(\lambda)_2$ is expressed as $\Delta\lambda$, and this difference is very narrow, it is assumed that:

$$E(\lambda) = E(\Delta\lambda) \cos\theta s \Delta\lambda, \tag{3.3}$$

Where $E(\Delta\lambda)$, is the mean irradiance between $(\lambda)_1$ and $(\lambda)_2$,

$$L = \frac{1}{\pi} \cdot E(\Delta\lambda) \cos\theta s \Delta\lambda \rho, \tag{3.4}$$

Therefore, if we know L from the above equation, we can deduce the power detected by the sensor, in addition to the ND originating from the original image, which is directly related to the radiance of the scene. Then, the radiance per pixel is expressed as:

$$L = (ND)k + L_{\min}, \tag{3.5}$$

Here, $L_{\min}$ and $L_{\max}$ are the maximum and minimum radiances detected by the

sensor and depend on the original calibration of the sensor. ND is a binary coded value of the intensity of light reflected from the Earth's surface, measured by the sensor using a particular combination of exposure settings (e.g., shutter speed, aperture, ISO/gain, etc.) (Cao et al., 2019).

Radiometric Calibration MicaSense RedEdge M

To perform the radiometric calibration process of the MicaSense RedEdge sensor, we use the manufacturer's radiometric conversion formula, which in this case is MicaSense, which converts ND values to absolute spectral radiance values (MicaSense, 2020).

$$L = V(x, y) \times \frac{a_1}{g} \times \frac{p - p_{BL}}{t_e + a_2 y - a_3 t_e y}, \tag{3.6}$$

Where,

- L: is the spectral radiance.
- $V(x, y)$: the polynomial vignetting function at pixel (x, y).
- a_1, a_2, and a_3: the radiometric calibration coefficients.
- g: the sensor gain setting.
- p: the normalized DN value.
- pBL: the black level shift.
- t: the exposure time of the image.

All these parameters required for the calculation of L are found in the calibration panel and in the image metadata (MicaSense, 2020).

Pixel Value Normalization

MicaSense sensors can save images in a 12 bit or 16 bit format. The radiometric model uses a normalized pixel value p, in the range 0 to 1. To compute the normalized pixel value, simply divide the raw digital number for the pixel by 2^N, where N is the number of bits in the image. For 16-bit images, divide by 65536. For 12-bit images, divide by 4096. This applies to both the pixel value and the black level value (MicaSense, 2020).

Vignette Model

The RedEdge uses a radial vignette model to correct for the fall-off in light sensitivity that occurs in pixels further from the center of the image. To apply the model, first read cx, cy, and the six polynomial coefficients from the image metadata, then compute the formula below to find a correction scale factor for each pixel intensity (MicaSense, 2020).

$$r = \sqrt{(x - c_x)^2 + (y - c_y)^2}, \tag{3.7}$$

$$k = 1 + k_0 r + k_1 r^2 + k_2 r^3 + k_3 r^4 + k_4 r^5 + k_5 r^6, \tag{3.8}$$

$$I_{\text{corrected}}(x, y) = \frac{I(x, y)}{k}, \tag{3.9}$$

Where,

- r is the distance of the pixel (x, y) from the vignette center, in pixels
- (x, y) is the coordinate of the pixel being corrected
- k is the correction factor by which the raw pixel value should be divided to correct for vignette
- $I(x, y)$ is the original intensity of pixel at x, y
- $I_{\text{corrected}}\ (x, y)$ is the corrected intensity of pixel at x, y

3.6 Machine learning and deep learning applications for nutrient estimation in crops

The integration of ML and DL with remote sensing technologies has further revolutionized crop yield predictions. Using large-scale, detailed observational data provided by aerial and satellite imagery, these technologies improve the analysis of weather conditions and soil characteristics. DL approaches, particularly CNNs, are adept at processing complex, high-dimensional data from remote sensing, offering unprecedented accuracy in predictive analysis (Bal and Kayaalp, 2021).

This synergy enables more accurate and informed agricultural planning. Using global coverage and temporal frequency of remote sensing to monitor crop health and predict

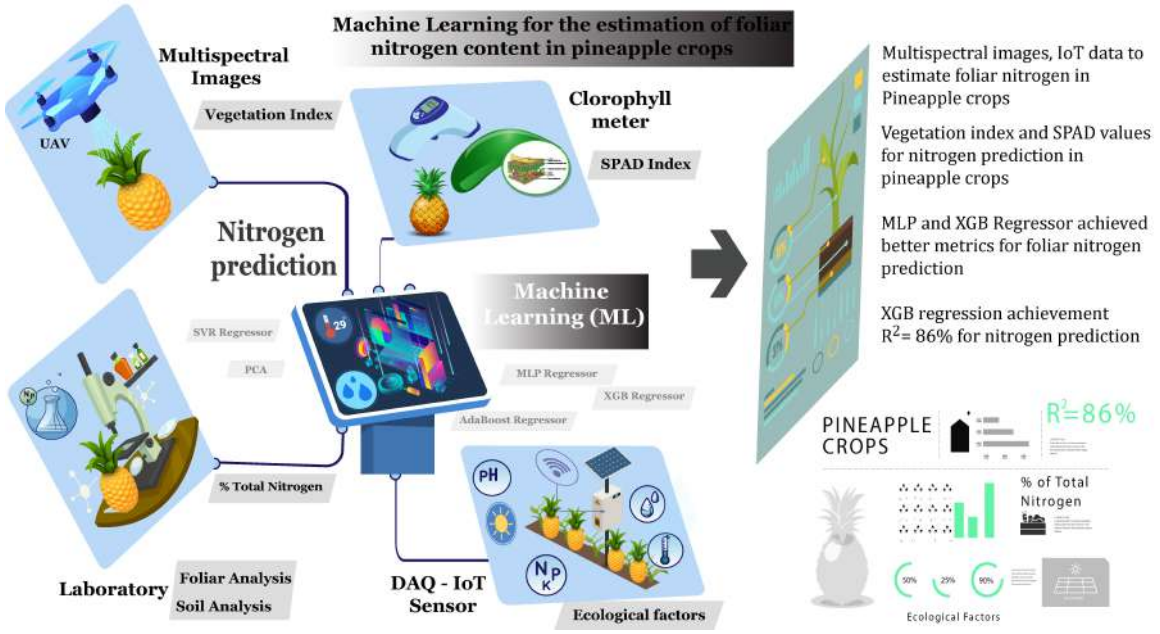

Figure 3.7: Graphical summary of the integration of machine learning models with imagery, IoT sensors, SPAD values and laboratory analysis to estimate nitrogen in pineapple crops. Source: Own elaboration.

yields with greater accuracy, thereby optimizing resources and maximizing productivity (Sharma et al., 2021).

In crop nitrogen estimation, several machine learning (ML) and deep learning (DL) techniques are used to analyze data from images and IoT. ML techniques include supervised algorithms such as linear regression, KNN, Random Forest, SVM, and artificial neural networks, as well as unsupervised algorithms such as K-means and DBSCAN (Bal and Kayaalp, 2021; Ennaji et al., 2023). In DL, convolutional neural networks (CNNs), recurrent neural networks (RNNs), and recurrent convolutional neural networks (CRNNNs) are used primarily. Predictor variables include multispectral images, taken by drones or satellites, and IoT sensor data such as soil moisture, temperature, and electrical conductivity, in addition to meteorological data. The resulting models can be regression, classification or mapping, and their application includes optimizing fertilizer use, early detection of nutrient deficiencies, and monitoring soil health (Sharma et al., 2021). However, they face challenges such as high-quality data availability, model complexity, and spatial variability of soil nitrogen. Accurate data collection, proper pre-

processing, careful selection of models, and interpretation of results are critical to the success of these applications in precision agriculture. Figure 3.7 details the integration of machine learning models with imagery, IoT sensors, SPAD values, and laboratory analysis to estimate nitrogen in pineapple crops. This is the most general methodology for estimating nutrients in any other type of crop.

Chapter 4

Materials and Methods

Chapters 3, 4 and 6 of this thesis constitute the core of the scientific contributions of this work. These chapters develop and validate predictive models for the estimation of nitrogen content in pineapple crops, using machine learning techniques based on information provided by multispectral images and sensor data analysis in IoT platforms. It is highlighted that part of the information presented in these chapters will be published in Elsevier's 'Journal of Agriculture and Food Research', a quartile one (Q1) publication.

In this PhD thesis, the use of multispectral imagery and sensors integrated in an IoT platform to predict nitrogen content in MD2 pineapple crops was investigated. The methodology includes multispectral image capture, foliar samples for nitrogen analysis, chlorophyll measurement using SPAD values, and soil, plant, and environmental data through sensors, as shown in the general methodology diagram in Figure 4.1.

4.1 Study area description

The study area is located in the municipality of Tauramena, in the department of Casanare, Colombia, with geographical coordinates WGS 84, N 5° 1′ 23.4″ - W 72° 45′ 4.7″ at an elevation of 340 meters above sea level. The experimental design was carried out at the facilities of the company "Agricola Santana de los Llanos S.A.S". This company has certified processes and registration as a producer of selected seeds of pineapple variety Gold MD2. Figure 4.2 shows the location of the crop in which the experiments and data recording were carried out.

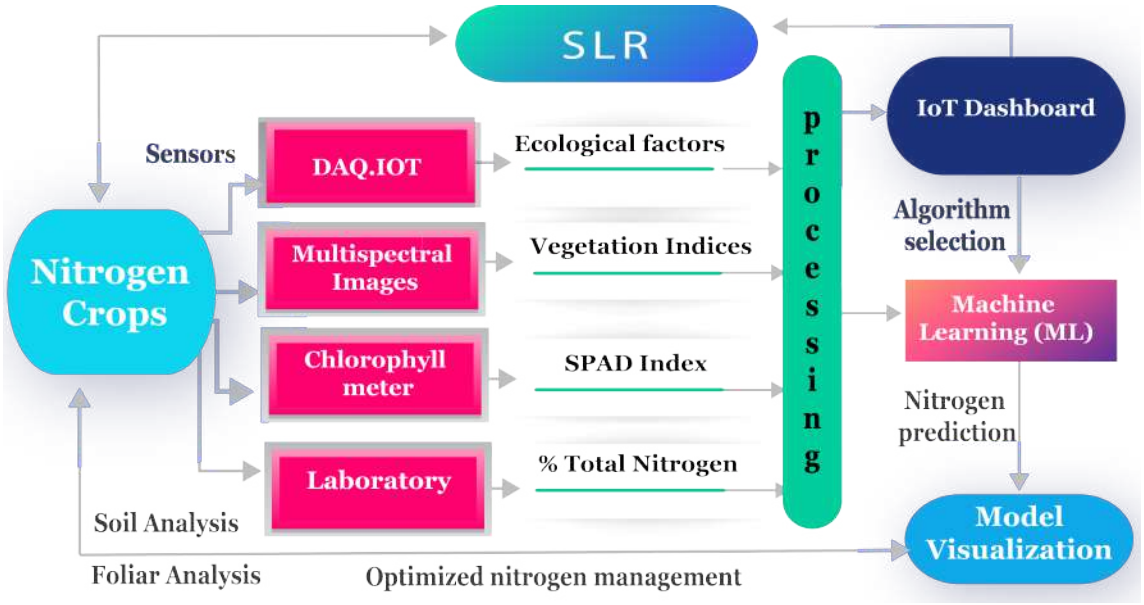

Figure 4.1: The overall methodology encompasses the following phases: Systematic Literature Review (SLR), leaf nitrogen sampling for laboratory analysis (Laboratory), IoT data logging of crop, soil, and environment (DAQ-IOT), multispectral image capture of crop leaf area (Multispectral Images), recording of SPAD values of leaf chlorophyll content (Chlorophyll Meter), and predictive model processing and development. Source: Own elaboration.

4.2 Experimental design

In order to have nitrogen variability, a complete randomized block experimental design was carried out, applying five different nitrogen treatments distributed in five blocks, for a total of 25 experimental units. Twelve applications were received over a six-month period, based on the methodology proposed by (Shendryk et al., 2020). In this case, the blocks were not used to measure the effect of treatment on biomass or crop yield but instead as a source of variability to obtain different samples of nitrogen content. Table 4.1 details the distribution and amount of nitrogen used in each of the treatments of the experimental design.

To guarantee the normal development of the crop, only the nitrogen content was varied; the rest of the nutritional elements, herbicides, and insecticides were applied according to the nutritional management plan established for the crop. Control treatment was number 3, with 6.7 grams of nitrogen per plant, following the recommendations of the Colombian Agricultural Research Corporation, AGROSAVIA.

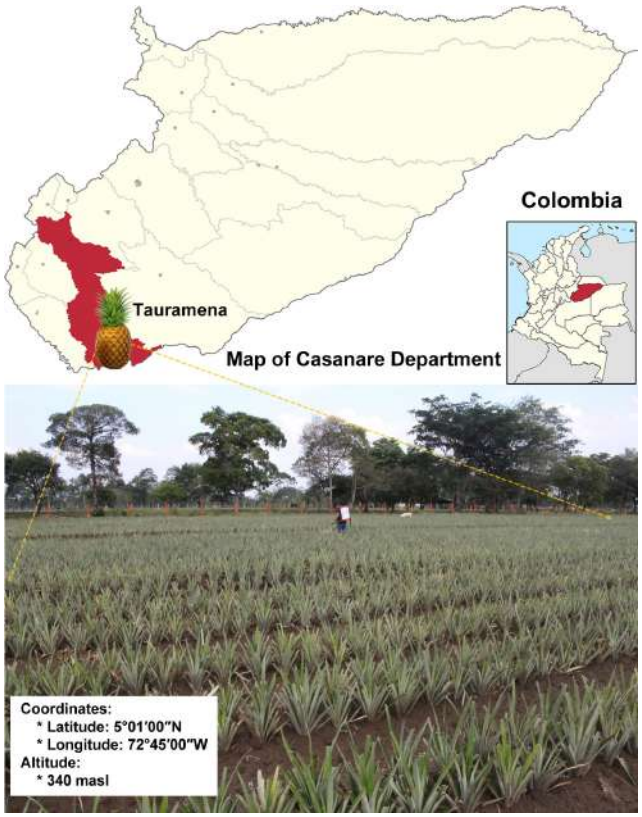

Figure 4.2: Study area located in the municipality of Tauramena; a Colombian municipality located in the department of Casanare, in the Eastern Plains region of the Colombian Orinoquia. Source: Own image of the place where the experimental design was developed.

Site selection and delimitation of sample plot sizes

For the experimental setup, five hectares were established and for each hectare five sampling sites were randomly selected. Each hectare corresponded to one furrow of the crop and these furrows were assumed as blocks, as can be detailed in the in Figure. 4.3.

Five hectares were established for the experimental layout and in each hectare five experimental units were established 30 meters apart to avoid possible effects on the results of the experiment. In each sample space or experimental unit, 10 pineapple fruits were selected, labeled with the block number and treatment, and marked with wooden stakes keeping a 3×1.5 meter ratio (the equivalent of 10 pineapple fruits), as shown in Figure. 4.4.

With the help of a professional agronomist, five foliar fertilization tables were prepared for 50 MD2 pineapple plants for each of the treatments. These tables contained information on the dates of application, the type and amount of nutritional element,

Table 4.1: Nitrogen values used per treatment and block distribution of the experimental design, unit of measurement, grams/plant.

	Blocks				
Treatments	B1	B2	B3	B4	B5
T1 = 0.0 g/p	T1	T2	T5	T4	T1
T2 = 3.3 g/p	T4	T1	T3	T2	T5
T3 = 6.7 g/p	T2	T4	T4	T5	T3
T4 = 9.3 g/p	T5	T3	T2	T3	T4
T5 = 12.0 g/p	T3	T5	T1	T1	T2

Table 4.2: Foliar fertilization table for treatment (T5), corresponding to 50 plants, nutritional elements applied in grams and amount of water in liters.

No	Date	**N**	K	Mg	Ca	Zn	B	H	H_2O
1	30/03/2022	**82**	30	10		3			1,5
2	13/04/2022	**92**	32	10	-	3	3	-	1,5
3	27/04/2022	**92**	32	12	8	-	3	1,3	1,5
4	04/05/2022	**100**	40	12	-	3	3		2
5	18/05/2022	**100**	40	14	9	-	3	1,3	2
6	01/06/2022	**108**	40	16	-	4	4	-	2
7	15/06/2022	**108**	50	17	10	-	4	1,3	2
8	29/06/2022	**117**	50	17	-	4	4	-	2
9	13/07/2022	**117**	50	20	12	-	4	1,4	2
10	27/07/2022	**126**	60	20	-	4	5	-	2,5
11	10/08/2022	**126**	60	20	13	-	5	1,5	2,5
12	24/08/2022	**132**	60	20	-	5	5	-	2,5

and the amount of water to be applied as described in Table 4.2.

Fertilizer and Herbicide Applications

Following the experimental design, granular foliar nitrogen (CH_4 N_2O - urea 46%) was applied during the twelve programmed dates for a period of six months, from March 1 to August 31, 2022, corresponding to the vegetative stage, as shown in Figure. 4.6. Foliar nitrogen was applied at this stage since, from the flowering stage, nitrogen promotes leaf growth rather than fruit growth. The application was made with a handheld sprayer, as detailed in Figure. 4.5.

Figure 4.3: Distribution of the five blocks (B1, B2, B3, B4 and B5) in the pineapple crop; each block is approximately 3 meters apart. Source: Own image of the place where the experimental design was developed.

Figure 4.4: Initial marking of sample spaces, 10 pineapple fruits were selected and demarcated with the block number and treatment. Source: Own image of the place where the experimental design was developed.

Figure 4.5: Application of treatments to the subplots through a manual fumigator. Source: Own image of the place where the experimental design was developed.

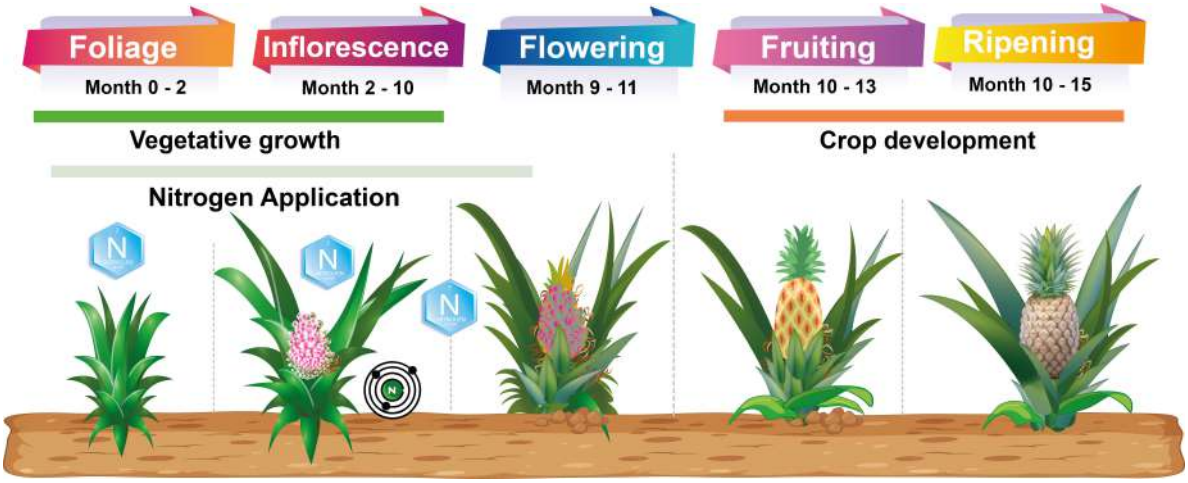

Figure 4.6: Phenological cycle of pineapple cultivation variety MD2. ***Foliage*:** After a certain period, new leaves appear. ***Inflorescence*:** Appears at the top of the stem wrapped inside the base of the leaves. ***Flowering*:** Appearance of flowers on the inflorescence. ***Fruiting*:** Fruit development and ripening. ***Ripening*:** The fruit reaches the typical size and color of the variety. Source: Own elaboration.

Chapter 5

Data Acquisition

This chapter comprehensively details the data acquisition process, the equipment used in data collection, and the methodological development used to analyze and process the information obtained. Given the interdisciplinary nature of this thesis, which integrates information from multiple sources for a holistic assessment of nitrogen content in pineapple crops, each type of collected data, its origin, and the justification for its use are described.

5.1 UAV Image acquisition and flight parameters

For the acquisition of multispectral images, the MicaSense RedEdge-M multispectral camera was used, installed on a DJI Phantom 4 Pro unmanned aerial vehicle (UAV).

This drone is equipped with an altitude hold mode that ensures stable flights and consistent flight times. The multispectral camera has dimensions of 9.4 cm x 6.3 cm x 4.6 cm, with a weight of 200 g (7 oz.). It incorporates GPS and five spectral bands spanning wavelengths from 470 to 840 nm: blue (470 nm), green (560 nm), red (680 nm), red edge (717 nm) and NIR (840 nm). The sensor has a spatial resolution of 1280 x 960 (1.2 MP per band) and a resolution (GSD) of 8 cm per pixel (per band) at 120 m (400 ft) AGL. Figure. 5.1 details the mounting of the drone and the multispectral camera.

Four samples were taken at 30-day intervals, between months 4 and 8 of the crop phenological cycle. The images were taken between 10:00 am and 3:00 pm, in order to maintain the same luminosity in the images. On the other hand, images were taken from a calibrated reflectance panel at the beginning and end of each flight. The Figure. 5.2 shows an image of the protocol for image acquisition, on the left side is the camera

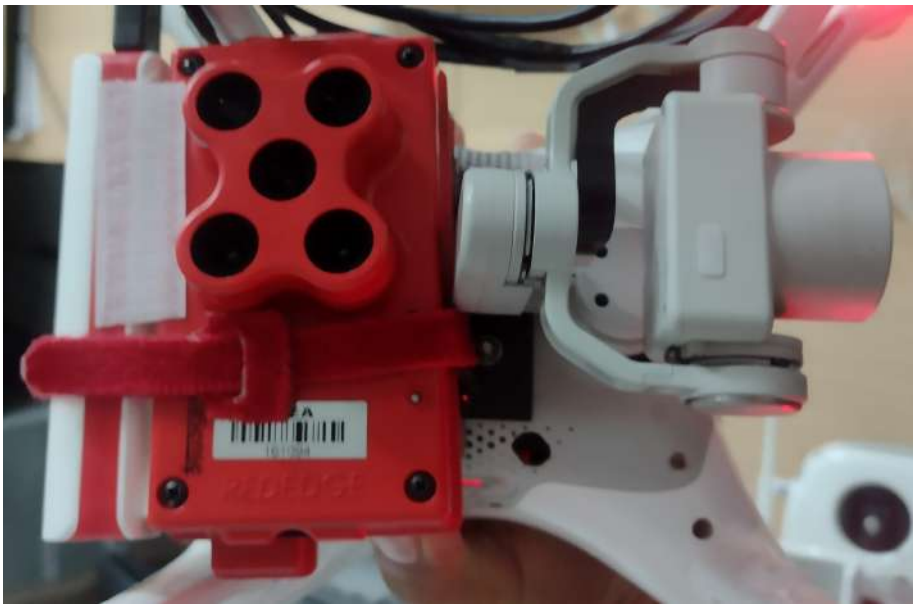

Figure 5.1: Mounting the MicaSense RedEdge-M multispectral camera on the Phantom 4 Pro (UAV). Source: Own image of the equipment used in the development of the experimental design.

calibration through the reflectance panel and on the right side is the stabilized flight at 12 meters.

A longitudinal and lateral overlap of 90% and 70%, respectively, was adopted for image capture. Flight planning was performed with the DJI ground station pro application for iPad. Figure. 5.3, shows the composition of an RGB image taken with the drone at an altitude of 12 meters. In this image, the label marked B4T4 can be seen at the beginning of the sample space, which is delimited by 4 white wooden stakes.

5.2 DAQ-IoT acquisition of information on ecological factors

To obtain agrometeorological data and ecological factors relevant to the crop, an IoT station was designed and implemented specifically for this project. Additionally, a mobile application was developed to facilitate the recording and visualization of the data collected. In order to validate and corroborate the accuracy of the information recorded, a backup weather station was installed to monitor environmental variables independently. In this case, the Logia: 7 in 1 Wi-fi Weather Station was chosen, which is solar powered

Figure 5.2: Camera calibration through the reflectance panel and stabilized flight at 12 meters altitude. Source: Own image of the equipment used in the development of the experimental design.

and has a remote monitoring system for indoors and outdoors. Among the variables measured by this station are: temperature, humidity, wind speed and direction, rainfall, UV index and relative humidity. The information collected by the Logia station is transmitted wirelessly to the Weathercloud platform for further analysis. Figure. 5.4 shows the Logia station installed in the crop as a backup of the data.

With regard to installed sensors, commercial sensors were used to have the possibility of replacing them in case of failure. Table 5.1 describes the monitored variables and the reference information of the sensors used.

5.2.1 Agrometeorological station developed for the acquisition of ecological and environmental factors.

An agrometeorological station composed of a Datalogger and a WiFi Gateway was developed. The Datalogger has the function of receiving and adapting the signal from the sensors, storing the information, preprocessing the data and then transmitting it to the WiFi Gateway. On the other hand, the WiFi Gateway facilitates the connection between the Datalogger and the IoT web platform. This device has a WiFi connection, 3 optocoupled inputs, an RS-232 channel for sensor modules, 3 visual indicators (LEDs), an audible indicator (buzzer) and 3 digital outputs for relay activation. The datalogger receives information from sensors for relative humidity, ambient temperature, precipitation, wind speed, solar radiation and pH. These sensors transmit to a data acquisition card which in turn transmits to a WiFi gateway responsible for communication with the

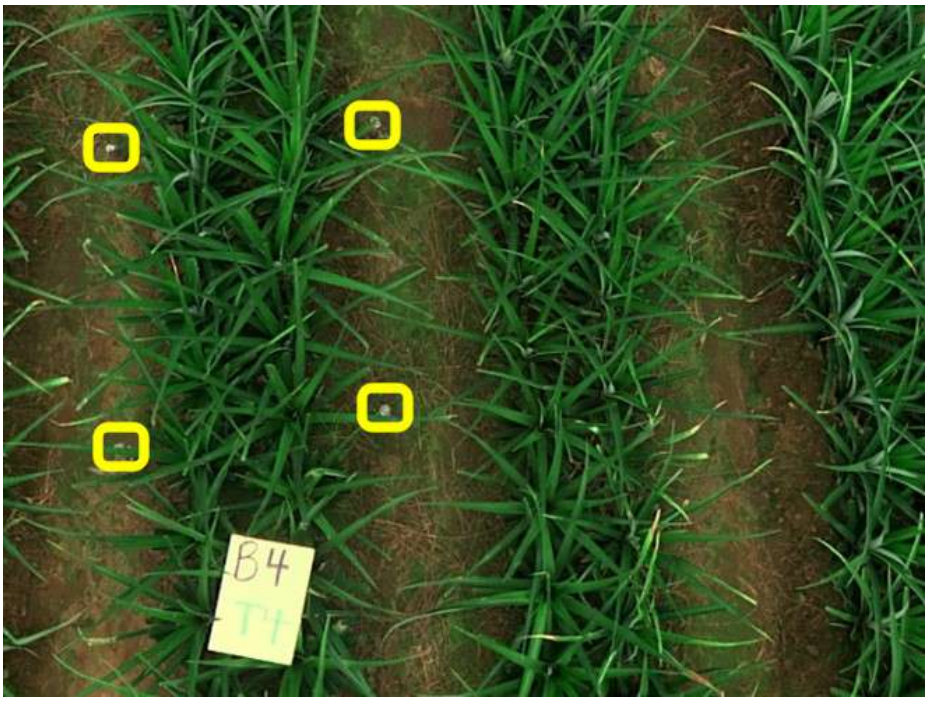

Figure 5.3: Image composed of red, blue and green bands. This image shows the sample space B4T4, block/treatment, which is made up of 10 pineapple fruits, demarcated with four stakes painted in white, as can be seen in the boxes marked in yellow. Source: Own image of the place where the experimental design was developed.

VPS. The system is totally autonomous and power is provided by a solar panel as shown in Figure. 5.5

To obtain data from sensors installed on the soil, measurement protocols were established. For soil moisture, the volumetric moisture method (H_g) was used, which is a relationship between the volume of the liquid fraction, water, or solution (V_a) and the volume of the sample (V_s) (Salman et al., 2021). This relationship is shown in Equation 5.1.

$$H_g = V_a/V_s \tag{5.1}$$

Regarding pH, three different sensors were used, as detailed in Table 5.1, two analog and one digital, with ranges between $3-8$ pH and an accuracy of ± 2 pH. The analog pH and soil moisture sensor is shown in the in Figure. 5.6, this sensor is analog and does not require batteries or electricity; it is simply inserted into the soil to obtain the pH value. However, for this project it was necessary to parameterize the sensor and convert the analog signal to digital so that it could be transmitted to the Datalogger.

Figure 5.4: Logia Wi-fi Weather Station: 7 in 1 installed in the crop for acquisition of environmental variables. Source: left image taken from amazon.com. Right image: own image of the equipment used in the development of the experimental design.

The RainWise RAINEW 111 rain gauge, known for its accuracy and low maintenance requirements, was used to measure rainfall. This device has a highly accurate, 8-inch (20.5 cm) diameter tipping bucket collector that meets NWS specifications for statistical accuracy. Figure. 5.5 shows a detail of this sensor on the upper right side of the weather station.

For more details on the sensors used, the variables monitored and the reference information for each of the sensors used in this research are described in Table. 5.1. The JL-FS2 sensor was employed to gauge the wind speed. This sensor provides an output signal in the range of 0 to 5 V (voltage signal), with a resolution of 0.1 ms and an effective measurement range of 0 to 30 ms.

5.2.2 Mobile application developed to facilitate the recording and integration of data in cultivation

In order to facilitate the recording of crop data and the integration of information from the two stations, a mobile application has been developed consisting of several modules, which are described below:

- **Irrigation Module:** it allows visualizing the last recorded values of volumetric humidity, as well as the evapotranspiration calculated from the data of meteoro-

Figure 5.5: IoT agrometeorological station designed and developed for this project. It records information on environmental variables and ecological factors. Source: own image taken from the agrometeorological station developed for this doctoral thesis.

logical sensors. Also graphs of the variables over time, date of the last recorded values and option to consult the last recorded data.

- **Climate Module:** Displays the last recorded value and the corresponding ranges for several climatic variables such as Air Humidity (%), Ambient Temperature (°C), Wind Speed (m/s), Precipitation (mm), Evapotranspiration (K) and Solar Radiation (W/m^2). It automatically generates graphs over time, indicates the date and time of the last value sent by the sensor module, and offers the option to consult and visualize the last recorded values.

- **Soil Module:** Displays the last value recorded and the corresponding ranges for the pH Level, Ambient Temperature and Soil Moisture variables. In addition, it shows graphically each of these variables over time, indicates the date and time of the last value sent by the sensor module, and offers the option to consult and visualize the last recorded values.

Figure 5.6: Analog pH and soil moisture sensor, this sensor was conditioned to transmit the signal to the agrometeorological station. Source: own image taken from the agrometeorological station developed for this doctoral thesis.

- **Calculate Irrigation Module:** Allows calculating the daily irrigation projection by entering the Kc constants and the irrigation system efficiency value. It also offers the option of plotting evapotranspiration vs. precipitation.
- **Logging Module:** Allows the operator to log daily irrigation data, selecting the date of the log, logger, batch, valve number, pressure (psi), start time of activation and end time of deactivation. It also displays the last recorded values and allows the user to enter specific observations for each valve.

Figure. 5.7 shows the main screen of the climate module.

5.2.3 ThingsBoard IoT WEB Platform for Efficient Data Collection and Management

The Open Source IoT platform ThingsBoard was installed and configured to receive information from sensors in the cloud. Based on Java, this platform streamlines the creation and extension of IoT applications, enabling the seamless collection, processing, visualization, and management of device data. An intuitive web interface empowers system users to manage their assigned devices. For this project, ThingsBoard was chosen due to its open source nature and its ability to store, visualize, and analyze data

Table 5.1: Variables monitored and references of sensors used to measure soil and environmental variables.

Environmental sensors	**Reference**	**Sampling Rate**
Rain	1AA800013 Station Logia	10 minutes
Relative humidity	DHT22 (AM2302) St Logia	10 minutes
Ambient temperature	DHT22 (AM2302) St Logia	10 minutes
Luminosity	BH1750	10 minutes
Solar Radiation	Station Logia	10 minutes
Wind speed	OEM Station Logia	10 minutes
Wind direction	Station Logia	10 minutes
Dew point	Station Logia	10 minutes
pH	MIOGREN/RCYAGO/Gain Express	Manual registration
Soil moisture	MIOGREN/RCYAGO/Gain Express	Manual registration
Soil Temperature	Sensor digital-MIOGREN	Manual registration

Although the 'Gain Express' sensor is an analog sensor, a specific electronic interface was designed and built to digitize its measurements. This card allows the capture and transmission of data to the weather station, configured with a sampling rate of 10 minutes..

transmitted by sensors. The ThingsBoard implementation was carried out on a VPS provided by Dongee, equipped with 1 CPU, 2 GB of RAM, 55 GB of SSD storage, and 2 TB of data transfer. The installation process was performed on Ubuntu 18.04 LTS, requiring the installation of Java 11 (OpenJDK) and the configuration of a PostgreSQL database. After the installation, we proceeded to the configuration of super administrators through User Management (Administrator Role). This role comprises Admin Role, granting the user administrative privileges, including management of other users, devices, sensor types, and relays. Additionally, the User Role was created, allowing users to manage assigned devices within limited capabilities. This role allows them to access reports, view the status and behavior of real-time sensors, and manage relays and sensors. The main features of the implemented ThingsBoard platform are as follows:

- **Device Management:** Administrators create devices with their respective sensors and relays, while users manage the assigned relays and sensors.
- **Sensor Management:** This section allows for visualizing the sensors installed in the field, adjusting their levels, and displaying information through various widgets and panels.
- **Telemetry:** An API facilitates the collection of time series data and related use cases.

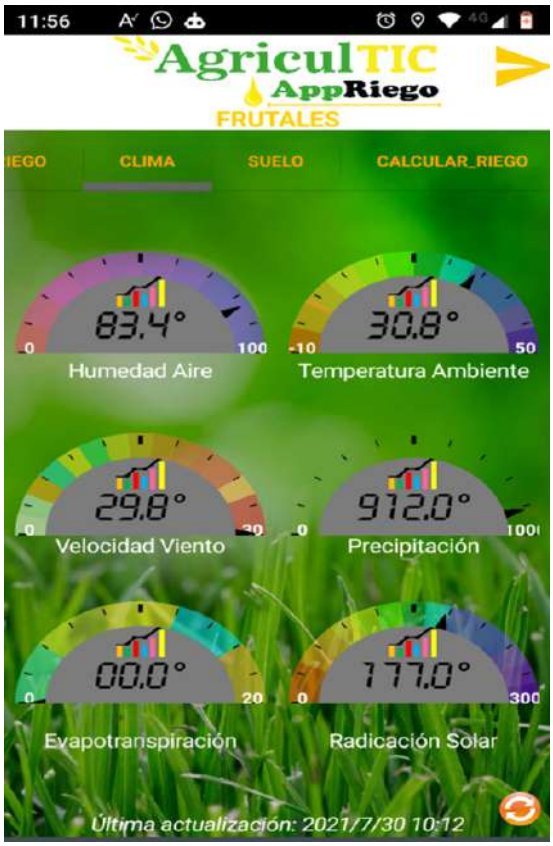

Figure 5.7: Main screen of the developed APP, the weather module is shown. Source: own image taken from the mobile application developed for this doctoral thesis.

- **Rules Engine:** This component handles data processing and actions based on telemetry and incoming events.
- **Reports:** This option allows the generation of reports for devices based on date ranges or data volume.

Figure. 5.8 shows a user interface that presents information from various sensors such as ambient temperature, precipitation and soil pH.

5.3 Capacitive parallel plate sensor for soil moisture determination

Within the framework of this doctoral thesis, a parallel plate capacitive sensor has been developed and validated, specifically designed for the integral measurement of soil

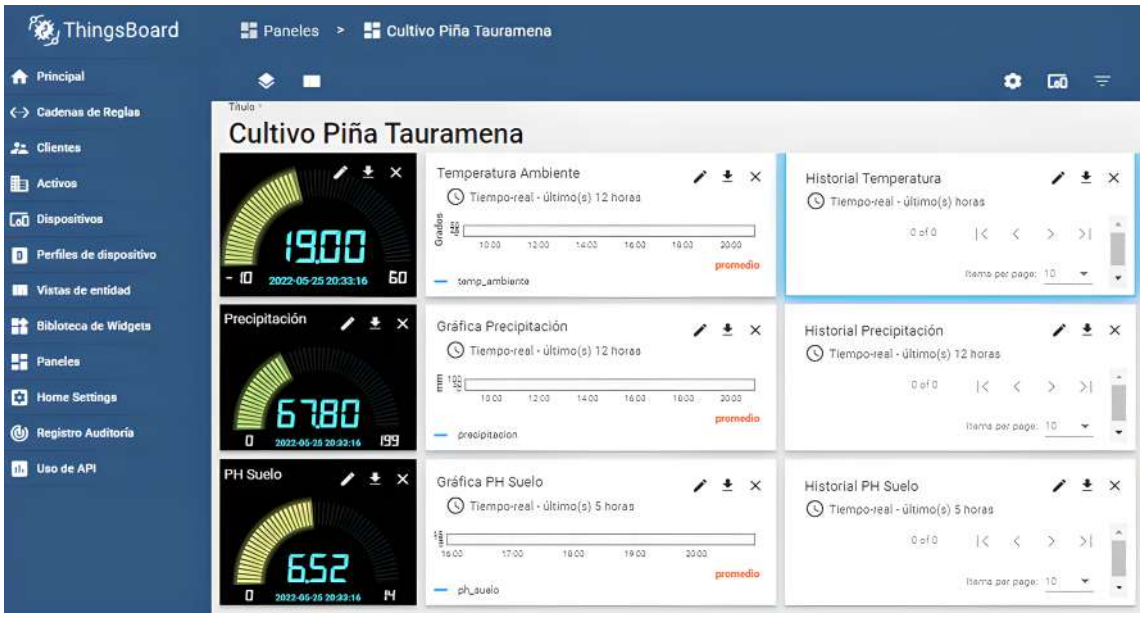

Figure 5.8: Main screen of the developed APP, the weather module is shown. Source: own image taken from the web application developed for this doctoral thesis.

moisture, relative humidity and temperature of both air and soil, with the capacity to transmit this data in real time through the Internet. This sensor is in the process of registration under national invention patent, with file number NC2022/0014133 before the Superintendence of Industry and Commerce. This development has been possible thanks to the support of the Ministry of Science and Technology MINCIENCIAS in the call 'Crearlo no es suficiente' of the year 2022, where it was recognized with the maximum score of 100 out of 100 possible, reflecting the innovation and potential impact of the technology. Part of the problem and solution is presented below. The theoretical underpinnings are described in more detail in Appendix C of this document.

Water plays a fundamental role in soil biophysical processes, acting as a limiting factor for plant growth. Therefore, precise control of soil moisture is crucial in agriculture. In this context, soil water content measurements are essential for irrigation management, both in agriculture and environmental sciences. Measurement-based irrigation allows for optimizing the use of water, a vital resource, and reducing negative environmental impact. However, measuring soil moisture is a complex task due to the influence of various soil biophysical factors, environmental and sensor characteristics.

Among the existing techniques to measure crop moisture, resistive moisture sensors have gained great popularity in agriculture due to their low cost, ease of use and fast response. These sensors work by measuring the electrical resistance of a conductive

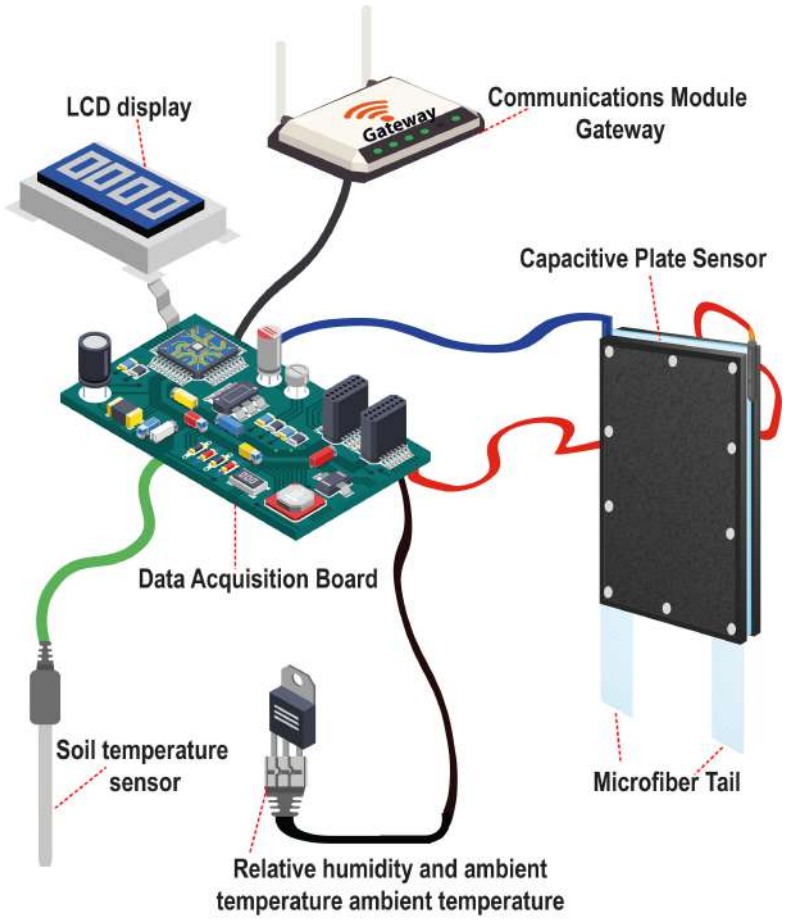

Figure 5.9: General diagram including each of the components of the developed parallel plate sensor. Source: Own image of parallel plate sensor architecture.

material, such as a polymer or salt, which is affected by the amount of water present in the soil. However, resistive moisture sensors have limitations in accuracy, as they require precise calibration. In addition, they are sensitive to soil temperature and salinity, factors that vary considerably depending on the spatial characteristics of the soil. To address these limitations, dielectric moisture sensors have been developed, which offer a more efficient and convenient method to measure soil moisture content. Dielectric sensors reduce the influence of salinity, texture, and other soil factors on the measurement by sensing at high frequency. However, their high manufacturing cost increases the price of the measurement circuit, making them difficult to deploy on a large scale in agricultural production. Figure. 5.9. shows the general architecture of the developed sensor.

In response to the limitations of conventional moisture sensors, an innovative circuit has been designed to improve the accuracy and application range of low-frequency ca-

pacitance sensors. This circuit is characterized by its high sensitivity, achieved through the use of medium-dimension parallel plates that enlarge the area of the capacitor, optimizing the relationship between capacitance and soil moisture. To compensate for temperature variations that affect moisture measurement, the circuit incorporates a commercial temperature sensor that monitors soil temperature. In addition, sensors are included to measure ambient temperature and relative humidity, allowing a more accurate assessment of the soil environment.

General operation of the circuit:

- **Capacitance Measurement:** The circuit measures the capacitance of the capacitor formed by the parallel plates. This capacitance is directly related to the amount of water present in the soil.
- **Temperature Compensatio**n: The commercial temperature sensor provides soil temperature data, which is fed into a formula to adjust the capacitance measurement and compensate for temperature effects.
- **Ambient Temperature and Relative Humidity Incorporation:** Ambient temperature and relative humidity measurements are also integrated into the adjustment formula, providing a more complete understanding of the soil environment and further improving the accuracy of the humidity measurement.

Circuit Enhancement Features:

- **Increased Accuracy:** Temperature compensation and the incorporation of environmental data significantly increase the accuracy of soil moisture measurements.
- **Wide Application Range:** The circuit operates effectively over a wide range of soil and temperature conditions due to its adaptability.
- **Low Cost:** The circuit design uses inexpensive and readily available components, making it a viable solution for large-scale agricultural applications.

As shown in Figure. 5.9, the parallel plate soil moisture sensor has a rectangular shape of 20 cm on each side. The distance between the plates is 4 mm, and the thickness of the plates is 2 mm. A cotton cloth is used as a dielectric material to absorb water from the soil. Unlike microfiber, cotton distributes water naturally throughout the material, which facilitates the detection of moisture in the soil.

To ensure that the sensor absorbs some of the soil water, two 8 cm tails were left in the dielectric material. This increases the ability to detect soil moisture and facilitates a more uniform distribution of water throughout the material, thus improving the detection of changes in capacitance. The parallel plates are equipped with two fully insulated metal connectors, allowing connections to be made to the sensor without moisture affecting its operation.

5.3.1 Calculation of the relative permittivity of the dielectric material used between the parallel plates

As dielectric material used between the parallel plates, a 100% cotton fabric material was used. Textiles have a low dielectric constant, therefore, when water is applied to it, this constant varies. Next, the dielectric constant of the material used is calculated, it should be noted that this constant is a reference for the material in dry state, since by adding water this constant changes, for this reason it will be found with the data obtained with the sensor in 0% water. The capacitance of a capacitor of parallel flat plates of area **A** and separation d is given by the following expression:

$$C = \frac{\varepsilon_0 A}{d} = \frac{\boldsymbol{K}_{\text{ref}} A}{d} \tag{5.2}$$

where,

- ε_0 = vacuum permittivity = 8.854×10^{-12} F/m
- $\boldsymbol{K}_{\text{ref}}$ = reference relative permittivity of the dielectric material used.
- d = Distance of separation of the parallel plates 4 mm = $0,4$ cm = $0,004$ m
- A = Area of the parallel plates of the capacitor = L $*$ L
- L = 20 cm = $0,2$ m
- $A = 0,2 \text{ m} * 0,2 \text{ m} = 0,04 \text{ m}^2$; The area of the capacitor will be constant

5.3.2 Data obtained from capacitive humidity sensor tests to find the permittivity of the dielectric material

To obtain these results, several tests were carried out by measuring the amount of water added to a 50 square centimeter area of dry soil. The soil was pre-dried in an oven and then the parallel plate capacitive sensor was placed to measure capacitance, capacitor frequency, soil temperature, relative humidity and air temperature. Subsequently, 10 cm^3 of water was added on top of the soil where the sensor was placed, and the same data

was recorded again. This procedure was repeated several times, incrementally adding 10 to 20 cm^3 of water, until the information detailed in the Table was obtained. Table. 5.2 shows the averaged data used to calculate the material permittivity reference constant $\boldsymbol{K}_{\text{ref}}$. Based on the data obtained experimentally, the reference dielectric constant of the material used is calculated. Since this dielectric constant is changeable, a reference constant $\boldsymbol{K}_{\text{ref}}$ is calculated for the data obtained when the material is completely dry.

$$C = \frac{\boldsymbol{K}_{\text{ref}} \varepsilon_0 A}{d} \tag{5.3}$$

$$C = 0.405\,\text{nF} = 0.000000000405\,\text{F} \tag{5.4}$$

$$k = \frac{C \cdot d}{\varepsilon_0 A} \tag{5.5}$$

$$\boldsymbol{K}_{\text{ref}} = \frac{0.0000000000405\,\text{F} \cdot 0.004\,\text{m}}{8.854 \times 10^{-12} \frac{\text{F}}{\text{m}} \cdot 0.04\,\text{m}^2} = 4.57 \tag{5.6}$$

$$\boldsymbol{K}_{\text{ref}} = 4.57 \tag{5.7}$$

$$\varepsilon = \boldsymbol{K}_{\text{ref}} \varepsilon_0 \quad ; \quad \varepsilon = 4.046 \times 10^{-11} \tag{5.8}$$

The relative permittivity of the dielectric material used between the plates is 4.57

Table 5.2: Data obtained from capacitive humidity sensor tests to find the permittivity of the dielectric material.

Capacitance (nF)	Frequency (Hz)	Soil temp (C)	Relative H (%)	Air temp (C)	Water (mm3)	Dielectric state
0.405	0.000.430	22	48	26	0	Dry
0.667	0.000.424	22	48	26.7	10	
0.78	0.000.414	22	50	27	20	
0.992	0.000.400	21	52	26	30	
1.076	0.000.388	21	53	23	40	
1.38	0.000.376	20	55	22	50	
1.48	0.000.363	20	57	22	60	
1.62	0.000.351	20	61	21	70	
1.72	0.000.349	20	65	20	80	
1.854	0.000.334	20	66	20	90	
1.97	0.000.329	20	71	20	100	High_ h

Figure. 5.10 shows the sensor built along with the tests performed.

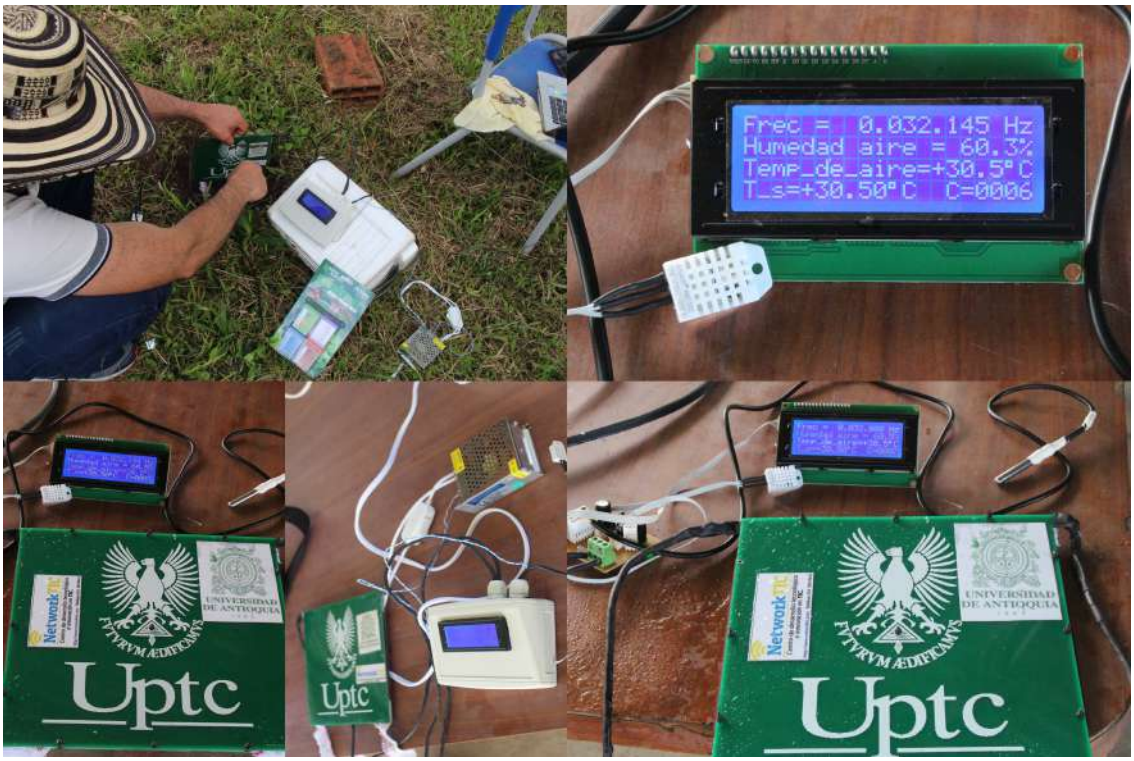

Figure 5.10: Images of the sensor and data log for the calculation of the permittivity of the capacitor dielectric material. Source: Own image of the tests performed on the parallel plate sensor.

5.3.3 Comparison tests of the parallel plate sensor with commercial sensors

Comparative tests were conducted with two commercial sensors:

- **Fivota brand sensor:** Comparative tests with the FIVOTA brand analog soil moisture sensor revealed that the capacitive parallel plate sensor offers higher resolution, since it delivers moisture values from 0 to 100%, while the commercial sensor provides three levels of analog moisture measurement: DRY, WET and MAXIMUM.

- **MIOGREN brand sensor:** Comparative tests were carried out with the MIOGREN digital soil moisture sensor. Unlike the analog sensor of the FIVOTA brand, the MIOGREN sensor provides the values digitally, maintaining the same measurement scales: DRY, WET and MAXIMUM. The results showed that the capacitive sensor in parallel plate offers higher resolution, with a measurement range from 0

to 100% humidity. This is because, when the dielectric material between the parallel plates is saturated with water, the capacitance varies rapidly, reaching response times on the order of milliseconds. The Figure 5.11 shows the three evaluated sensors: the two commercial sensors in conjunction with the capacitive sensor on the parallel plate.

Figure 5.11: Comparative tests with commercial sensors Fivota and MIOGREN. Source: Own image of the tests performed on the parallel plate sensor.

5.4 Foliar samples for laboratory analysis

Plant tissue analysis is a useful diagnostic tool for determining the nutritional status of a plant. It has the advantage of measuring the total content of nutrients and not just the fraction called available, allowing the diagnosis of deficiency or toxicity (Mello Prado, 2021). For sample collection, six plants were selected from the center of each experimental unit, and of these, 3 "D leaves" were randomly chosen (Suparna Sinha, 2021). The "D leaves" are the youngest among the adult leaves and physiologically the most active. The selected leaves were cut on the same day the images were taken and sent to the laboratory; this procedure was repeated in the 25 sample spaces during the four dates sampled. The laboratory performed the (NT)analysis of the 100 samples

processed during the six months of the experiment, using the Kjeldhal method (Sáez-Plaza et al., 2013), the extraction was carried out by digestion H_2SO_4 and the redox volumetry technique.

5.5 Measurement of plant chlorophyll content

To measure plant chlorophyll, the *SPAD-502* Plus chlorophyll meter was used (SPAD-502Plus, 2021). The samples were taken on the same "D leaves" before being cut to be sent to the laboratory, under the same lighting conditions in which the multispectral images were obtained. Figure 5.12 describes this procedure to record the values of *SPAD* .

Figure 5.12: Procedure for measuring chlorophyll content using the *SPAD-502* Plus instrument. Source: Own image of the development of the experimental design.

5.6 Data processing and analysis

5.6.1 Leaf nitrogen evaluation

In this research, the total nitrogen (TN) content was considered as the response variable, with a sample size of 100 observations ($n = 100$), corresponding to the results obtained on four sampling dates. These measurements were carried out at 25 sampling

points with the objective of capturing the variability in (TN) content throughout the experiment. The sampling dates were as follows: date 1 = 30 June 2022; date 2 = 26 July 2022; date 3 = 5 August 2022; and date 4 = 23 August 2022. It should be clarified that the main objective of the experimental design carried out in this research was not to measure the effect of treatments on crop biomass or yield, but rather as a source of variability to obtain different samples of the (TN) content of the leaf area for multispectral imaging. Statistical analysis revealed significant variability in content (TN), particularly on later sampling dates, as shown in Figure 5.13. This variability allowed multispectral images to be obtained with varying levels of TN, thus facilitating the development of machine learning models. To support the existence of significant differences between treatments and ensure consistency in the variability of TL at the four sampling dates, the p-values and confidence intervals were calculated. The results revealed p-values of 0.1476, 0.0685788, 0.0022363 and 0.00018 for dates 1, 2, 3, and 4, respectively. As can be seen in the last two dates, the values ($P < 0.05$) are significantly less than 0.05. This indicates that there is sufficient statistical evidence to reject the null hypothesis with a confidence level of 95%. Furthermore, it was observed that the confidence intervals progressively narrowed with each sampling date, indicating greater precision in estimating the treatment means as the amount of nitrogen accumulated in the plants increased.

The results of laboratory analyzes reveal a clear trend: the p-value decreases with each sampling date, suggesting an increase in the statistical significance of the differences between treatments over time. This pattern indicates a possible cumulative effect of treatments on the amount of (TN) in pineapple leaves. Figure 5.13 shows that on the first sampling date, the values (TN) in T1 and T2 were around 1.5 (TN), while the values in T3, T4, and T5 were close to 1.8 (TN). This initial variability could be explained by the short growth time of the crop and the varied location of the sampling points. From the second sampling date, variation in nitrogen levels was observed in the five treatments, with notable differences between T1 and T5. On the last two sampling dates (dates 4 and 5), a significant change is observed in treatment T1 compared to T4 and T5. Specifically, on date 4, T1 exhibited a (TN) of 1.11, while T4 and T5 showed (TN) of 2.34 and 2.31, respectively, as shown in Figure 5.13.

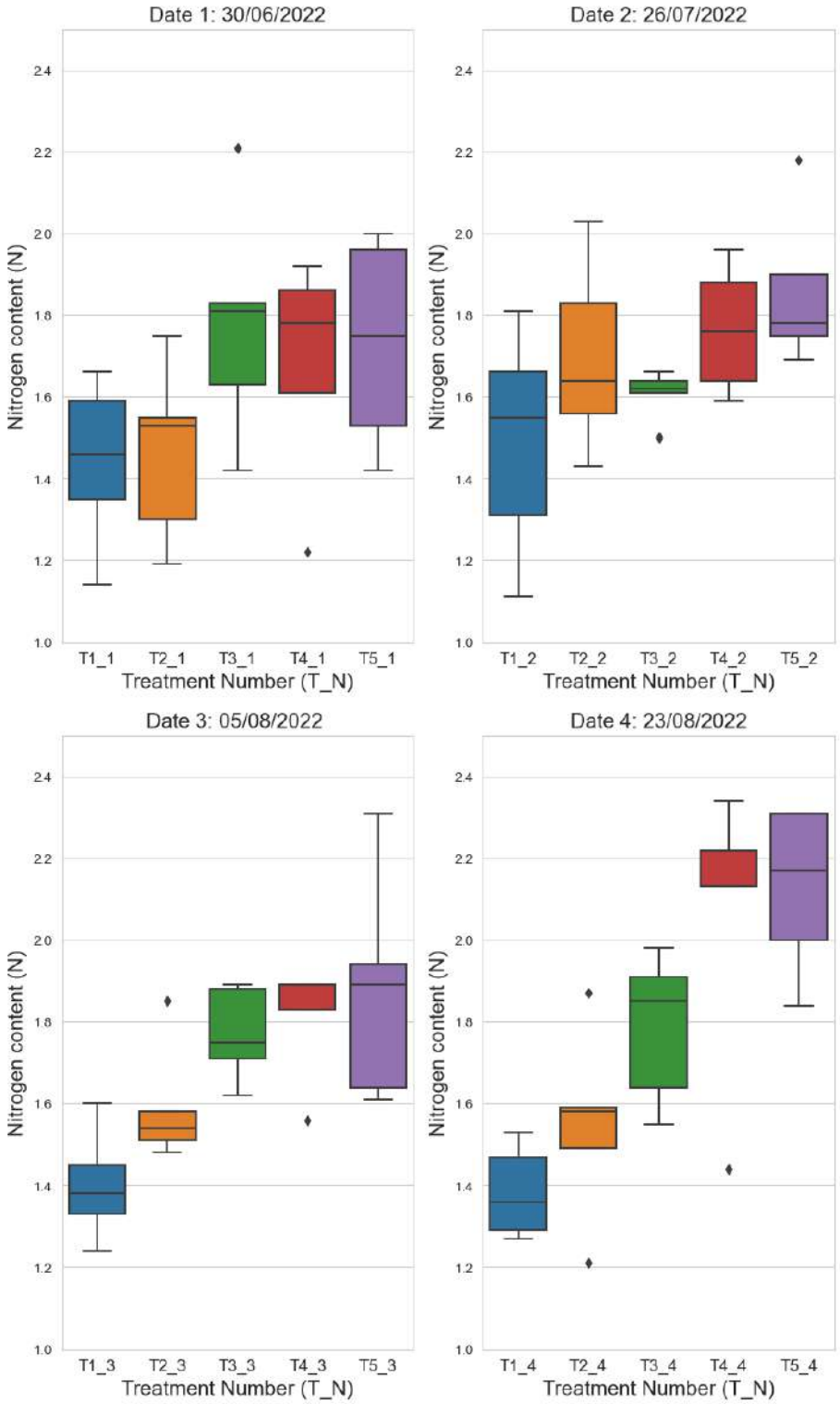

Figure 5.13: Laboratory results of foliar samples of (TN) as a function of the 5 treatments or fertilizer application rates. Each image represents a sampling date, and for each sampling date 25 records corresponding to 5 Blocks per 5 treatments are displayed.

On the first sampling date, values (TN) were observed in T1 and T2 close to 1.5 (TN) and T3, T4 and T5 values close to 1.8 (TN). From the second sampling date, nitrogen levels began to vary in the five treatments, with a difference observed between treatments T1 and T5. On the last two sampling dates corresponding to dates 3 and 4, a significant change (TN) in treatment T1 can be observed with respect to treatments T4 and T5. In the data obtained in the sampling carried out on the third and fourth dates, a significant difference was achieved between treatment T1 and treatments T4 and T5. On date 4, treatment T1 = 1.11 and treatment T4 = 2.34 and T5 = 2.31 as shown in Figure 5.13.

5.6.2 UAV data processing and ecological factors

Since the data in the spectral images are digital levels (ND) that do not represent biophysical variables directly, it was necessary to calculate the radiance and reflectance in each image. This process consisted of two stages: radiometric calibration and conversion of radiance to apparent reflectance (Cao et al., 2019; MicaSense, 2022).

- ***Radiometric calibration***

The purpose of this calibration is to transform the observation values (DN) of the images into absolute values of the spectral radiance $\left(\frac{W}{m^2}/\text{sr}/\text{nm}\right)$.

The formula compensates for sensor black level, sensitivity, gain and exposure settings, and lens vignetting effects (MicaSense, 2022). The implementation of this process was carried out with the help of Python and the use of Micasense libraries, the formula to calculate the spectral radiance L was performed from the pixel value p according to Equation 5.9:

$$L = V(x, y) \times \frac{a_1}{g} \times \frac{\rho - \rho_{BL}}{t_e + a_2 y - a_3 t_e y}, \tag{5.9}$$

where,

- L: the spectral radiance.
- $V(x, y)$: the polynomial vignetting function at pixel (x, y).
- a_1, a_2, a_3: the radiometric calibration coefficients.
- g: the sensor gain setting.

- ρ: the normalized DN value.
- ρ_{BL}: the black level shift.
- t: the exposure time of the image.

All these parameters required for the calculation of L are found in the calibration panel and in the image metadata.

- **Conversion of radiance to reflectance**

Before this process, it is necessary to calibrate the RAW images from the camera into reflectance maps. To do this, the normalized pixel value is calculated by dividing the raw digital pixel number by 2^n, where N is the number of bits in the image. Now that flat- and calibrated-radiance images are available, they are converted to reflectance. To do this, we used the radiance values from the known reflectance panel image to determine the scale factor between radiance and reflectance. In this case, the following values were used for each of the bands: blue: 0.67, green: 0.69, red: 0.68, red edge: 0.67 and red: 0.61 (MicaSense, 2022).

This process is shown in Figure 5.14 and is detailed below: initially, the five images are loaded along with their respective calibration panels. The software automatically detects the panel in each image and extracts the following information:

- Detected panel serial number: **RP02-1618086-SC**
- Extracted panel statistics:
  - Mean: **44,794.40**
  - Standard deviation: **796.99**
  - Panel pixel count: **14,524**
  - Saturated pixel count: **0**

The described information is obtained for each of the spectral bands. Figure 5.14, shows the reflectance panel corresponding to the blue band. For image calibration, it is necessary to compensate the panel values with the information obtained from the image. This process is crucial to detect the calibration panels of the MicaSense camera and extract data related to the Lambertian surface of the panel. A Lambertian surface reflects incident radiation uniformly in all directions and is considered an ideal reflector. Figure

5.15 illustrates the complete process, while Figure 5.16 presents the final histogram of the image, after applying the uniform radiation distribution procedure in all directions.

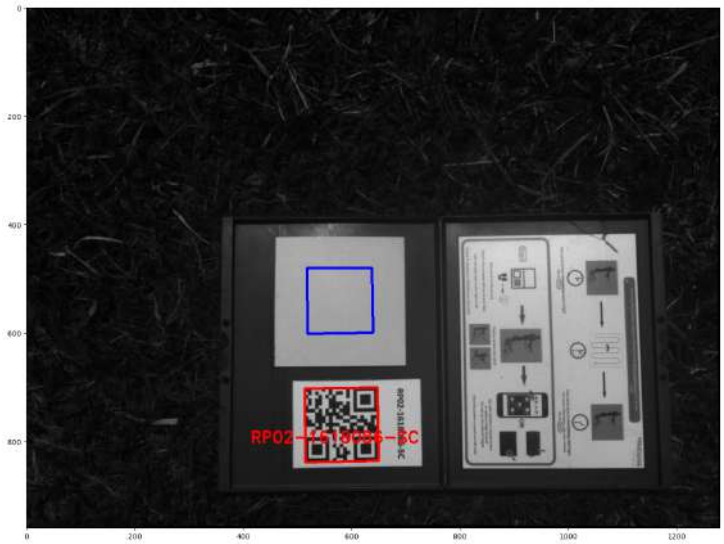

Figure 5.14: Capture of information from the image calibration panel.

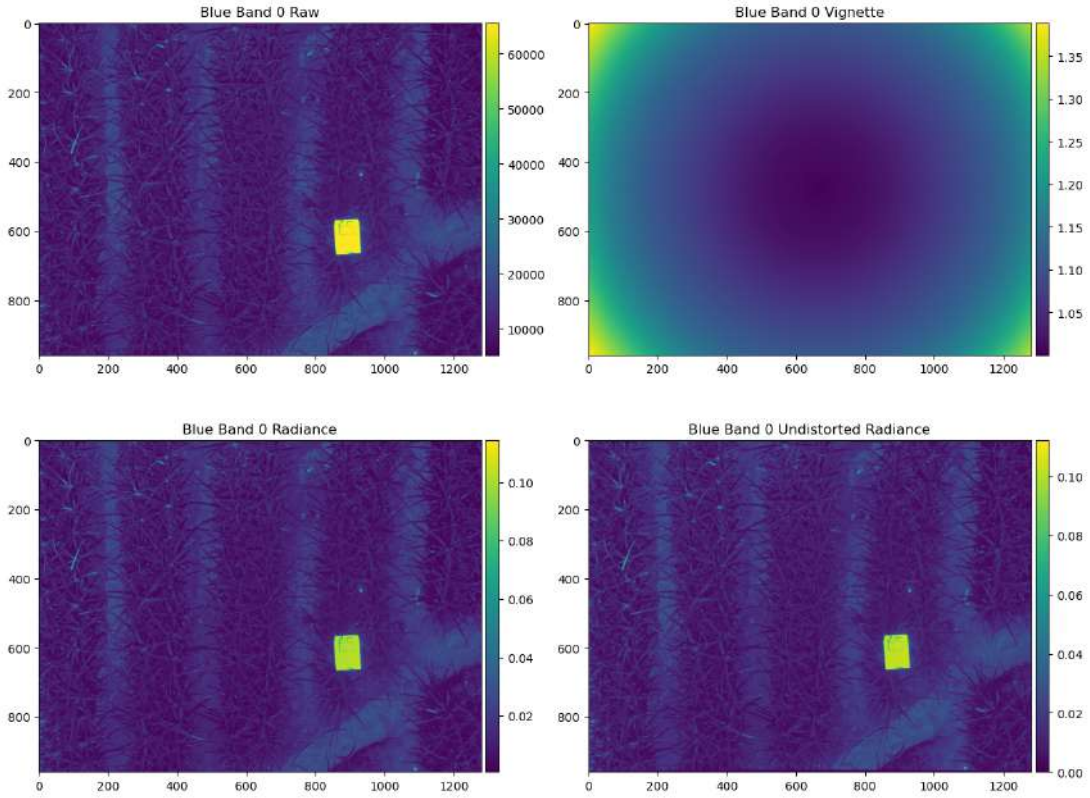

Figure 5.15: Capture of information from the image calibration panel.

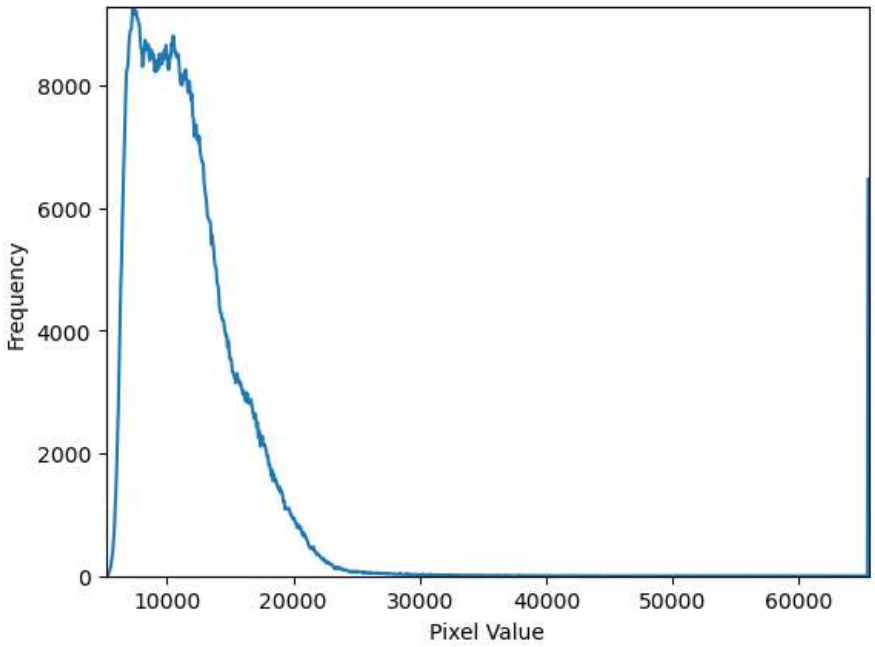

Figure 5.16: Capture of information from the image calibration panel.

- **Spectral band alignment**

After completing the conversion of the images to radiance and reflectance, it was essential to align the five spectral bands to allow algebraic operations between them, a crucial step in obtaining vegetation indices. The alignment of the images was performed using software built in Python and is an integral part of the workflow developed, based on the information provided by the MicaSense camera manufacturer. The applied methodology consists of three main steps. First, the unwinding of the images was performed using the built-in lens calibration, with the objective of correcting optical distortions. This radial calibration counteracts the curvature of the lens, ensuring that the spectral bands are not distorted. The second step consisted in the transformation between the bands, where each band is aligned with respect to a reference band; in this case, the green band (band 4). To achieve this alignment, a homographic transformation `(3×3 matrix)`, capable of handling rotation, translation, scaling and perspective changes, was applied. This transformation was calculated using the `cv2.MOTION_HOMOGRAPHY` mode in the alignment software. Finally, an image pyramid was implemented to optimize the alignment process. This method consists of reducing the resolution of the images to several levels, starting with the lowest resolution images, which allows for a quick initial solution. Subsequently, the results are refined to higher resolution until the alignment is

complete. In this case, three pyramid levels (`pyramid_levels = 3`) were used, to ensure the balance between precision and efficiency. Once aligned, the images were combined and cropped, removing pixels that did not match in all bands, thus ensuring an accurate and consistent overlay for use in further analysis. Figure 5.17, shows three spectral bands: Blue, Green and Red. Then, the composition of these three bands (R, G, B) is shown without applying an alignment process, which allows observing the misalignments between them. In Figure 5.18, the same three bands (R, G, B) are displayed after having undergone the alignment process, showing the correction of the initial discrepancies and achieving an accurate overlapping of the bands.

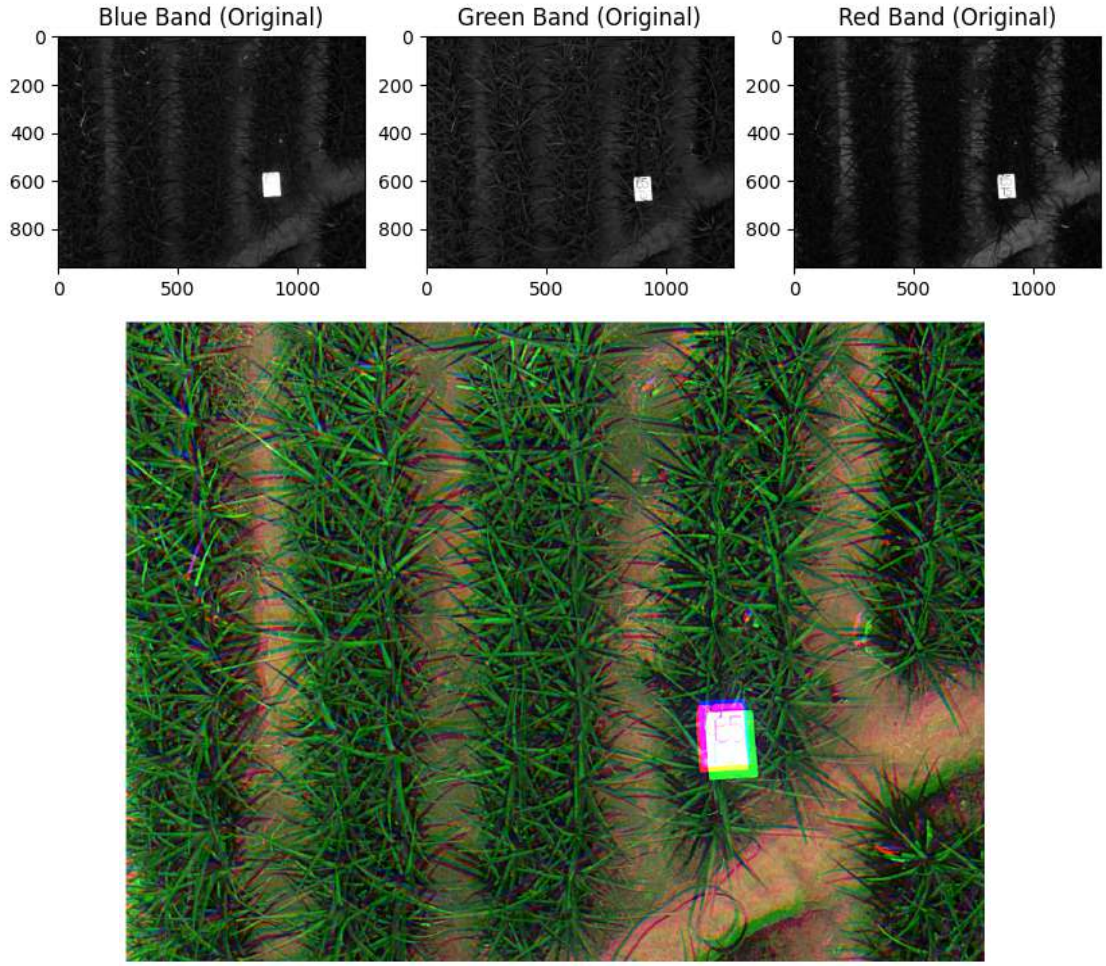

Figure 5.17: At the top are three multispectral images, the blue (B), green (G) and red (R) band. The following image shows the unaligned rgb combination

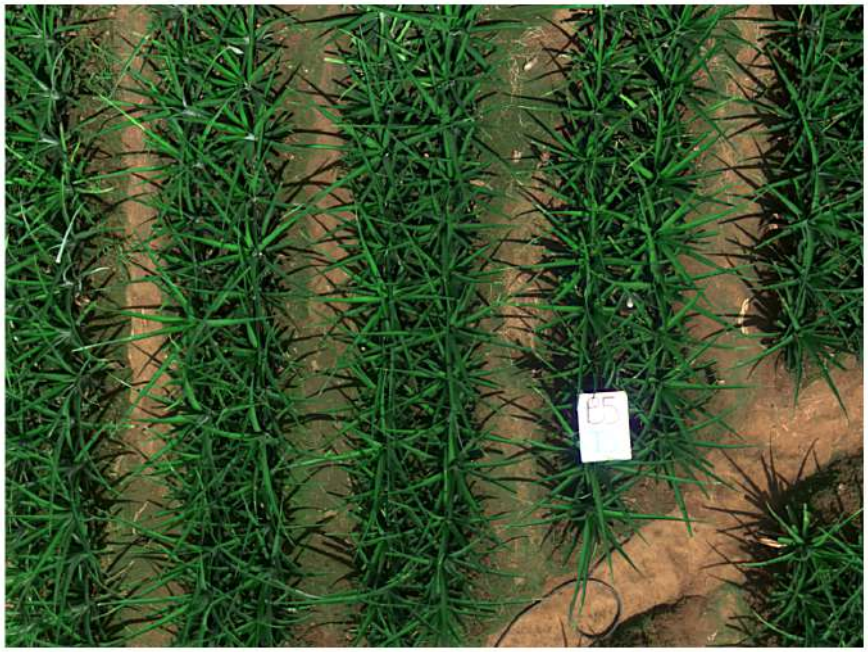

Figure 5.18: The image shows the composition of R,G,B bands after performing the alignment process according to the three steps mentioned above.

5.6.3 Vegetation indices used in this study

Vegetation indices (VI) have been widely used in agricultural research to estimate and monitor the nutritional status of crops, especially the nitrogen and chlorophyll content (Chungcharoen et al., 2022; Qiao et al., 2022; Verma et al., 2022). Chlorophyll strongly absorbs energy in the bands centered at 0.45 and 0.67 µm; this is why our eyes perceive healthy vegetation as green, due to the high absorption in blue and red by the leaves and reflection in green (Qiao et al., 2022). The nitrogen shortage in crops reduces chlorophyll, increasing reflectance in the red and giving leaves a yellowish hue. This is exploited by vegetation indices combining different spectral bands(Tsoulias et al., 2023; Verma et al., 2022).

In this study, 16 vegetation indices (VI) were selected as characteristic variables to estimate the nitrogen content of the canopy in pineapple crops. Table 5.3 describe the vegetation indices implemented with their respective formulas, including the most common indices related to the foliar nitrogen content (NDVI, NDRE, GNDVI, MACI, VARI, IPVI), as well as soil-regulated indices such as (EVI, SAVI, OSAVI, ARVI) and indices related to the chlorophyll content, such as (CVI, SCCCI, TCARI, MCARI, GCI, RECI). These vegetation indices have previously been used to find the nitrogen content

in cotton, corn, wheat, rice, and sugarcane crops (Chungcharoen et al., 2022; Mouazen et al., 2023; Shendryk et al., 2020).

Table 5.3: Vegetation indices used for the implementation of predictive models. The values of the spectral bands are assumed as follows, R=red, G=green, B=blue, RE=red edge, NIR=near infrared.

No	**Index Name**	**Equation**
1	Normalized difference vegetation index (NDVI)	(NIR- R) / (NIR+R)
2	Normalized Difference Red Edge Index (NDRE)	(NIR-RE) / (NIR+RE)
3	Green NDVI (GNDVI)	(NIR-G) / (NDVI+G)
4	Enhanced Vegetation Index (EVI)	2.5(NIR-R) / (NIR+6R-7.5B+1)
5	Modified Anthocyanin Content Index (MACI)	NIR / G
6	Optimized Soil Adjusted Vegetation Index (OSAVI)	(1+0.16)(NIR-R) / (NIR+R+0.16)
7	Simplified Canopy Chlorophyll Content Index (SCCCI)	NDRE / NDVI
8	Transformed Chlorophyll Absorption and Reflectance Index (TCARI)	3(RE-R-0.2(RE/G)(RE/R)) / OSAVI
9	Visible Atmospherically Resistant Index (VARI)	(G·R)(G+R-B)
10	Infrared Percentage Vegetation Index (IPVI)	NIR / (NIR+R)
11	Atmosphere Resistant Vegetation Index (ARVI)	(NIR - 2R + B) / (NIR + 2R +B)
12	Chlorophyll vegetation index (CVI)	(NIR/G)(R/G)
13	Atmosphere Resistant Vegetation Index (ARVI)	(NIR - 2R+B) / (NIR + 2R+B)
14	Green Chlorophyll Index (GCI)	(NIR / G) - 1
15	Red Edge Chlorophyll Index (RECI)	(NIR /RE) - 1
16	Modified Chlorophyll Absorption Ratio Index (MCARI)	((VNIR - R)-0.2(VNIR - G))(VNIR / R)

Removal of Background Noise

Background noise in the multispectral images was removed using an NDVI mask, excluding elements such as soil, water, and weeds. Non-plant pixels were removed by setting those with NIR reflectance less than 20% to zero. This ensured that ground noise did not affect the histograms of the 16 vegetation indices found in the study.

Statistics used in this study

After noise elimination, the ROI region of interest was selected. For this, the 10 pine cones were selected in each of the treatments (25 regions of interest on each of the four sampling dates). Figure 5.19 shows the image of the NDRE vegetation index based on the RGB image. This image is marked in red, which corresponds to the 10 pineapple clumps, and a label with the treatment number and block at the beginning of the region of interest is also observed.

After selecting the ROI region of interest, we proceeded to find five statistics: maximum, minimum, average, standard deviation, and variance.

Ecological Factors

The ecological factors were obtained from the sensors installed in the crop, as well as from the SPAD value meter and from the manual data records. These variables were part of the predictor variables used in the machine learning models. The ecological factors registered with the IoT platforms are described in Table 5.4.

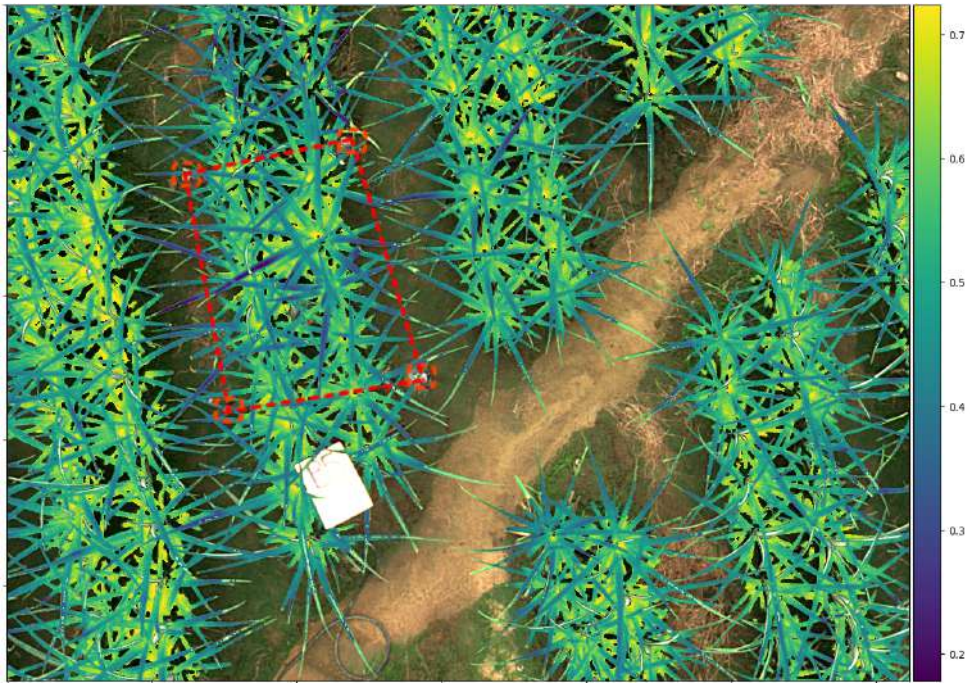

Figure 5.19: Vegetation index NDRE on RGB image.The image shows the region of interest, ROI, demarcated in red; the vegetation index statistics used in the predictive models are calculated on this region. Source: Own image of multispectral image processing results.

Table 5.4: Ecological factors recorded with IoT platforms, including environmental variables, soil variables and plant variables.

Ecological Factor	**Description**
pH	pH of each region of interest (ROI)
H soil (%)	Soil moisture of each ROI
T soil(°C)	Soil temperature of each ROI
T ambient (°C)	Ambient temperature of the location
Humidity (%)	Relative humidity of the location
Atm pressure (hPa)	Atmospheric pressure of the location
Wind speed (m/s)	Wind speed of the location
Gust of wind (m/s)	Wind gusts of the location
Wind direction	Wind direction of the location
Rain (mm)	Average rain at the site
Average SPAD	SPAD value of chlorophyll of ROI

Chapter 6

Predictive Models

This chapter is devoted to the detailed presentation of the predictive models implemented in this doctoral thesis, which constitute a central piece of the research. The theoretical foundations, the machine learning methodologies applied, and the data analysis techniques used to develop and validate each model are described. The models implemented range from advanced regression techniques to Artificial Neural Network algorithms, each selected and adapted to optimize the accuracy of nitrogen content estimation in pineapple crops.

6.1 Correlation analysis

Figure 6.1 shows the correlation matrices of the predictor variables of dates 1 and 4 corresponding to 30/06/2022 and 23/08/2022. On the graph of date 30/06/2022, the variables that had the highest correlation with it (TN) can be seen. Most of these correspond to statistical values of multispectral images, of which 14 variables obtained correlations greater than 60%. The average OSAVI obtained the highest correlation of around 76%, followed by the maximum OSAVI with 70%, as seen in Figure 6.1.

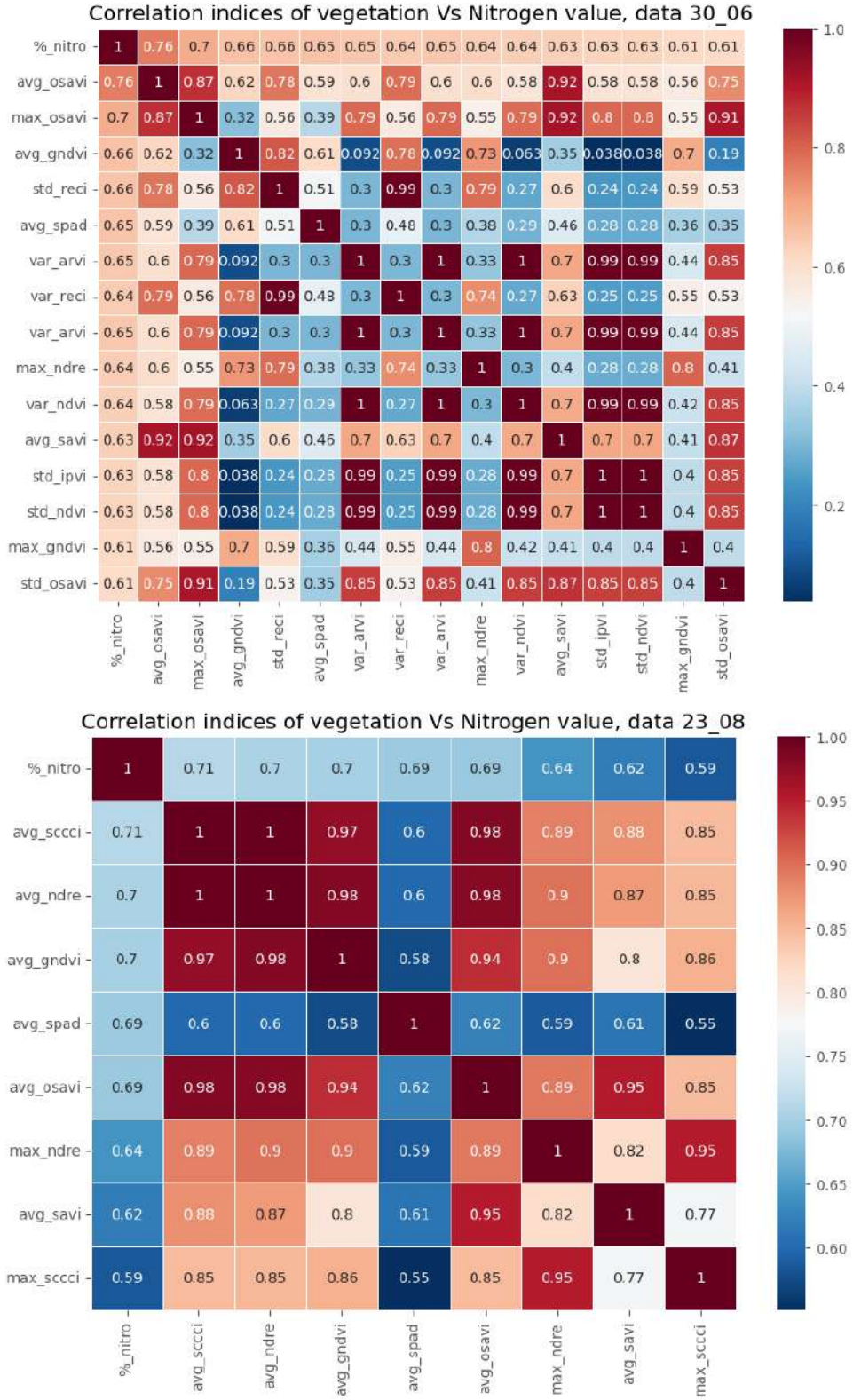

Figure 6.1: Correlation matrix of the predictor variables with respect to the nitrogen value, date one 30/06/2022, and data four 23/08/2022.

Sampling date 2 corresponding to 27/07/2022 presented the lowest correlation among the 4 dates sampled. The highest values on this date corresponded to the mean SPAD value of 64%, followed by soil moisture with 54%. For date 3 corresponding to 05/08/2022, the highest values were obtained for the mean SPAD with 68%, followed by soil moisture with 61%. On the last sampling date, corresponding to 23/08/2022, the highest values correlated with the percentage of (TN) correspond to the vegetation index statistics of the multispectral images, followed by the SPAD value observed in Figure 6.1. Mean SCCCI 71.2%, mean NDRE 70.44%, mean GNDVI 70.14%, and mean SPAD 69.34%.

6.2 Dimensionality reduction

The dataset used as predictor variables to estimate the amount of nitrogen corresponds to 80 multispectral predictors resulting from the statistical values of the 16 vegetation indices plus 4 ecological factors including SPAD values for a total of p=84 predictors and n=50 observations. Since p>n, this creates a high-dimensional regression environment (Shendryk et al., 2020). To eliminate the high dimensionality, a principal component analysis (PCA) was used. Using PCA, predictors were reduced to a few variables, which, in turn, allowed reducing multicollinearity. In Figure 6.2, it can be seen that for date 1 corresponding to 30/06/2022, the first five principal components explain about 60% of the variables. By using only the first five principal components as predictors, a notable reduction in the dimensionality of the data was achieved, while capturing most of the variability present. It is important to note that estimating foliar nitrogen content in tropical pineapple crops, where the four seasons interact, using images, sensors, and SPAD values, presents a challenge due to the high variability of the data caused by the interaction of multiple ecological and environmental factors. In this context, reaching a level of explained variance of approximately 60% can be considered significant and useful to understand the relationships between variables and nutrient concentration in pineapple leaves. However, it is essential to emphasize that the percentage of variance explained alone does not provide a complete assessment of the quality of the models. Other aspects, such as the validity of the assumptions of the models, the robustness of the predictions, and the replicability of the results, must be considered to determine the purposes of this study. On the other hand, when analyzing the five most weighted variables in the first principal component of the data, in order, were the OSAVI vegetation index, GNDVI, RECI, SPAD values and the ARVI index. This information is also very relevant, as it provides insight into the most effective vegetation indices for estimating

nitrogen in pineapple leaves.

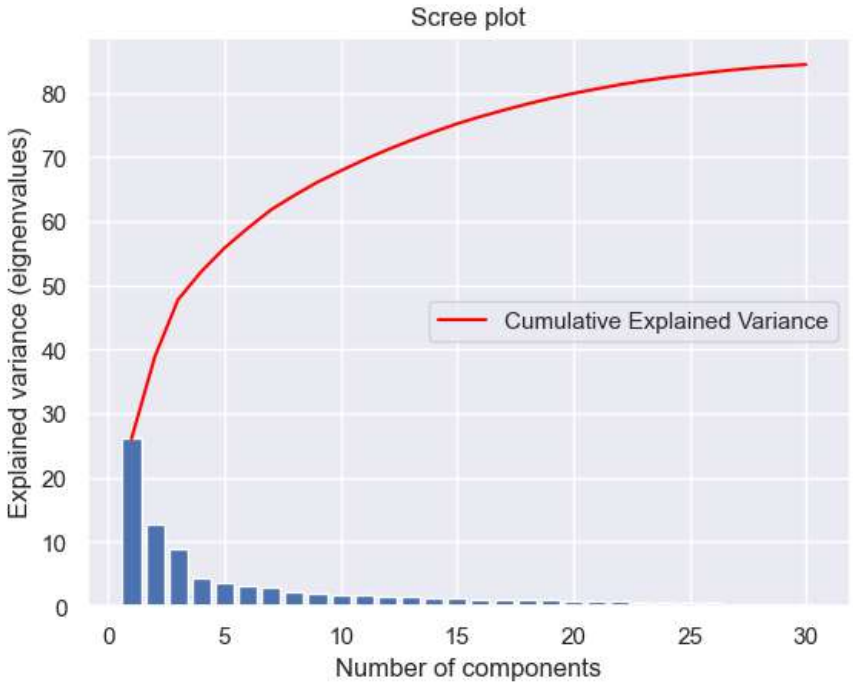

Figure 6.2: Explanation of variance according to the number of principal components date 30/06/2022.

6.3 Model construction and evaluation

Nine regression models were used to predict nitrogen levels in the pineapple crop from the information of the five principal components. The algorithms used included the following: Linear Regression, Support Vector Machines (SVM), Decision Tree Regressor, Random Forests Regressor, XGB Regressor, AdaBoost Regressor, Lasso Regressor, Ridge Regressor, and MLP Regressor. To assess the effectiveness of these models, two performance metrics were used: the determination coefficient R^2 and the root mean squared error (RMSE). The coefficient R^2 reflects the amount of variation in the response variable explained by the independent variables X in the linear regression model. A higher value of R^2 indicates a better explanation of the variability by the linear regression model. However, RMSE can be considered as the standard deviation of unexplained variance and is expressed in the same units as the response variable. Lower RMSE values

indicate a better fit to the model.

$$R^2 = 1 - \frac{SS_{RES}}{SS_{TOT}} = 1 - \frac{\sum_i (y_i - \hat{y}_i)^2}{\sum_i (y_i - \bar{y})^2} \tag{6.1}$$

where:

SS_{RES} is the sum of squared residuals (i.e., the sum of squared errors)

SS_{TOT} is the total sum of squares (i.e., the sum of squared deviations from the mean)

$$RMSE = \sqrt{\frac{1}{n}\sum_{i=1}^{n} (y_i - \hat{y}_i)^2} \tag{6.2}$$

Where: y_i = present value or current value, $\hat{y}_i$ = predicted value, n = sample size.

6.3.1 Models that obtained the highest metrics

XGBRegressor is a supervised learning algorithm that belongs to the family of gradient boosting techniques. It is a part of the **XGBoost (Extreme Gradient Boosting)** framework, which is known for its efficiency, speed, and performance in predictive modeling tasks, particularly in regression and classification problems (Ennaji et al., 2023).

XGBRegressor works by combining the predictions of several weak learners, typically decision trees, in an iterative manner. In each iteration, the algorithm trains a new decision tree that attempts to correct the errors made by the previous trees. This process is called *boosting*. The key idea is that by adding multiple weak learners, the final model can minimize the residuals (errors) of the previous predictions and improve accuracy.

The main advantages of XGBRegressor include:

- **Regularization**: XGBRegressor includes L_1 (Lasso) and L_2 (Ridge) regularization terms, which help in reducing overfitting by penalizing complex models.
- **Handling missing data**: The algorithm can automatically handle missing data by learning the best direction to follow in the decision trees when encountering missing values.
- **Parallel computation**: XGBRegressor supports parallel processing, allowing faster computation, especially when dealing with large datasets.

- **Gradient boosting**: It minimizes the loss function by iteratively fitting decision trees to correct the errors of previous models, resulting in a powerful ensemble model.
- **GPU support**: XGBoost has built-in support for using GPUs to speed up training, which is especially beneficial for large datasets.

Overall, XGBRegressor is widely used due to its scalability, flexibility, and ability to deliver superior performance in both small and large datasets. It is commonly applied in fields such as finance, healthcare, and marketing, where predictive modeling is essential.

XGBoost and Learning/Validation curves

The XGBRegressor learning curve shows a model that fits the training data well and improves its generalization ability as more training samples are provided. The curves tend to converge, indicating a good balance between bias and variance. The model benefits from adding more data, but after a certain point, the marginal gain decreases, suggesting that the model is reaching its limit in terms of learning. In Figure 6.3 shows the XGBRegressor Learning Curve.

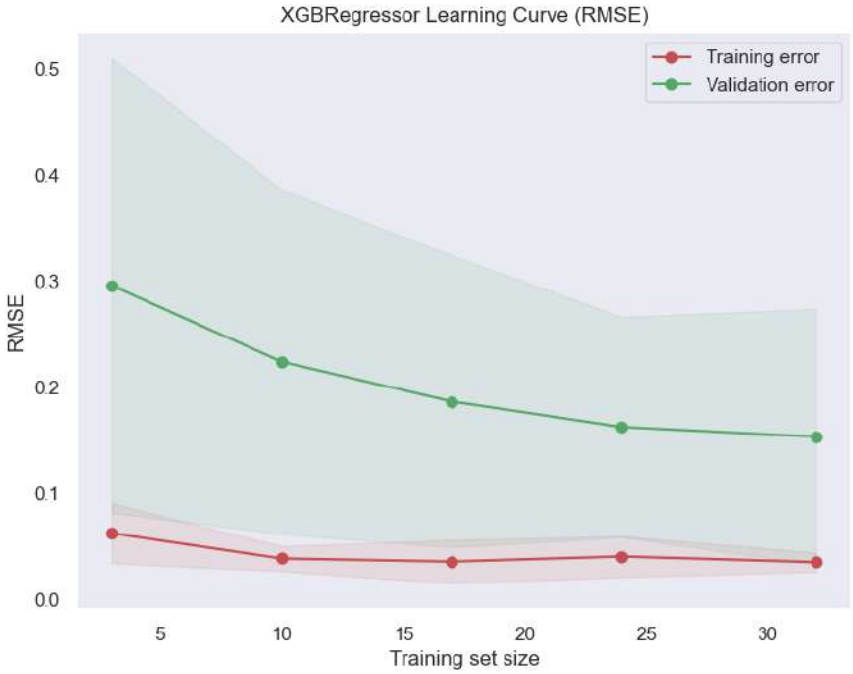

Figure 6.3: XGBRegressor Learning Curve

Hardware and model training parameters

The following is a list of the details of the hardware used to train the models.

The **XGBRegressor** model was trained using the following hardware:

- **Processor**: Intel(R) Xeon(R) w5-3433 1.99 GHz
- **RAM**: 64.0 GB
- **Operating System**: Windows 10 and 11 Professional
- **GPU**: NVIDIA RTX A4500
- **Programming Language**: Python 3
- **Graphical User Interface (GUI) used**: Anaconda Navigator

The training time for the **XGBRegressor** model was **0.1447 seconds**.

6.3.2 MLPRegressor Model (Multilayer Perceptron - MLP)

The **MLPRegressor** is a multilayer perceptron (MLP) model designed for regression tasks. MLPRegressor trains iteratively since at each time step the partial derivatives of the loss function with respect to the model parameters are computed to update the parameters. It can also have a regularization term added to the loss function that shrinks model parameters to prevent overfitting. In the provided code, the following configuration is used:

- **Hidden layers**: A single hidden layer with 100 neurons is used.

```
hidden_layer_sizes=(100)
```

- **Activation function**: The selected activation function is `identity`, which is a linear activation function $f(x) = x$. This option is unusual for neural networks as it does not introduce non-linearity. However, it can be useful in certain regression problems.

```
activation='identity'
```

- **Optimization algorithm**: The optimizer used is `Adam`, which is a stochastic gradient-based optimization algorithm. Adam is popular due to its efficiency on large datasets and high-dimensional problems.

  ```
  solver='adam'
  ```

- **Regularization parameter** α: This parameter controls the L_2 penalty to reduce overfitting. In this case, it is set to $\alpha = 10^{-4}$.

  ```
  alpha=1e-4
  ```

- **Maximum iterations**: Up to 10,000 iterations are allowed to ensure that the algorithm has enough time to converge.

  ```
  max_iter=10000
  ```

- **Stopping criterion**: Training stops if the improvement in error is less than 1×10^{-4} over two consecutive iterations.

  ```
  tol=1e-4
  ```

MLPRegressor and Learning/Validation curves

The MLPRegressor learning curve shows a constant low training error, indicating low bias. The validation error decreases with more data, suggesting that the model benefits from a larger training set and generalizes well. The small shaded area reflects low variability, which means that the model is stable and consistent. In this sense, MLPRegressor balances fit and generalization well, showing low bias and controlled variance. In Figure 6.4 shows the MLPRegressor Learning Curve.

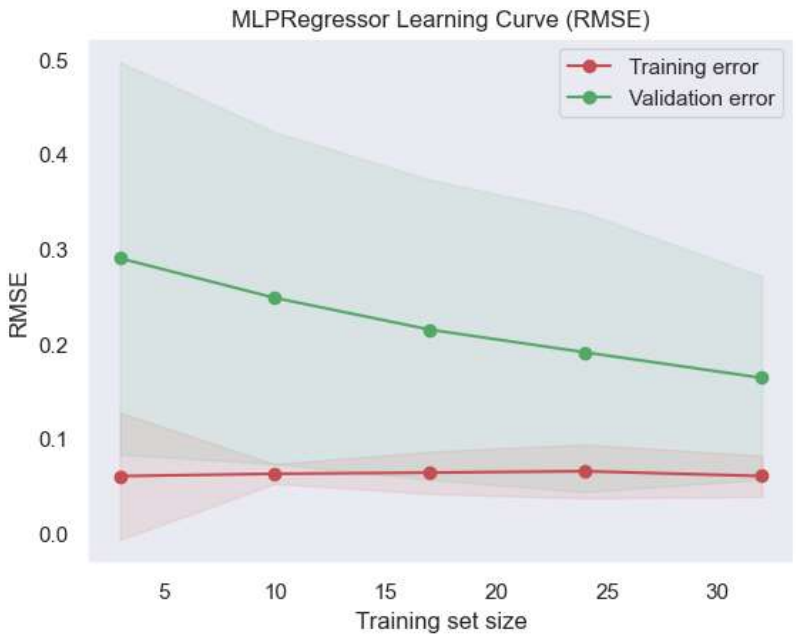

Figure 6.4: XGBRegressor Learning Curve

The hardware used for training is the same as that used for XGBRegressor and training time for the **MLPRegressor** model was **1.515 seconds**.

6.3.3 Foliar Nitrogen Prediction

Due to changes in leaf physicochemical composition, biomass, height, diameter and noise caused by factors such as weeds and water during the vegetative stage of the crop, it was necessary to implement predictive models for each of the four observation dates. The five main components were used as predictor variables and (TN) was used as the variable to be predicted. The approach used to train and validate the regression models involved dividing the data into 80% for training and 20% for validation. To ensure randomization of the data, the `random_state` parameter of scikit-learn's `train_test_split` function was used. In addition, both training and validation were performed using cross-validation to compare performance, and the results obtained both ways were very similar. This approach ensures a robust and reliable evaluation of the performance of the models, which is crucial for their application in real situations.

On the first sampling date, the XGB Regresor algorithm achieved a R^2 of 86.98%, which was the highest metric among the four observation dates, as detailed in Table 6.1. It should be noted that the nine regression models implemented obtained the R^2 metrics

above 78% in this initial sampling phase. On date 2, corresponding to 26/07/2022, the lowest performance metrics were obtained among the four sampled dates. In the date 2 column of Table 6.1, it can be observed that the MLP Regressor algorithm achieved the highest R^2 with 59.11%. On this second date, five algorithms obtained R^2 metrics above 50%, but no model reached R^2 higher than 60%.

On date three, corresponding to 05/08/2022, the algorithm that showed the best performance was the XGB regressor, which obtained an R^2 of 68%. Finally, in the last column of Table 6.1, corresponding to the date 23/08/2022; it can be observed that the algorithm with the highest R^2 was the MLP Regressor with a R^2 of 70%. Likewise, eight of the nine implemented models reached R^2 higher than 65

Table 6.1: Results of the R^2 and RMSE performance metrics of the nine models implemented in the four sampling dates performed.

No	**Models**	**Date 1**		**Date 2**		**Date 3**		**Date 4**	
		R^2	RMSE	R^2	RMSE	R^2	RMSE	R^2	RMSE
1	LinearRegression	0,8109	0,1222	0,5829	0,1378	0,4136	0,2123	0,6936	0,1831
2	DecisionTreeRegressor	0,8562	0,1066	0,2509	0,2386	0,6036	0,1746	0,1936	0,2970
3	RandomForestRegressor	0,8286	0,1164	0,3695	0,1694	0,6149	0,1721	0,6706	0,1898
4	SVR_linear	0,7856	0,1302	0,5565	0,1421	0,3684	0,2204	0,6719	0,1894
5	**XGBRegressor**	**0,8699**	**0,1014**	0,2113	0,2348	**0,6801**	**0,1568**	0,4511	0,2450
6	AdaBoostRegressor	0,8428	0,1115	0,3977	0,1656	0,5331	0,1895	0,6471	0,1965
7	LassoRegressor	0,8109	0,1223	0,5828	0,1378	0,4135	0,2123	0,6936	0,1831
8	RidgeRegressor	0,7981	0,1263	0,5538	0,1425	0,3842	0,2176	0,6643	0,1916
9	**MLPRegressor**	0,8036	0,1246	**0,5911**	**0,1364**	0,4113	0,2127	**0,6992**	**0,1829**

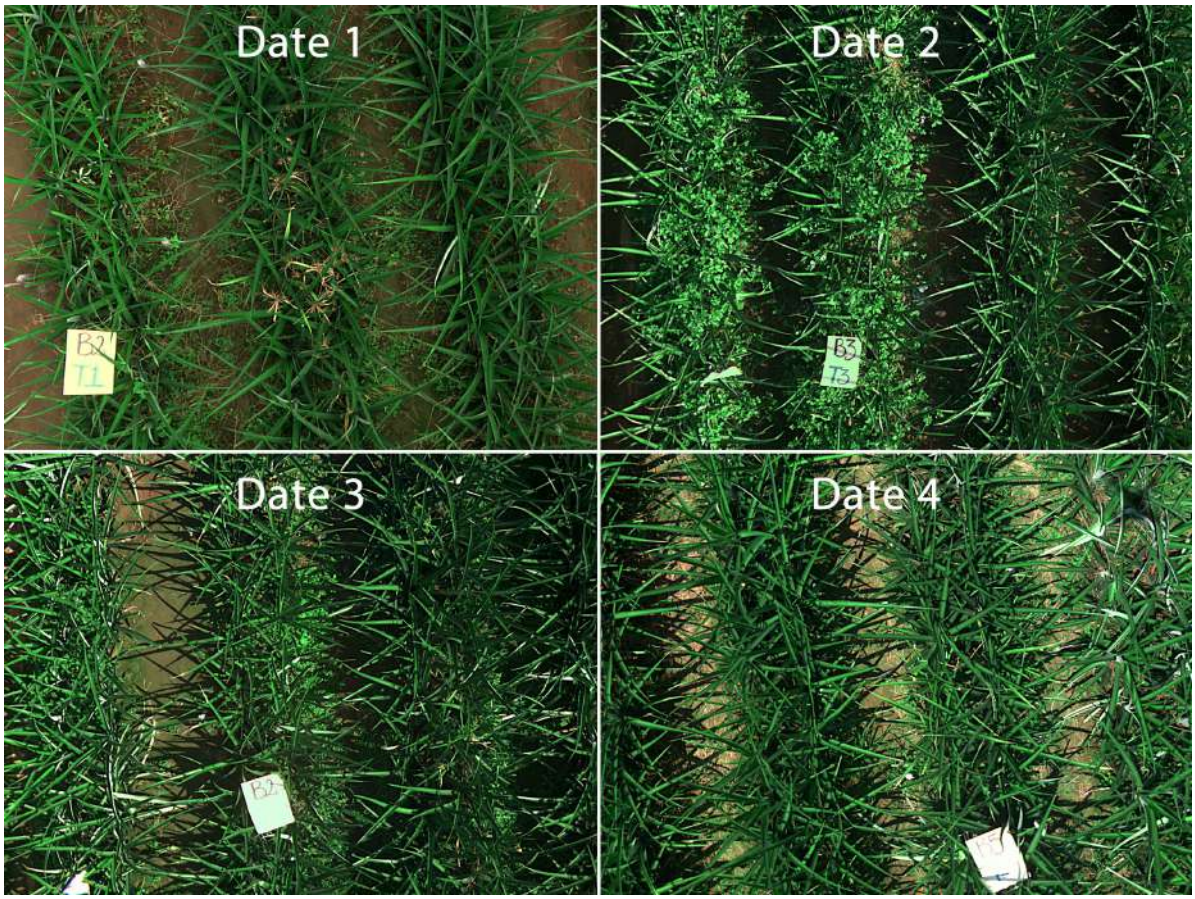

Figure 6.5: Images of the sample spaces of the four sampling dates. Date 1 corresponds to images from 30/06/2022; date 2 on 26/07/2022; date 3 on 05/08/2022 and date 4 on 23/08/2022. Source: Own image of multispectral image processing results.

In Figure 6.6, the algorithms that obtained the highest R^2 on each of the four sampling dates are shown. These graphs present the current values of (%N) along with the values predicted by the algorithms. In the upper left corner, the XGB Regressor algorithm, which obtained the highest R^2 on the first sampling date, is detailed. In the upper right corner, the MLP Regressor algorithm, which obtained the highest R^2 on the second date, is shown. In the lower left corner, we observe the XGB Regressor algorithm, which obtained the highest metric on the third date, and in the lower right corner, we observe the plot of the last sampling date with the MLP Regressor algorithm that obtained the highest R^2.

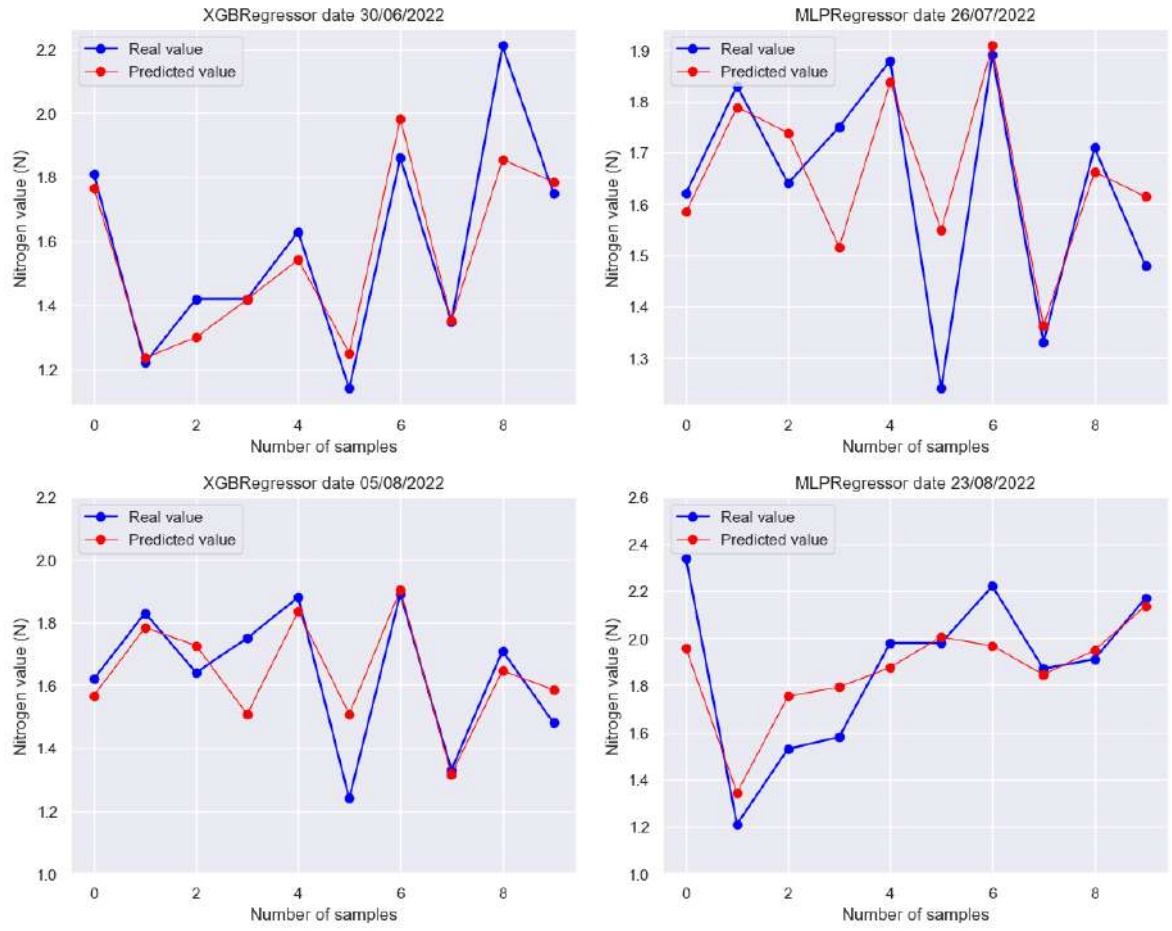

Figure 6.6: Behavior of predicted versus current values of (TN) percentage of leaf area during the four sampling dates.

Explanation of the metrics of one sampling date from the other two dates

The general purpose of these tests was to evaluate the generality and explanatory capacity of the regression models from the information of the other sampling dates, excluding date number 2 due to its lower correlation with the percentage of (TN). However, this omission does not compromise the overall validity of the results; in contrast, it provides a valuable guideline for future research in this type of crop. It was observed that the abundant presence of grass and weeds on date 2 introduced noise in the measurements, which makes data processing difficult due to the similarity in color and shape between pineapple leaves and grass, which is evident in Figure 6.6 and in the lower correlation values presented in Table 6.1. Addressing this issue is discussed in depth in the discussion session section of this Thesis. Based on the above, in order to evaluate the generality and explanatory power of the regression models using the information from

the two remaining sampling dates, the following process was implemented. 1. Training and validation with data from the same date: Initially, the models were trained and validated with data corresponding to the same sampling date. 2. Evaluation with data from other dates: Models trained in stage 1 were subsequently evaluated with all data from the other two remaining dates. This allowed us to evaluate the ability of the models to generalize to data not seen during training. The results of this evaluation are presented in Table 6.1.

At the top of this table is the sampling date used for training, called the "Train Date". In the next row, there are three columns with the data that were used to perform the tests, called "Test Date". In these columns, one is shaded gray and corresponds to the R^2 results obtained with the training and test data from the same date, where 80% was used for training and 20% for validation. The other two columns show the R^2 obtained through training with the entire data set and validation with the data from the other two dates mentioned.

In the Train Date 1 column, the XGBRegressor algorithm obtained the highest R^2 values on the three validation dates; however, these values decrease as the validation dates move away from the training date. Regarding the Train Date 3 column, XGBRegressor maintains the highest metric value when the models are trained and validated with data from the same date. However, when validation was performed with data from date 1, AdaBoostRegressor obtained the highest value and when validation was performed with data from date 4, LassoRegressor and LinearRegression obtained the highest metrics. The results show higher metrics when the validation data are closer to the training date. Finally, in the column in Train Data 4, when validation was performed with data from date 1, a metric of 0.35 was obtained in three algorithms, LassoRegressor, RidgeRegressor, and LinearRegression. When validation was performed with data for date 3, the MLPRegressor obtained the highest metric. On this date, it can also be seen that the performance metrics are higher when the validation is performed with data from the same date or data from nearby dates.

Table 6.2: Training and validation with data from the same date and training with full data and validation with data from other dates.

Models	**Train Data 1**			**Train Data 3**			**Train Data 4**		
	Test Data 1 R^2	**Test Data 3** R^2	**Test Data 4** R^2	**Test Data 1** R^2	**Test Data 3** R^2	**Test Data 4** R^2	**Test Data 1** R^2	**Test Data 3** R^2	**Test Data 4** R^2
LinearRegression	0.8109	0.3015	0.3709	0.3454	0.4136	**0.5285**	**0.3454**	0.4310	0.6936
DecisionTreeRegressor	0.8562	0.1965	0.0182	0.2757	0.6036	0.1499	0.2757	0.0146	0.1936
RandomForestRegressor	0.8286	0.5331	0.2718	0.2672	0.6149	0.3065	0.2672	0.4593	0.6706
SVR_linear	0.7856	0.0414	0.3681	0.2037	0.3684	0.4445	0.2037	0.2379	0.6719
XGBRegressor	**0.8699**	**0.5654**	**0.4555**	0.3617	**0.6801**	0.1396	0.2617	0.2285	0.4511
AdaBoostRegressor	0.8428	0.4197	0.3231	**0.4706**	0.5331	0.2631	0.4706	0.4619	0.6471
LassoRegressor	0.8109	0.3016	0.3708	0.3453	0.4135	**0.5284**	**0.3453**	0.4310	0.6936
RidgeRegressor	0.7981	0.3089	0.3615	0.3467	0.3842	0.5016	**0.3467**	0.4341	0.6643
MLPRegressor	0.8036	0.3264	0.3346	0.3361	0.4113	0.4994	0.3361	**0.4723**	**0.6992**

Chapter 7

Discussion

7.1 Implications of the results for the management and improvement of the pineapple crop

Pineapple plant nutrition is critical for growth, yield, and fruit quality. Nitrogen, in particular, is an essential element for healthy plant development, promoting high growth rates and contributing to optimum yields (Mohsin et al., 2020). For growers, accurate application of nutrients at the right time and place is a priority. In this regard, the results of this research indicate the effectiveness of the proposed models to predict the foliar nitrogen content in pineapple leaves during the vegetative stage of the crop. This finding is of great relevance for nutrient management programs, since it allows the application of fertilizers to the specific needs of the crop and soil in real time. In this way, the use of resources is optimized and the environmental impact is minimized, contributing to a more sustainable agriculture.

An example of practical application of these models is the generation of dynamic fertilization plans, which can be generated from real-time predictions of foliar nitrogen content. These dynamic plans would adjust nitrogen doses to the specific needs of each crop zone, avoiding uniform and static applications such as the current ones (three stages and 15 biweekly applications prior to flower induction). This strategy would optimize the absorption of nutrients by plants, reducing environmental impact, input costs, and ultimately improving crop yield. A relevant aspect to highlight in this study is the monitoring capacity of the pineapple leaf, which varies between 45 and 50 leaves, with dimensions of about one meter in height and width in adulthood, which facilitates its evaluation through images. However, the literature in this field is scarce, and in

the particular case of Colombia, it is attributed to the late introduction of the MD2 pineapple variety in the country in 2004 and to the continuation of its exploitation with the application of technology developed abroad.

7.2 Multisensor data fusion and machine learning for N status diagnosis in pineapple crop

It is important to note that, in order to develop these noninvasive nutrient monitoring techniques, proper weed and grass management is essential. Since the MD2 pineapple plant (A. comosus), being a low herbaceous perennial, the lack of weed control can cause confusion between weeds and pineapple leaves in the captured images. Although multispectral images offer high spatial resolution and more information about crop characteristics than RGB images, they also present greater background noise due to shadows, weeds, and waterlogging, among others. Therefore, it is crucial to consider strategies to reduce this noise prior to analysis. In this study, background noise removal was performed by applying a filter with the NDVI vegetation index. This process removes pixels that do not belong to plants, setting to zero those where the NIR reflectance is less than 20%. However, this technique has limitations in that it does not differentiate between weeds with a similar color to pineapple leaves, which can lead to pixel confusion as observed in the Figure 6.5 (Date 2). The results indicated that the XGBoost Regressor and MLP Regressor algorithms showed the best metrics for predicting nitrogen content in the pineapple crop. However, it is important to note that the effectiveness of these models is closely linked to the quality of the multispectral images and their proper processing, as previously mentioned. The superiority of the yield metrics on the first sampling date (Date 1) can be explained by several reasons. First, the crop was only a few months old and the pineapple leaves were small, which helped to reduce noise in the pineapple canopy images. Second, the soil was free of weeds and waterlogging, which also helped minimize interference. These factors allowed the vegetation indices to more accurately capture nitrogen content. On this date, an R^2 of 86.98% was achieved with the XGB regressor algorithm, which is a high performance metric considering the complexity of this type of open field agricultural system. On the second sampling date, (date 2), the lowest correlation was observed between the predictor variables and the percent (TN). This pattern was reflected in the performance metrics, where the MLP Regressor algorithm achieved an R^2 of 59.11%, being the highest for that date, but

the lowest among the four dates sampled. A possible explanation lies in the presence of weeds and waterlogging in the crop on that date, which made it difficult to extract the weeds in the image processing due to their similarity in color to pineapple leaves. On the third date, the XGB Regressor algorithm achieved an R^2 of 68%, while, on the fourth date, the MLP Regressor obtained an R^2 of 69.41%. In contrast, the integration of information from multiple sensors, including multispectral imagery, ecological factors obtained with IoT sensors, and SPAD chlorophyll values, demonstrated an increase in predictive model efficiency of approximately 7% compared to models based on images alone. One factor that may have decreased the performance of the predictive models is the sample size (n=100) relative to the large number of predictors (p=84). This situation may negatively affect the accuracy of the models. To address this problem, principal component analysis (PCA) was employed to reduce the dimensionality to only five principal components. While PCA can be useful in reducing noise and multicollinearity, there is also the possibility that it may have decreased predictive power by removing relevant information contained in the original variables.

7.2.1 Comparison of performance metrics with related work

It is important to note that the results of the performance metrics obtained in this work exceed those of other research that has used similar methodologies for data collection, processing, and model development for nitrogen estimation in other crops. An example of this is the work of (Shendryk et al., 2020) on sugarcane crops. In this study, a complete randomized block design with five nitrogen levels was implemented and 160 observations were obtained (40 observations in four time periods). Using the principal components of the vegetation indices derived from multispectral images, a R^2 value of 0.57 was achieved for nitrogen prediction. Similarly, (Liang et al., 2023), addressed the estimation of nitrogen status in corn crops. Their experiment was based on a split-plot design with six nitrogen levels. For this, they used multispectral data collected with an unmanned aerial vehicle (UAV) and obtained R^2 values ranging from 0.64 to 0.79. For their part, (Wang et al., 2023b) combined vegetation, color and texture indices with hyperspectral parameters and machine learning methods to estimate nitrogen concentration in rice stems and leaves. In this case, R^2 values of 0.50, 0.51 and 0.63 were achieved.

7.2.2 Analysis with respect to R^2 and RMSE performance metrics

In the second chapter of the Systematic Literature Review, an analysis of the machine learning techniques used in the estimation of nitrogen content in crops was carried out. In this context, it is observed that models based on machine learning techniques, such as Random Forests (RF), Support Vector Machines (SVM), Artificial Neural Networks (ANN) and Multilayer Neural Networks (MLP), have shown outstanding performance, with values of R^2 between 0.64 and 0.99. However, most studies agree on an average R^2 of 0.75, attributed to this consistent trend to the inherent complexity of agroecological and environmental systems, where various variables interact in different compartments (Dong et al., 2022; Fan et al., 2022a; Jiang et al., 2023; Wang et al., 2023b). In this research study, the yield metrics R^2 of 86.98% were achieved, as well as others close to 70%, except for the sampling date number two. These results are within the average R^2 mentioned in chapter 2 of the paper. It is important to note that the R^2 metrics obtained in this investigation correspond to current values achieved only with the fitting of hyperparameters and the reduction in dimensions. No outlier eliminations were performed, since we sought to obtain metrics that reflect the reality of the agroecological and environmental systems, avoiding statistical adjustments that could artificially increase the R^2 metrics, but would distort the true nature of the systems studied.

Chapter 8

Conclusions and Future Work

This chapter summarizes the main contributions and advances achieved throughout the research presented in this thesis. It details the results obtained in the estimation of the optimum nitrogen density in MD2 pineapple crops, using non-invasive techniques that integrate machine learning with data obtained from multispectral images and field sensors. In addition, the implications of these findings in the field of precision agriculture are discussed and several lines of future research are proposed that could expand and deepen the knowledge acquired, exploring new applications, technological improvements and effective implementation strategies.

8.1 Conclusions

The results obtained confirm that it is feasible to estimate the required amount of nitrogen in pineapple crops, especially during the early phenological stages, with a high degree of precision. Using noninvasive techniques, the accuracy of the estimation of 86. 98% was achieved employing advanced machine learning algorithms, including multilayer neural networks and extreme gradient boosting (XGBoost) algorithms. These methods were shown to be optimal for these tasks, allowing accurate and efficient estimation, which represents a significant advance in precision agriculture and agronomic management of the pineapple crop.

- In order to identify the main parameters, variables, and information necessary for the construction of predictive models of nitrogen demand in pineapple crops, a systematic review of the literature was carried out. This exhaustive analysis allowed synthesizing the key factors used in various scientific investigations to

estimate foliar nitrogen content using noninvasive techniques. During the review, different relevant articles were analyzed, identifying an average R^2 coefficient of determination of 75% in similar projects, a figure that aligns with field standards and validates the methodological approaches used. This systematic review not only served to consolidate the theoretical basis of the research but also guided the selection and definition of the most relevant variables and statistical analysis methods used in this thesis.

- Over a period of six months, crop leaf area data were collected through multispectral imaging, sensor measurements of ecological factors, and SPAD values indicating leaf chlorophyll content. This experimental design also explored nitrogen variability across five distinct treatments. Statistical analyses of the results are especially significant on the last two sampling dates, revealing p-values of 0.1476, 0.0685788, 0.0022363 and 0.00018 for the four dates, respectively. The values on the last two dates indicate statistically significant differences, confirming that the data on which the models are trained have significant variations in nitrogen content among treatments.

- The results validated the effectiveness of these techniques, with special attention to the Extreme Gradient Boosting (XGB) and Multilayer Perceptron (MLP) regression algorithms, reaching coefficients of determination R^2 of 86.98%. In addition, it was shown that the models can generalize and explain the results when using data from dates other than the training dates. However, the metrics decrease as the validation data moves away from the training date. Despite this, the XGB Regressor algorithm remained stable and provided the highest metrics.

- The presence of green weeds similar to pineapple leaves generates interference in the images and reduces the effectiveness of the predictive models. To avoid this problem, it is essential to capture images when the crop is free of weeds and grasses. This ensures the generation of cleaner images and allows for better correlation with leaf nitrogen content.

- The great advantage of these methodologies lies in their ability to capture spatial and temporal variability in crop nutritional status, something that conventional laboratory analysis cannot offer due to their static nature and long turnaround times. By avoiding the typical weeks-long delays in obtaining laboratory results, growers can respond more quickly to the changing needs of the crop, resulting in

more efficient use of resources and reduced risk of nitrogen leaching into the soil and nearby water bodies.

- The capacitive sensor on parallel plates has a lower susceptibility to variations in the physicochemical composition of the soil, such as salinity and conductivity, compared to resistive sensors. This is because the capacitive measurement principle is based on the dielectric constant, which is less influenced by these factors than the electrical resistance. In addition, the integration of a soil temperature sensor into the capacitive sensor design allows temperature variations to be compensated for, which significantly improves the accuracy of the measurement. In contrast, resistive sensors are highly sensitive to salinity and temperature, which can lead to inaccurate measurements.

8.2 Future Work

The results of this research highlight the potential of machine learning techniques and the combination of data from various sources, such as multispectral images, environmental sensors, soil sensors, and plant sensors, such as SPAD chlorophyll content values, to estimate the nitrogen content in MD2 pineapple crops. Future research should focus on integrating thermal, hyperspectral and LiDAR sensors to complement multispectral data and improve prediction accuracy; developing dynamic and adaptive fertilization models based on real-time data to optimize resource use and minimize environmental impact; and conducting extensive field trials in diverse geographical locations in order to better generalize results. In addition, it is crucial to conduct temporal analyses and longitudinal studies to optimize the timing of nutrient applications and to assess the economic and environmental benefits of these techniques. It is also important to expand the research to include the estimation of other essential nutrients, such as phosphorus and potassium, for more comprehensive nutrient management strategies. These lines of research will advance precision agriculture, making it more sustainable and beneficial to the environment and the farming community.

Appendix A

Annexes Chapter 2

A.1 Matrix of the results of the systematic literature review article searches. They are organized by tables according to the topics of the four research questions.

Table A.1: Machine learning algorithms for crop nutrient estimation from spectral and sensor images (Part 1)

Crop type	**MLRA**	**Metrics: R^2 - RMSE**	**Explanatory Variables**	**Sensor**	**Ref.**
Soil (N)	PLSR and SVR	SVR: R^2: 0,82. PLSR: R^2: 0,73	pH, EC (dS/m), OC (%), N (ppm), P (ppm), Zn (ppm), Clay (%), Sand (%)	Sentinel 2	(Singha et al., 2023)
Groundnut and Rice	MobileNet	Accuracy = 94%	pH, EC (dS/m), OC (%), N (ppm), P (ppm), Silt (%)	Raspberry Pi. Multispectral camera device	(Venkatesh and Naik, 2024)
Winter Wheat	PLSR and RFR	PLSR: R^2= 0.88 RMSE= 3.35	Canopy chlorophyll content and Nitrogen N	Hyperspectral remote sensing	(Liu et al., 2023a)
Maize	RF	(R^2= 0.64-0.79)	Nitrogen N, leaf and stem shape.	(UAV) DJI FC6510, Inspire 2	(Liang et al., 2023)
Maize	RF	(R^2= 0.63 and R^2= 0.56-0.57)	Corn N index compared with GreenSeeker and ACS-430.	Data fusion from multiple sensors	(Wang et al., 2023b)
Winter Wheat	DNN, LSTM, RF	DNN: R^2= 0.83-0.96 MTL:R^2 = 0.81-0.96	Proximal sensing and meteorological data	Crop sensor and meteorological	(Ruan et al., 2023)
Maize	RF	RFR:R^2=0.81-0.82	NDVI, RVI, NDRE, RERVI used for N status diagnosis	GreenSeeker and CropCircle ACS	(Wang et al., 2023e)
Maize	RF, SVM and MLR.	R^2 =0.96, RMSE= 26.85	Leaf chlorophyll density (CCD), and Leaf area index (LAI).	Unmanned Aerial Vehicle (UAV)	(Zhou et al., 2023)
Rice	GPR	RMSE = 6.84%	Nitrogen from canopy reflectance	Unmanned Aerial Vehicle (UAV)	(Li et al., 2023a)
Winter Wheat	GPR, RF, ElasticNet	R^2= 0.726, RMSE= 3.20	Analyse the Total, Nitrogen Content in Winter Wheat	Unmanned Aerial Vehicle (UAV)	(Li et al., 2023b)
Ryegrass, barley	LR	R^2= 0.75, RMSE= 3.20	Canopy nitrogen concentration	ASD HandHeld, spectroradiometer	(Patel et al., 2024)
Winter Wheat	RF, Lasso, ANN	RF: R^2= 0.69-0.93, ANN: 0.65-0.71	Analyse the Total, Nitrogen	UAV and images Sentinel 2	(Jiang et al., 2023)
Ginger	ANN, MLP, RBF	MLP: R^2= 0.99	Estimating and optimizing 6-gingerol	Environmental factors	(Sahoo et al., 2023)
Winter Wheat	RF, SVR	RF: R^2= 0.63-0.93, SVR: 0.53-0.67	Nitrogen balance index (NBI)	Canopy features	(Fan et al., 2022a)
Maize	FR, SVR	R^2= (0.81 – 0.83)	Nitrogen status indicators across growth stages	Leaf fluorescence sensor Dualex	(Dong et al., 2022)
Maize, cotton	CB, QRF	R^2= of 71% - 52%.	pH, Soil organic carbon SOC N (%), pH	Digital soil mapping	(Hounkpatin et al., 2022)
Maize	RR, SVR, RF, GP	BMA: R^2= 0.888 - 0.929 for LAI	Phenotypic and nitrogen content	(UAV) and multiple sensors data.	(Shu et al., 2022)
Wheat	MLR, ANN	MLR: R^2= 0.662, ANN: R^2= 0.744	Leaf nitrogen content (LNC)	(UAV) and multispectral sensors	(Fu et al., 2022)
Sugarcane	PLS, BPNN, ELM	Best accuracy, (R^2= 0.79, RMSE= 0.11)	Canopy nitrogen concentration (CNC)	Unmanned aerial vehicle (UAV)	(Patil et al., 2023)

Table A.2: Machine learning algorithms for crop nutrient estimation from spectral and sensor images (Part 2)

Crop type	**MLRA**	**Metrics: R^2 - RMSE**	**Explanatory Variables**	**Sensor**	**Ref.**
Grape leaves	PLS, RF, SVM, ELM	In general, R^2= 0.65-0.75	Leaf nitrogen content (LNC)	Unmanned aerial vehicle (UAV)	(Peng et al., 2022)
Maize	SVM and RF	SVM: R^2= 0,74 0,90, RF: R^2=0,84-0,93	Genetics, environmental on N rate, irrigation, and pre-plant N rate	RapidSCAN CS-45 active canopy sensor	(Li et al., 2022a)
Rice	NNA	R^2= 0,85	Abundance-adjusted vegetation index (AAVI) Green Pixel Vegetation Index (GPVI)	Unmanned aerial vehicle (UAV)	(Wang et al., 2022a)
Winter Wheat	RF	R^2= 0.82- 0.87	Plant N accumulation (PNA) and N nutrition.	Multispectral imaging, agronomic data.	(Jiang et al., 2022)
Rice	SMLR, RF	SMLR: R^2= 0,80, RMSE= 0,11, RFR: R^2= 0,75 RMSE= 11,4	Diagnosis and recommendation of N in terms of rice yield	Data fusion from multiple sources	(Lu et al., 2022a)
Winter Wheat	RFR	R^2= 0.72 - 0.86	N state estimation	Climatic factors, vegetation index	(Zhang et al., 2022b)
Maize	LR	R^2= 0.67	N nitrogen life cycle	Hyperspectral and multispectral data	(Han et al., 2022)
Sugarcane	RF, SVR	RF: R^2= 0,59. RVS: R^2= 0,58	N state estimation	Sentinel-2	(Minaei et al., 2022)
Cotton	LR, SVR, CNN	R^2= 0.80 and RMSE= 1.67 g kg	N state estimation. Canopy images	(UAV) Canopy RGB images	(Kou et al., 2022)
Potato	MLR), K-NN, and RF	RF: R^2= 0,79, MLR: R^2= 0,80, K-NN: R^2= 0,76	Vegetation indices in visible light (VI) and morphological parameters (MP)	Unmanned aerial vehicle (UAV)	(Fan et al., 2022b)
Wheat	ResNet, EfficientNet	Accuracy (0.96)	Prediction Nitrogen. Spectral Attention Block (SAB).	UAV digital aerial imagery	(Zhang et al., 2022a)
Winter Wheat	SVR, ELM, RF	SVR: R^2= 0.61,RF: R^2=0.62, ELM: R^2=0.72	Leaf nitrogen concentration (LNC)	Unmanned aerial vehicle (UAV)	(Lu et al., 2022b)
Maize	DNN	R^2= 0.82-0.84, RMSE=0.89	Chlorophyll monitoring established	SPAD-502 monitor	(Putra et al., 2022)
Winter Wheat	NNA	R^2=0,7920 RMSE=0,1431	Monitoring of total nitrogen (TN)	Features fusion method called PNMF-MCR.	(Tian et al., 2022)
Soil nitrogen	PLSR, LSSVM	PLSR: R^2=0.92, RMSE=0.77% LSSVM: R^2=0.96,	Different types of soil nitrogen	Near-infrared hyperspectral imaging (NIR-HSI)	(Chen et al., 2022)
Maize	PLS	R^2=0.88	Canopy nitrogen content (CNC)	(VI) and wavelet functions	(Wang et al., 2022b)
Winter Wheat	PLSR	R^2=0.52	Canopy nitrogen content (CNC, kg/ha)	Sentinel 2, vegetation indices (VI)	(Bossung et al., 2022)
Cotton	MLR, PLSR, and SVR	R^2= 0.532 0.665	Leaf nitrogen concentration (LNC)	30 hyperspectral vegetation indices	(Ma et al., 2022)

Table A.3: Applications of UAV and satellite spectral imagery for estimation of nitrogen and other crop parameters

Key aspects	Crops	Type of image	Type of Variables	References
Evaluar el rendimiento de tres modelos de aprendizaje automático: (SVM), la red neuronal de retropropagación (BPNN) y el refuerzo de gradiente extremo (XGB).	Cotton	Multispectral imaging from (UAV) - MicaSense sensor	Nitrogen nutrition index (NNI)	(PEI et al., 2023)
A multi-stage time-series GY prediction model combining VI and EM abundance	Rice	UAV-based multispectral vegetation indices - MiniMCA-6 and AIRPHEN multispectral camera	Crop yield	(Su et al., 2023)
Variation in spectral signature of rice grown at different altitudes and nutrient management practices using spectroradiometers	Rice	Spectrometer (FieldSpec4)	Essential spectral and agronomic data	(Gopinath et al., 2024)
Inferring chlorophyll content in sugarcane crops at the canopy level using unmanned aerial vehicles (UAVs) and vegetation spectral indices.	Sugarcane crops	Multispectral imaging from (UAV) - DJI P4 multispectral Sensor	Leaf chlorophyll, vegetation spectral indices	(Narmilan et al., 2022)
Evaluated the potential of UAV-based modeling to monitor crop growth under different water and nutrient supplies considering different phenological stages of maize.	Maize	Multispectral imaging from (UAV) - MicaSense RedEdge-M	Leaf area index, leaf chlorophyll concentration and aerial dry matter	(Zhu et al., 2022)
Nitrogen variability within pasture fields was predicted using UAV and satellite data.	Grass fields	Sentinel 2A and Multispectral imaging from (UAV) - MicaSense RedEdge-M	Plant N content (PNC), aboveground biomass (AGB), and nutritional nitrogen index (NNI)	(Pereira et al., 2022)
A Micro-Scale Approach for Cropland Suitability Assessment of Permanent Crops Using Machine Learning and a Low-Cost UAV	Mandarin plantations	UAV with an RGB sensor Mavic 2 Pro	Leaf nitrogen content (LNC)	(Lukáš et al., 2023)
Automated temporal and spatial identification and individualization of crop images from UAVs.	Sugar beet	Multispectral imaging from (UAV) - Micasense Altum multispectral camera	Cercospora leaf spot (a fungal disease)	(Günder et al., 2022)
Evaluate the accuracy of corn weed infestation mapping using multi-temporal data from (UAV) and PlanetScope.	Maize	Multispectral images from UAV - MicaSense RedEdge-MX and PlanetScope	Leaf area of weed infestations	(de Villiers et al., 2023)
Accurate estimation of aboveground biomass (AWB) in grasslands using UAV remote sensing.	Pasture production	Multispectral imaging from (UAV) - MicaSense RedEdge-M	Accurate aboveground biomass (AGB)	(Freitas et al., 2022)
LNC prediction method based on the combination of deep learning methods and mechanistic models.	Wheat Leaf	UAV Hyperspectral Images - ImspectorV10, Spectral Imaging	Leaf nitrogen content (LNC)	(Chen et al., 2022)
Objective to investigate the ability of UAV-based multispectral imagery to monitor leek nitrogen uptake and dry biomass in multiple fields and seasons.	Leek	Multispectral imaging from (UAV) - MicaSense RedEdge sensor	Dry-Biomass and Nitrogen Uptake	(Haumont et al., 2022)
Spectral indices under different irrigation water and nitrogen fertilizer management in terms of monitoring and estimation of corn biomass.	Maize	Multispectral imaging from (UAV) - Sequoia sensor	Effect of different levels of irrigation water and nitrogen.	(Feizolahpour et al., 2023)
A Machine-Learning Model Based on the Fusion of Spectral and Textural Features from UAV Multi-Sensors to Analyse the Total Nitrogen Content	Winter Wheat	Multispectral imaging from (UAV) -RedEdge MX multispectral	Total nitrogen content- Images of leaf area	(Li et al., 2023b)
The ability of four different sensors to estimate nitrogen in winter wheat was evaluated.	Winter Wheat	UAV with an RGB sensor - Sony DSC-QX100 digital RGB camera	Wheat leaf N concentration (LNC)	(Song et al., 2022)

Table A.4: Summary of works developed with multispectral images, separated by vegetation indices.

Objective	Vegetation Index Used	Crop	Image type	Ref
Estimation of fractional cover of nonphotosynthetic and photosynthetic vegetation	NDVI-NSSI, EVI-NSSI	Rice	Feature space, using the NPV soil separation index (NSSI).	(Zhu et al., 2023)
To evaluate the performance of different IVs in the estimation of canopy chlorophyll content (CCC).	NDVI, PNSI,RDVI and IPVI	Wheat	RGB-NIR, RedEdge	(Zhang et al., 2022b)
Characteristics of the vegetation index such as delimitation, low or propagation of errors.	NDVI and kNDVI	Maize	RGB, NIR, RedEdge	(Wang et al., 2023d)
Measure the quantity and size of fruits, related to the quality and chlorophyll and maturity of the fruit.	NDVI	Fruit	RGB, NIR, Red Edge	(Nikos Tsoulias, 2023)
Detection of irrigation dates from integration of Sentinel-2-derived leaf area index values into the Optirrig crop model.	CWSI	Maize	NIR, Red Edge, RGB, Green	(Hamze et al., 2023)
Estimating nitrogen level in corn from multispectral images taken with unmanned aerial vehicles (UAV)	NDVI, SAVI, RI, DI	Corn	NIR, Red Edge, RGB	(Chen et al., 2022)
Detection and mapping of vegetation stress using AVIRIS NG hyperspectral imagery	(NDVI, NSI 2, SWST, SRWI, NWI, CSVI, HMSSI, and ARI 1)	Vegetation	Hyperspectral data	(Kayet et al., 2023)
Spatial and temporal trends of global dryland vegetation were investigated based on multiple model and satellite	NDVI, VOD DI	Global land vegetation	NIR, Red Edge, RGB, Green, Blue	(Liu et al., 2023a)
Four data processing methods - (VI), (BPNN), (XGBoost) and PLSR compared their ability to estimate LNC	GNDVI, EVI and NDRE	Wheat	NIR, Red Edge, Blue and RGB	(He et al., 2022)
Five vegetation indices and three specific chlorophyll indices were compared individually and in combination.	MSAVI, MCARI, NDVI, EVI, LAI, RGR	Multispecies trees	Sentinel 2	(Thinley et al., 2024)
Different (VI) extracted from RGB aerial images to differentiate the nutritional and water status.	MDVI, NDVI, MGRVI	Hass avocado	RGB acquired with UAV	(Salazar-Reque et al., 2023)
The optimized vegetation indices (Opt-VIs) could resist spectral saturation.	RVI, NDVI	Potato	UAV hyperspectral imagery	(Liu et al., 2024)
Different types of remote sensing parameters have good potential for monitoring nitrogen	VARI, MGRVI, RGBVI, NGRDI	Rice	Hyperspectral parameters with UAV	(Wang et al., 2023a)

Table A.5: Vegetation indices used in the articles, with abbreviation, full name and Equation

Index	**Spectral index name**	**Equation**
NDVI	Normalized difference vegetation index	$\text{NDVI} = \frac{NIR-RED}{NIR+RED}$
MNDI	Modified normalized difference index	$\frac{R_i-R_j}{R_i+R_j-2R_{445}}$
CVI	Chlorophyll vegetation index	$CVI = \frac{NIR}{\text{Green}} \times \frac{\text{Red}}{\text{Green}}$
IPVI	Infrared percentage vegetation index	$IPVI = \frac{NIR}{NIR+RED}$
CWSI	Crop Water Stress Index	$CWSI = \frac{T_c-T_{\text{wet}}}{T_{dry}-T_{\text{wet}}}$
MSR	Modified simple ratio	$\frac{R_i-R_{445}}{R_i-R_{445}}$
SAVI	Soil-adjusted vegetation index	$\text{SAVI} = \frac{NIR-RED}{NIR+RED+L} * (1 + \text{L})$
DI	Difference index	DI=N I R-R E D
GNDVI	Green Normalized difference vegetation index	$GNDVI = \frac{(NIR-\text{ Green })}{(NIR+\text{ Green })}$
LSWI	Land Surface Water Index	$LSWI = \frac{\rho_{\text{nir}}-\rho_{\text{swir}}}{\rho_{\text{nir}}+\rho_{\text{swir}}}$
NDWI	Normalized Difference Water Index	$\text{NDWI} = (\text{Green - NIR})/(\text{Green + NIR})$
EVI	Enhanced vegetation Index	$EVI = 2.5 * \frac{(NIR-Red)}{(NIR+6* \text{Red } -7.5* \text{ Blue } +1)}$
NDRE	Normalized difference red edge index	$NDRE = \frac{NIR-REDGE}{NIR+REDGE}$
RI	Ratio index	$\text{RI} = \frac{NIR}{RED}$
RGBVI	Red-green blue vegetation index	$\frac{\text{Green }^2-(\text{ Blue } * \text{ Red})}{\text{Green }^2+(\text{ Blue } * \text{ Red })}$
RVI	Ratio vegetation index	$\frac{\text{NIR}}{\text{Red}}$
TVI	Transformed vegetation index	$\sqrt{\text{NDVI } + 0.5}$
VIN	Vegetation index number	$\frac{\text{NIR}}{\text{Red}}$
GRVI	Green-red vegetation index	$\frac{\text{Green-Red}}{\text{Green+Red}}$
M-MTCI	Modified MERIS terrestrial chlorophyll index	$\frac{\text{NIR-Rededge}}{\text{Rededge-Red}}$
MSAVI2	Modified soil adjusted vegetation index	$\frac{2\times \text{ NIR } +1-\sqrt{(2\times NIR+1)^2-8(\text{ NIR-Red})}}{2}$

Table A.6: Analysis of works developed with Internet of Things (IoT) applications, oriented to agriculture.

Objective	Communication Technologies	Application	Sources
Smart irrigation system using cloud computing, embedded systems and Internet of Things (IoT)	Module (DHT22), water level and humidity sensors, connected to the system (ESP32).	Intelligent irrigation system	(Morchid et al., 2024b)
It combines sensor, actuator, and cloud platform technologies to build an intelligent greenhouse control system.	STM32F407ZGT6 microcontroller. Beidou/GPS module ATK-1218-BD. Wind cup wind speed sensor	Agricultural and environmental variables	(Song et al., 2024)
The testbeds available for agriculture based on IoT have been studied.	PotatoNet is a wireless sensor network system with 9 INGA nodes in the field.	Potato	(Vangala et al., 2022)
Moisture, pH, temperature, and soil moisture sensors are used in agricultural fields to collect data.	Common Raspberry PI 3 (RPI3) controller module, which was used to control all of these sensors	Disease detection	(Hasan et al., 2022)
Discusses a smart irrigation system that is based on the Internet of Things and a cloud-based architecture.	Raspberry Pi, DHT11/DHT22 Humidity Sensor and YL-69 Soil Moisture Sensor	Agricultural irrigation	(Phasinam et al., 2022)
He objective is to develop an integrated IoT solution adapted to fruit and vegetable crops, facilitating higher productivity	The transmitter node realized with sensors and an Arduino for LoRa communication and the receiver node with ESP32.	Fruit and vegetable crops	(Ting and Chan, 2024)
Design and implementation of an innovative real-time water quality monitoring system	Combination of an Arduino microcontroller-based board for real-time data capture and transmission to a LoRaWAN gateway.	Quality of water resources	(Jabbar et al., 2024)
System that uses intelligent sensors whose real-time records are managed according to the concept of fuzzy sets.	Capacitive soil moisture sensor v1.2, DHT22 sensor, (LDR sensor) and passive infrared receiver (PIR sensor)	Mushroom cultivation	(Irwanto et al., 2024)
How IoT benefits agriculture to ensure less resource waste, healthier yields.	Arduino, sensors humidity, temperature, pH and (NPK)	Greenhouse environment	(Maraveas et al., 2022)
This paper presents a hybrid ML model with IoT for performance prediction.	Extreme Learning Machine (ELM) and IoT	Water	(Hundal et al., 2023)
It proposes an intelligent optimization model to develop sustainable agriculture using ML.	Remote sensing	Soil and crop conditions	(Saba et al., 2023)
This work explores an efficient integration of IoT devices based on context awareness in the agricultura.	(WSN), (ML)	Irrigation systems	(Javaid, 2023)
The proposed system focuses on automatic water irrigation and detection of plant diseases.	K-Nearest Neighbor and support vector	Automatic water irrigation.	(Mathi et al., 2023)
Monitor air temperature, humidity and ambient light intensity in a crop in order to measure and control different parameters.	(WSN), (ML)	Ecological factors	(Kumar Singh and Sobti, 2022)
An intelligent system to accurately track and schedule irrigation using IoT, LoRa-based machine learning (ML) is presented.	Humidity sensors	Ecological factors	(Prasanna Lakshmi et al., 2023)
Integrated edge-fog-cloud architecture to improve energy efficiency of agricultural systems and carbon emissions.	LPWA, LoRa	Ecological factors	(Karaman et al., 2023)

Appendix B

Publications and Patents

B.1 Invention Patents

Application for Patent of Invention

- **Title of the Invention:** Capacitive sensor of parallel plates to determine humidity in soils.
- **File No.** NC2022/0014133. Super Intendencia de Industria y Comercio (Superintendence of Industry and Commerce).
- **Filing Date:** September 30, 2022
- Type of filing: National Patent of Invention
- **Applicant:** Centro de Desarrollo Tecnologico e Innovacion en TIC NetworkTIC S.A.S, University of Antioquia UdeA, Universidad Pedagogica y Tecnologica de Colombia UPTC.
- **Inventor:** Jose Edinson Aedo Cobo, Nelson Barrera Lombana, Jorge Enrique Chaparro Mesa.
- **Funding:** Ministry of Science, Technology and Innovation MINCIENCIAS through the "Convocatoria Crearlo no es Suficiente". National call to encourage patent protection of I+D+i results that promote economic empowerment of the business sector.

B.2 Publications

Published article

- **Title:** Machine Learning for estimation of leaf nitrogen content in pineapple crops using multispectral imaging and Internet of Things (IoT) platforms.
- **Authors:** Chaparro Mesa Jorge Enrique, Felipe Lumbreras Ruiz, Jose Edison Aedo.
- **Journal: Journal of Agriculture and Food Research.** Online ISSN: 2666-1543.

  Subject areas: Agricultural and Biological Sciences (General).

  Link Journal: www.sciencedirect.com/journal/journal-of-agriculture-and-food-research
  Link SJR: https://www.scimagojr.com/journalsearch.php?q
- **Year:** 2024

Published Scientific Article

- **Title:** Remote Terminal Module for data acquisition, monitoring and control of Agroindustrial processes - AgriculTIC.
- **Authors:** Chaparro Mesa Jorge Enrique, Barrera Lombana Nelson, Leon Socha Fredy.
- **Journal: Ingeniare. Chilean Engineering Journal.** ISSN 0718-3291 Printed Version. ISSN 0718-3305 Online version.

  Link to the Journal: https://ingeniare.uta.cl/?numid=172. Link SJR:

  https://www.scimagojr.com/journalsearch.php?q=11600154153tip=sidexact=no
- **Year:** 2021

Appendix C

Theoretical and technical information patent parallel plate capacitive humidity sensor

The parallel plate soil moisture sensor has a capacitance variation as a function of the variation of the dielectric constant, and this in turn varies as a function of the water concentration between the plates, in this particular case, the area of the plates and the distance between them remain constant; thus, the variation of the capacitance as a function of the parameters involved can be expressed as shown in Equation C.1.

$$C = \frac{k^* {\varepsilon_o}^* A}{d} \tag{C.1}$$

As mentioned, C is the capacitance in farads, A is the area of the plates in square meters, d is the distance between the plates in meters, ϵ_0 is the constant of dielectric vacuum permittivity, and k is the relative dielectric permittivity of the material between the plates, which varies as a function of the water concentration in the latter.

To determine changes in capacitance and, indirectly, changes in soil moisture, an astable multivibrator circuit was designed using the LM555 integrated circuit. This component, introduced by Signetics in the 1970s, is still widely used today. The constructed circuit is shown in Figure C.1.

Figure C.2, it can be seen that the capacitor C is charged by the resistors R1 and R2, in this case the transistor T1 is represented by a switch that will be in open state so it will not operate; the differential equation that represents this circuit can be seen in Equation C.2.

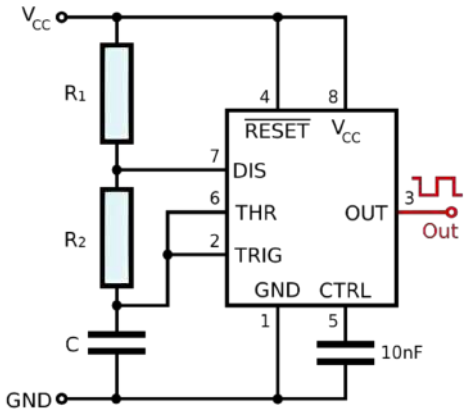

Figure C.1: Astable multivibrator schematic used in the design of the parallel plate sensor circuit designed to measure soil moisture. Figure from (Ennaji et al., 2023)

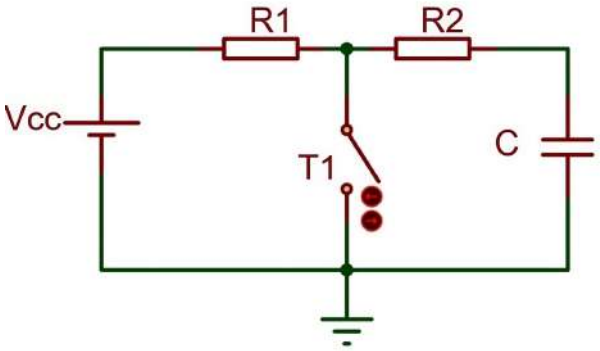

Figure C.2: Equivalent capacitor charging circuit C. Figure from (Ennaji et al., 2023)

$$Vcc = (R1 + R2)^{*} i(t) + \frac{1}{C}\int_{0}^{t} i(\tau)^{*} d\tau \tag{C.2}$$

Solving differential Equation C.2, considering that the initial charge of C is zero, yields the solution given in Equation C.3.

$$i(t) = \frac{Vcc}{(R1 + R2)} e^{-t/(R1+R2)^{*}C)} \tag{C.3}$$

Figure C.2, shows that the current is uniform throughout the circuit, so i(t) in equation three describes the current through capacitor C, which in this case is the capacitor of the parallel-plate soil moisture sensor. In addition, the voltage across a capacitor is given by Equation C.4.

$$Vc(t) = \frac{1}{C}\int_0^t i(\tau)^* d\tau \tag{C.4}$$

Since $i(\tau)$ is the current through the capacitor, replacing equation three in equation four gives an expression for the charge on the capacitor when the bistable is in set mode, operating as described in Figure C.2. Thus, the voltage across the capacitor $V_c(t)$ is expressed as in Equation C.5.

$$Vc(t) = Vcc^* \left[1 - e^{-t/((R1+R2)^*C)}\right] \tag{C.5}$$

When the voltage across the capacitor $V_c(t)$ reaches $Vcc/3$, according to the schematic in Figure C.3, the two comparators will produce low voltages, bringing the biconductor to a state without change.

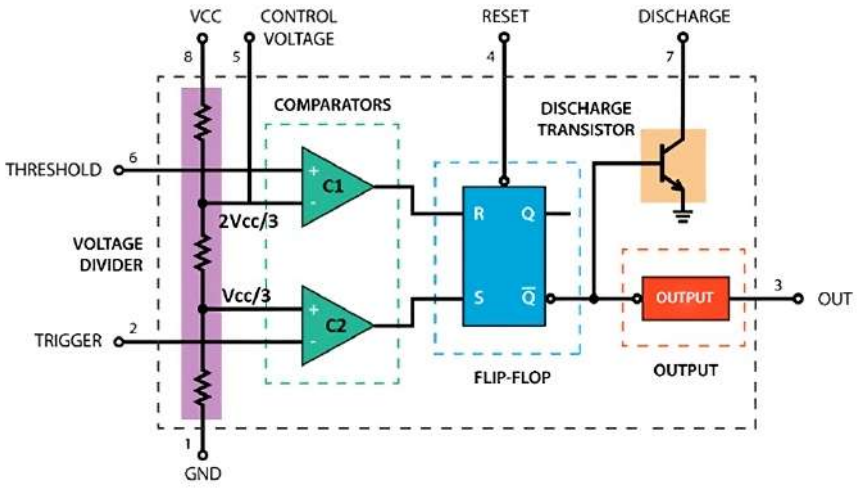

Figure C.3: Internal construction LM555 Integrated Circuit. Figure from (Ennaji et al., 2023)

The output of the circuit will remain high and the transistor will remain in the cut-off state. This time interval, from when the circuit is energized until the voltage reaches $Vcc/3$, is called t1 (time 1). After that, the capacitor will continue to charge up to $2Vdc/3$. When the voltage across the capacitor reaches this value, a total time called t2 will have elapsed. At this point, according to the schematic in textcolormycolorFigure C.3, comparator C1 will produce a high voltage and C2 a low voltage, which will reset the bistable, causing the transistor to go into saturation, discharging the capacitor and causing the output of the subsystem to take a low logic value. This new equivalent circuit is shown in Figure C.4.

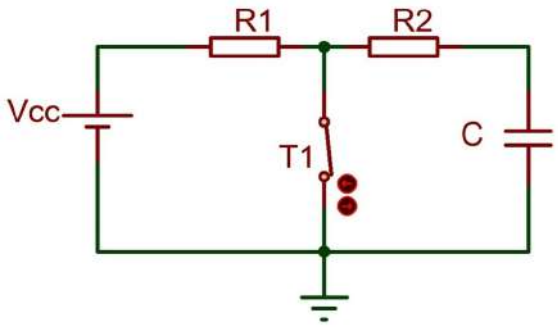

Figure C.4: Equivalent capacitor discharge circuit C. Figure from (Ennaji et al., 2023)

Based on the above, Figure C.4, shows that the capacitor, with an initial voltage condition equal to $2Vdc/3$, will now discharge through resistor $R2$, while the source is connected to ground through $R1$. For this reason, R1 cannot be a low resistance, as it would drain an excess charge to the ground, which could cause a short circuit. The differential equation describing the capacitor discharge voltage $V_c(t)$ is shown in Equation C.6.

$$\frac{Vc(t)}{R2} + C\frac{d[Vc(t)]}{dt} = 0 \tag{C.6}$$

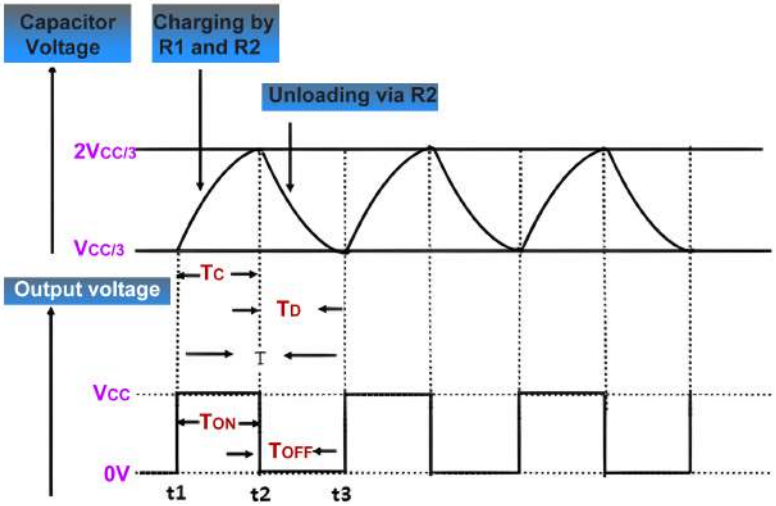

Figure C.5: Voltage signals involved in astable multivibrator. Source: Own elaboration.

According to Figure C.5, the capacitor charging time between $Vcc/3$ and $2Vcc/3$, called T_{ON}, is given by the difference $t2-t1$. The T_{OFF} time, which is the interval during which the capacitor is discharged, is given by the difference $t3-t2$. Furthermore, it must

be considered that the output frequency of the monostable multivibrator is defined by Equation C.7.

$$f = \frac{1}{T_{ON} + T_{OFF}} \tag{C.7}$$

For the calculation of $t1$, Equation C.5, describing the capacitor charge is used, thus $t1$ is given when the voltage across the capacitor reaches the value of $Vcc/3$, thus, replacing it, we obtain Equation C.8.

$$\frac{Vcc}{3} = Vcc * \left[1 - e^{-t'_1((R1+R2)^*C)}\right] \tag{C.8}$$

Finally, from Equation C.7, it is possible to calculate the frequency of the astable multivibrator circuit from the capacitance of the parallel plate capacitive soil moisture sensor, this synthesis is shown in Equation C.9.

$$f = \frac{1}{\ln(2) * (R1 + 2 * R2)^*C} \tag{C.9}$$

As can be seen, there is a non-linear relationship between frequency and capacitance. The values of $R1$ and $R2$ are arbitrary but constant, therefore, the frequency will be a function of the capacitance variation only. This capacitance variation depends on the dielectric constant of the capacitor, which varies with the water concentration between the plates of the parallel plate soil moisture sensor.

References

Rabiya Abbasi, Pablo Martinez, and Ahmad. The digitization of agricultural industry – a systematic literature review on agriculture 4.0. *Smart Agricultural Technology*, 2: 100042, 12 2022. ISSN 2772-3755. doi: 10.1016/J.ATECH.2022.100042. URL https://linkinghub.elsevier.com/retrieve/pii/S2772375522000090. (page 14)

Yaganteeswarudu Akkem, Saroj Kumar Biswas, and Aruna Varanasi. Smart farming using artificial intelligence: A review. *Engineering Applications of Artificial Intelligence*, 120:105899, 4 2023. ISSN 0952-1976. doi: 10.1016/J.ENGAPPAI.2023.105899. URL https://linkinghub.elsevier.com/retrieve/pii/S0952197623000830. (page xxiii)

Tarek Alahmad, Miklós Neményi, and Anikó Nyéki. Applying IoT Sensors and Big Data to Improve Precision Crop Production: A Review. *Agronomy 2023, Vol. 13, Page 2603*, 13(10):2603, 10 2023. ISSN 2073-4395. doi: 10.3390/AGRONOMY13102603. URL https://www.mdpi.com/2073-4395/13/10/2603/htmhttps://www.mdpi.com/2073-4395/13/10/2603. (page 14)

Angelos Alexopoulos, Konstantinos Koutras, Sihem Ben Ali, Stefano Puccio, Alessandro Carella, Roberta Ottaviano, and Athanasios Kalogeras. Complementary Use of Ground-Based Proximal Sensing and Airborne/Spaceborne Remote Sensing Techniques in Precision Agriculture: A Systematic Review. *Agronomy 2023, Vol. 13, Page 1942*, 13(7):1942, 7 2023. ISSN 2073-4395. doi: 10.3390/AGRONOMY13071942. URL https://www.mdpi.com/2073-4395/13/7/1942/htmhttps://www.mdpi.com/2073-4395/13/7/1942. (page 14)

Narmilan Amarasingam, Arachchige Surantha Ashan Salgadoe, Kevin Powell, Luis Felipe Gonzalez, and Sijesh Natarajan. A review of UAV platforms, sensors, and applications for monitoring of sugarcane crops, 4 2022. ISSN 23529385. (pages 39 and 40)

Fatih Bal and Fatih Kayaalp. Review of machine learning and deep learning models in agriculture. *International Advanced Researches and Engineering Journal*, 05(02): 309–323, 2021. doi: 10.35860/iarej.848458. URL www.dergipark.org.tr/en. (pages 48 and 49)

Wasana Bandara and Rehan Syed. The role of a protocol in a systematic literature review. *Journal of Decision Systems*, 10 2023. ISSN 21167052. doi: 10.1080/12460125.2023.2217567. URL https://www.tandfonline.com/doi/abs/10.1080/12460125.2023.2217567. (page 10)

Clara Oliva Gonçalves Bazzo, Bahareh Kamali, Christoph Hütt, Georg Bareth, and Thomas Gaiser. A Review of Estimation Methods for Aboveground Biomass in Grasslands Using UAV. *Remote Sensing 2023, Vol. 15, Page 639*, 15(3):639, 1 2023. ISSN

2072-4292. doi: 10.3390/RS15030639. URL https://www.mdpi.com/2072-4292/15/3/639/htmhttps://www.mdpi.com/2072-4292/15/3/639. (pages 12 and 42)

Katja Berger, Jochem Verrelst, Jean-Baptiste Féret, Tobias Hank, Matthias Wocher, Wolfram Mauser, and Gustau Camps-Valls. Retrieval of aboveground crop nitrogen content with a hybrid machine learning method. *International Journal of Applied Earth Observation and Geoinformation*, 92:102174, 10 2020a. ISSN 03032434. doi: 10.1016/j.jag.2020.102174. URL https://www.sciencedirect.com/science/article/pii/S0303243420303500. (page 38)

Katja Berger, Jochem Verrelst, Jean-Baptiste Féret, Zhihui Wang, Matthias Wocher, Markus Strathmann, Martin Danner, Wolfram Mauser, and Tobias Hank. Crop nitrogen monitoring: Recent progress and principal developments in the context of imaging spectroscopy missions. *Remote Sensing of Environment*, 242:111758, 6 2020b. ISSN 00344257. doi: 10.1016/j.rse.2020.111758. URL https://linkinghub.elsevier.com/retrieve/pii/S0034425720301280. (page xxiii)

Christian Bossung, Martin Schlerf, and Miriam Machwitz. Estimation of canopy nitrogen content in winter wheat from Sentinel-2 images for operational agricultural monitoring. *Precision Agriculture*, 23(6):2229–2252, 12 2022. ISSN 15731618. doi: 10.1007/S11119-022-09918-Y/FIGURES/6. URL https://link.springer.com/article/10.1007/s11119-022-09918-y. (pages 18, 19, and 110)

Marie Aure Bourgeon, Jean Noël Paoli, Gawain Jones, Sylvain Villette, and Christelle Gée. Field radiometric calibration of a multispectral on-the-go sensor dedicated to the characterization of vineyard foliage. *Computers and Electronics in Agriculture*, 123: 184–194, 4 2016. ISSN 0168-1699. doi: 10.1016/J.COMPAG.2016.02.019. (pages 44 and 45)

Achilles D. Boursianis, Maria S. Papadopoulou, Panagiotis Diamantoulakis, Aglaia Liopa-Tsakalidi, Pantelis Barouchas, George Salahas, George Karagiannidis, Shaohua Wan, and Sotirios K. Goudos. Internet of Things (IoT) and Agricultural Unmanned Aerial Vehicles (UAVs) in smart farming: A comprehensive review. *Internet of Things*, page 100187, 3 2020. ISSN 25426605. doi: 10.1016/j.iot.2020.100187. (pages xxiii, 8, 13, and 14)

Hang Thanh Bui, Hamed Aboutorab, Arash Mahboubi, Yansong Gao, Nazatul Haque Sultan, Aufeef Chauhan, Mohammad Zavid Parvez, Michael Bewong, Rafiqul Islam, Zahid Islam, Seyit A. Camtepe, Praveen Gauravaram, Dineshkumar Singh, M. Ali Babar, and Shihao Yan. Agriculture 4.0 and beyond: Evaluating cyber threat intelligence sources and techniques in smart farming ecosystems. *Computers & Security*, 140:103754, 5 2024. ISSN 0167-4048. doi: 10.1016/J.COSE.2024.103754. (page 3)

Sen Cao, Brad Danielson, Shari Clare, Shantel Koenig, Carlos Campos-Vargas, and Arturo Sanchez-Azofeifa. Radiometric calibration assessments for UAS-borne multispectral cameras: Laboratory and field protocols. *ISPRS Journal of Photogrammetry and Remote Sensing*, 149:132–145, 3 2019. ISSN 0924-2716. doi: 10.1016/J.ISPRSJPRS.2019.01.016. (pages xii, 45, 46, 47, and 76)

M. K. V. Carr. The water relations and irrigation requirements of pineapple (Ananas comosus). *Experimental Agriculture*, 48(4):488–501, 10 2012. doi: 10.1017/S0014479712000385. URL https://www.cambridge.org/core/product/identifier/S0014479712000385/type/journal_article. (page 3)

Sandra Cerón, González Paola. Contexto cadena de la piña en Colombia. Technical report, Corporación colombiana de investigación agropecuaria, Bogota, 2022. URL https://oec.world/en/profile/hs92/pineapples-fresh-or-dried. (page 1)

Subhash Chander, Roopa Kumari, F. N.U. Sadarat, and Sindhu Luhana. The Evolution and Future of Intensive Care Management in the Era of Telecritical Care and Artificial Intelligence. *Current Problems in Cardiology*, 48(10):101805, 10 2023. ISSN 0146-2806. doi: 10.1016/J.CPCARDIOL.2023.101805. (page 13)

Daosheng Chen, Fei Zhang, Mou Leong Tan, Ngai Weng Chan, Jingchao Shi, Changjiang Liu, and Weiwei Wang. Improved Na+ estimation from hyperspectral data of saline vegetation by machine learning. *Computers and Electronics in Agriculture*, 196, 5 2022. ISSN 01681699. doi: 10.1016/j.compag.2022.106862. URL https://www.sciencedirect.com/science/article/pii/S016816992200179X#t0015. (pages 23, 24, 110, 111, and 112)

Yun-ping Chen, Jie HU, Zhi-wen CAI, Jing-ya YANG, Wei ZHOU, Qiong HU, Cong WANG, Liang-zhi YOU, and Bao-dong XU. A phenology-based vegetation index for improving ratoon rice mapping using harmonized Landsat and Sentinel-2 data. *Journal of Integrative Agriculture*, 5 2023. ISSN 2095-3119. doi: 10.1016/J.JIA.2023.05.035. (pages xxiii, 39, and 40)

Thatchapol Chungcharoen, Irwin Donis-Gonzalez, Kittisak Phetpan, Vasu Udompetaikul, Panmanas Sirisomboon, and Rattapong Suwalak. Machine learning-based prediction of nutritional status in oil palm leaves using proximal multispectral images. *Computers and Electronics in Agriculture*, 198, 7 2022. ISSN 01681699. doi: 10.1016/j.compag.2022.107019. (pages 81 and 82)

Daniel Cozzolino, Madeleine F Dupont, Aaron Elbourne, Vi Khanh Truong, Aoife Power, and James Chapman. Chapter 9 - Role of sensors in fruit nutrition. In A K Srivastava and Chengxiao Hu, editors, *Fruit Crops*, pages 111–119. Elsevier, 2020. ISBN 978-0-12-818732-6. doi: https://doi.org/10.1016/B978-0-12-818732-6.00009-5. URL https://www.sciencedirect.com/science/article/pii/B9780128187326000095. (pages xxiii, 37, and 38)

Pedro V. de Azevedo, Cleber B. de Souza, Bernardo B. da Silva, and Vicente P.R. da Silva. Water requirements of pineapple crop grown in a tropical environment, Brazil. *Agricultural Water Management*, 88(1-3):201–208, 3 2007. ISSN 03783774. doi: 10.1016/j.agwat.2006.10.021. (page 3)

Colette de Villiers, Cilence Munghemezulu, Zinhle Mashaba-Munghemezulu, George J. Chirima, and Solomon G. Tesfamichael. Weed Detection in Rainfed Maize Crops Using UAV and PlanetScope Imagery. *Sustainability 2023, Vol. 15, Page 13416*, 15(18):13416, 9 2023. ISSN 2071-1050. doi: 10.3390/SU151813416. URL https://www.mdpi.com/2071-1050/15/18/13416/htmhttps://www.mdpi.com/2071-1050/15/18/13416. (page 111)

Sinan Demir, Mert Dedeoğlu, and Levent Başayiğit. Yield prediction models of organic oil rose farming with agricultural unmanned aerial vehicles (UAVs) images and machine learnaing algorithms. *Remote Sensing Applications: Society and Environment*, 33:101131, 1 2024. ISSN 2352-9385. doi: 10.1016/J.RSASE.2023.101131. (page 2)

Carlos A Devia, Juan P Rojas, E Petro Carol, Martinez Ivan, F Mondragon D Patino, and J Colorado. High-Throughput Biomass Estimation in Rice Crops Using UAV Multispectral Imagery. *Journal of Intelligent & Robotic Systems*, 2019. URL https://link.springer.com/article/10.1007/s10846-019-01001-5. (page 4)

Rui Dong, Yuxin Miao, Xinbing Wang, Fei Yuan, and Krzysztof Kusnierek. Combining leaf fluorescence and active canopy reflectance sensing technologies to diagnose maize nitrogen status across growth stages. *Precision Agriculture*, 23(3):939–960, 6 2022. ISSN 15731618. doi: 10.1007/S11119-021-09869-W/METRICS. URL https://link.springer.com/article/10.1007/s11119-021-09869-w. (pages 20, 23, 104, and 109)

Oumnia Ennaji, Leonardus Vergütz, and Achraf El Allali. Machine learning in nutrient management: A review. *Artificial Intelligence in Agriculture*, 9:1–11, 9 2023. ISSN 2589-7217. doi: 10.1016/J.AIIA.2023.06.001. (pages xv, 9, 11, 49, 90, 118, 119, and 120)

Eduardo Esteves, Guilherme Locatelli, Neus Alcon Bou, and Rhuanito Soranz Ferrarezi. Sap analysis: A powerful tool for monitoring plant nutrition. *Horticulturae*, 7(11), 11 2021. ISSN 23117524. doi: 10.3390/HORTICULTURAE7110426. (page 36)

Kai Fan, Fenling Li, Xiaokai Chen, Zhenfa Li, and David J. Mulla. Nitrogen Balance Index Prediction of Winter Wheat by Canopy Hyperspectral Transformation and Machine Learning. *Remote Sensing 2022, Vol. 14, Page 3504*, 14(14):3504, 7 2022a. ISSN 2072-4292. doi: 10.3390/RS14143504. URL https://www.mdpi.com/2072-4292/14/14/3504/htmhttps://www.mdpi.com/2072-4292/14/14/3504. (pages 17, 18, 20, 104, and 109)

Yiguang Fan, Haikuan Feng, Xiuliang Jin, Jibo Yue, Yang Liu, Zhenhai Li, Zhihang Feng, Xiaoyu Song, and Guijun Yang. Estimation of the nitrogen content of potato plants based on morphological parameters and visible light vegetation indices. *Frontiers in Plant Science*, 13:1012070, 10 2022b. ISSN 1664462X. doi: 10.3389/FPLS.2022.1012070/BIBTEX. (pages 19 and 110)

FAO. Estadísticas sobre costos de producción agrícola. *Manual de estadísticas sobre costos de producción agrícola*, 2016. URL https://www.fao.org/3/ca6411es/ca6411es.pdf. (page 5)

Hafiz Umar Farid, Zahid Mahmood Khan, Muhammad Naveed Anjum, Aamir Shakoor, and Huzaifa Shahzad Qureshi. Precision Nitrogen Management for Cotton Using (GreenSeeker) Handheld Crop Sensors. *Environmental Sciences Proceedings 2022, Vol. 23, Page 12*, 23(1):12, 12 2022. ISSN 2673-4931. doi: 10.3390/ENVIRONSCIPROC2022023012. URL https://www.mdpi.com/2673-4931/23/1/12/htmhttps://www.mdpi.com/2673-4931/23/1/12. (page 23)

Farid Feizolahpour, Sina Besharat, Bakhtiar Feizizadeh, Vahid Rezaverdinejad, and Behzad Hessari. An integrative data-driven approach for monitoring corn biomass

under irrigation water and nitrogen levels based on UAV-based imagery. *Environmental Monitoring and Assessment*, 195(9):1–20, 9 2023. ISSN 15732959. doi: 10.1007/S10661-023-11697-6/METRICS. URL https://link.springer.com/article/10.1007/s10661-023-11697-6. (page 111)

Rodrigo G. Freitas, Francisco R.S. Pereira, Aliny A. Dos Reis, Paulo S.G. Magalhães, Gleyce K.D.A. Figueiredo, and Lucas R. do Amaral. Estimating pasture aboveground biomass under an integrated crop-livestock system based on spectral and texture measures derived from UAV images. *Computers and Electronics in Agriculture*, 198: 107122, 7 2022. ISSN 0168-1699. doi: 10.1016/J.COMPAG.2022.107122. (page 111)

Zhaopeng Fu, Shanshan Yu, Jiayi Zhang, Hui Xi, Yang Gao, Ruhua Lu, Hengbiao Zheng, Yan Zhu, Weixing Cao, and Xiaojun Liu. Combining UAV multispectral imagery and ecological factors to estimate leaf nitrogen and grain protein content of wheat. *European Journal of Agronomy*, 132:126405, 1 2022. ISSN 1161-0301. doi: 10.1016/J.EJA.2021.126405. (pages 9, 19, and 109)

J. P. Goffart, F. Ben Abdallah, D. Goffart, Y. Curnel, and V. Planchon. Potato Crop Nitrogen Status Monitoring for Sustainable N Fertilisation Management: Last 15 Years and Future-Expected Developments with Reference Method and Use of Optical Sensors. *Potato Research 2023 66:4*, 66(4):1257–1303, 8 2023. ISSN 1871-4528. doi: 10.1007/S11540-023-09644-6. URL https://link-springer-com.udea.lookproxy.com/article/10.1007/s11540-023-09644-6. (pages 11 and 42)

Girish Gopinath, U. Surendran, J. Vishak, Nimmi Sasidharan, and Muhamed Fasil CT. Hyperspectral data and vegetative indices for paddy: A case study in Kerala, India. *Remote Sensing Applications: Society and Environment*, 33:101109, 1 2024. ISSN 2352-9385. doi: 10.1016/J.RSASE.2023.101109. (page 111)

Maurice Günder, Facundo R. Ispizua Yamati, Jana Kierdorf, Ribana Roscher, Anne Katrin Mahlein, and Christian Bauckhage. Agricultural plant cataloging and establishment of a data framework from UAV-based crop images by computer vision. *GigaScience*, 11:1–14, 12 2022. ISSN 2047217X. doi: 10.1093/GIGASCIENCE/GIAC054. URL https://dx.doi.org/10.1093/gigascience/giac054. (page 111)

Antoine Haddon, Loïc Kechichian, Jérôme Harmand, Cyril Dejean, and Nassim Ait-Mouheb. Linking soil moisture sensors and crop models for irrigation management. *Ecological Modelling*, 484:110470, 10 2023. ISSN 0304-3800. doi: 10.1016/J.ECOLMODEL.2023.110470. (page 35)

Mohamad Hamze, Bruno Cheviron, Nicolas Baghdadi, Madiop Lo, Dominique Courault, and Mehrez Zribi. Detection of irrigation dates and amounts on maize plots from the integration of Sentinel-2 derived Leaf Area Index values in the Optirrig crop model. *Agricultural Water Management*, 283:108315, 6 2023. ISSN 0378-3774. doi: 10.1016/J.AGWAT.2023.108315. (page 112)

Liang Han, Guijun Yang, Xiaodong Yang, Xiaoyu Song, Bo Xu, Zhenhai Li, Jintao Wu, Hao Yang, and Jianwei Wu. An explainable XGBoost model improved by SMOTE-ENN technique for maize lodging detection based on multi-source unmanned aerial vehicle images. *Computers and Electronics in Agriculture*, 194:106804, 3 2022. ISSN 0168-1699. doi: 10.1016/J.COMPAG.2022.106804. (page 110)

S. B. Hareesh. The latest applications of remote sensing technologies for soil management in precision agriculture practices. *Remote Sensing in Precision Agriculture: Transforming Scientific Advancement into Innovation*, pages 105–135, 1 2024. doi: 10.1016/B978-0-323-91068-2.00008-4. (page 4)

Muhammad Zulkifl Hasan, Zurina Mohd Hanapi, Muhammad Zunnurain Hussain, Masnida Hussin, Nadeem Sarwar, and Mohammad Yahya Akhlaqi. Deep Insight into IoT-Enabled Agriculture and Network Protocols. *Wireless Communications and Mobile Computing*, 2022, 2022. ISSN 15308677. doi: 10.1155/2022/5617903. (pages 25 and 114)

Muhammad Hariz Bin Hasni and Salsabila Ahmad. Cost Effective MD2 Pineapple Smart Farming IoT Monitoring System in Chuping, Perlis. *2022 International Conference on Green Energy, Computing and Sustainable Technology, GECOST 2022*, pages 215–220, 2022. doi: 10.1109/GECOST55694.2022.10010624. URL https://ieeexplore.ieee.org/document/10010624. (page 1)

Jérémie Haumont, Peter Lootens, Simon Cool, Jonathan Van Beek, Dries Raymaekers, Eva Ampe, Tim De Cuypere, Onno Bes, Jonas Bodyn, and Wouter Saeys. Multispectral UAV-Based Monitoring of Leek Dry-Biomass and Nitrogen Uptake across Multiple Sites and Growing Seasons. *Remote Sensing 2022, Vol. 14, Page 6211*, 14 (24):6211, 12 2022. ISSN 2072-4292. doi: 10.3390/RS14246211. URL https://www.mdpi.com/2072-4292/14/24/6211/htmhttps://www.mdpi.com/2072-4292/14/24/6211. (page 111)

Li He, Meng Ran Liu, Yu Long Guo, Yong Kang Wei, Hai Yan Zhang, Xiao Song, Wei Feng, and Tian Cai Guo. Angular effect of algorithms for monitoring leaf nitrogen concentration of wheat using multi-angle remote sensing data. *Computers and Electronics in Agriculture*, 195, 4 2022. ISSN 01681699. doi: 10.1016/j.compag.2022.106815. URL https://www.sciencedirect.com/science/article/pii/S0168169922001326. (page 112)

Kpade O.L. Hounkpatin, Aymar Y. Bossa, Yacouba Yira, Mouïnou A. Igue, and Brice A. Sinsin. Assessment of the soil fertility status in Benin (West Africa) – Digital soil mapping using machine learning. *Geoderma Regional*, 28:e00444, 3 2022. ISSN 2352-0094. doi: 10.1016/J.GEODRS.2021.E00444. (page 109)

Gaganpreet Singh Hundal, Chad Matthew Laux, Dennis Buckmaster, Mathias J. Sutton, and Michael Langemeier. Exploring Barriers to the Adoption of Internet of Things-Based Precision Agriculture Practices. *Agriculture (Switzerland)*, 13(1):163, 1 2023. ISSN 20770472. doi: 10.3390/AGRICULTURE13010163/S1. URL https://www.mdpi.com/2077-0472/13/1/163/htmhttps://www.mdpi.com/2077-0472/13/1/163. (pages 24 and 114)

Firdaus Irwanto, Umar Hasan, Eric Saputra Lays, Ntivuguruzwa Jean De La Croix, Didacienne Mukanyiligira, Louis Sibomana, and Tohari Ahmad. IoT and fuzzy logic integration for improved substrate environment management in mushroom cultivation. *Smart Agricultural Technology*, 7:100427, 3 2024. ISSN 2772-3755. doi: 10.1016/J.ATECH.2024.100427. (pages 25 and 114)

Md Abrar Istiak, M. M.Mahbubul Syeed, Md Shakhawat Hossain, Mohammad Faisal Uddin, Mahady Hasan, Razib Hayat Khan, and Nafis Saami Azad. Adoption of Unmanned Aerial Vehicle (UAV) imagery in agricultural management: A systematic literature review. *Ecological Informatics*, 78:102305, 12 2023. ISSN 1574-9541. doi: 10.1016/J.ECOINF.2023.102305. (pages 9, 12, and 42)

Waheb A. Jabbar, Tan Mei Ting, M. Fikri I. Hamidun, Ajwad H. Che Kamarudin, Wenyan Wu, Jamil Sultan, Abdul Rahman A. Alsewari, and Mohammed A.H. Ali. Development of LoRaWAN-based IoT system for water quality monitoring in rural areas. *Expert Systems with Applications*, 242:122862, 5 2024. ISSN 0957-4174. doi: 10.1016/J.ESWA.2023.122862. (pages 26 and 114)

Nadeem Javaid. Integration of context awareness in Internet of Agricultural Things. *ICT Express*, 9(2):189–196, 4 2023. ISSN 2405-9595. doi: 10.1016/J.ICTE.2021.09.004. (pages 24 and 114)

Jie Jiang, Peter M. Atkinson, Jiayi Zhang, Ruhua Lu, Youyan Zhou, Qiang Cao, Yongchao Tian, Yan Zhu, Weixing Cao, and Xiaojun Liu. Combining fixed-wing UAV multispectral imagery and machine learning to diagnose winter wheat nitrogen status at the farm scale. *European Journal of Agronomy*, 138:126537, 8 2022. ISSN 1161-0301. doi: 10.1016/J.EJA.2022.126537. (pages 20 and 110)

Jie Jiang, Peter M. Atkinson, Chunsheng Chen, Qiang Cao, Yongchao Tian, Yan Zhu, Xiaojun Liu, and Weixing Cao. Combining UAV and Sentinel-2 satellite multi-spectral images to diagnose crop growth and N status in winter wheat at the county scale. *Field Crops Research*, 294:108860, 4 2023. ISSN 0378-4290. doi: 10.1016/J.FCR.2023.108860. URL https://www.sciencedirect.com/science/article/pii/S0378429023000539. (pages 18, 20, 104, and 109)

Bilal Karaman, Sezai Taskin, Daudi S. Simbeye, Mbazingwa E. Mkiramweni, and Aykut Kurtoglu. Design and development of smart cover system for vineyards. *Smart Agricultural Technology*, 3:100064, 2 2023. ISSN 2772-3755. doi: 10.1016/J.ATECH.2022.100064. URL https://linkinghub.elsevier.com/retrieve/pii/S2772375522000296. (pages 25 and 114)

Narayan Kayet, Khanindra Pathak, C.P. Singh, Bimal K. Bhattacharya, Rajiv Kumar Chaturvedi, Anjanikumar SV Brahmandam, and Chinmoy Mandal. Detection and mapping of vegetation stress using AVIRIS-NG hyperspectral imagery in coal mining sites. *Advances in Space Research*, 3 2023. ISSN 0273-1177. doi: 10.1016/J.ASR.2023.03.002. (pages 24 and 112)

Mahlatse Kganyago, Clement Adjorlolo, Paidamwoyo Mhangara, and Lesiba Tsoeleng. Optical remote sensing of crop biophysical and biochemical parameters: An overview of advances in sensor technologies and machine learning algorithms for precision agriculture. *Computers and Electronics in Agriculture*, 218:108730, 3 2024. ISSN 0168-1699. doi: 10.1016/J.COMPAG.2024.108730. (page 13)

Jasenka Gajdoš Kljusurić, Tamara Jurina, Davor Valinger, Maja Benkovi, and Ana Jurinjak Tušek. NIR spectroscopy and management of bioactive components, antioxidant activity, and macronutrients in fruits. *Fruit Crops*, pages 95–109, 2020.

doi: 10.1016/b978-0-12-818732-6.00008-3. URL https://www.sciencedirect.com/science/article/pii/B9780128187326000083. (page xxiii)

Jinmei Kou, Long Duan, Caixia Yin, Lulu Ma, Xiangyu Chen, Pan Gao, and Xin Lv. Predicting Leaf Nitrogen Content in Cotton with UAV RGB Images. *Sustainability 2022, Vol. 14, Page 9259*, 14(15):9259, 7 2022. ISSN 2071-1050. doi: 10.3390/SU14159259. URL https://www.mdpi.com/2071-1050/14/15/9259/htmhttps://www.mdpi.com/2071-1050/14/15/9259. (pages 22 and 110)

Rohit Kumar Kasera, Shivashish Gour, and Tapodhir Acharjee. A comprehensive survey on IoT and AI based applications in different pre-harvest, during-harvest and post-harvest activities of smart agriculture. *Computers and Electronics in Agriculture*, 216: 108522, 1 2024. ISSN 0168-1699. doi: 10.1016/J.COMPAG.2023.108522. (pages 3, 4, 24, and 26)

Dushyant Kumar Singh and Rajeev Sobti. Long-range real-time monitoring strategy for Precision Irrigation in urban and rural farming in society 5.0. *Computers & Industrial Engineering*, 167:107997, 5 2022. ISSN 0360-8352. doi: 10.1016/J.CIE.2022.107997. URL https://linkinghub.elsevier.com/retrieve/pii/S0360835222000675. (pages 24 and 114)

Maqsood Ahmed Lakho, Mushtaque Ahmed Jatoi, Najamuddin Solangi, Adel Ahmed Abul-Soad, Muneer Ahmed Qazi, and Gholamreza Abdi. Optimizing in vitro nutrient and ex vitro soil mediums-driven responses for multiplication, rooting, and acclimatization of pineapple. *Scientific Reports 2023 13:1*, 13(1):1–10, 1 2023. ISSN 2045-2322. doi: 10.1038/s41598-023-28359-9. URL https://www.nature.com/articles/s41598-023-28359-9. (page 1)

Dan Li, Yuxin Miao, Curtis J. Ransom, Gregory Mac Bean, Newell R. Kitchen, Fabián G. Fernández, John E. Sawyer, James J. Camberato, Paul R. Carter, Richard B. Ferguson, David W. Franzen, Carrie A.M. Laboski, Emerson D. Nafziger, and John F. Shanahan. Corn Nitrogen Nutrition Index Prediction Improved by Integrating Genetic, Environmental, and Management Factors with Active Canopy Sensing Using Machine Learning. *Remote Sensing 2022, Vol. 14, Page 394*, 14(2):394, 1 2022a. ISSN 2072-4292. doi: 10.3390/RS14020394. URL https://www.mdpi.com/2072-4292/14/2/394/htmhttps://www.mdpi.com/2072-4292/14/2/394. (page 110)

Jiating Li, Yufeng Ge, Laila Puntel, Derek Heeren, Guillermo Balboa, and Yeyin Shi. Combining machine learning with a mechanistic model to estimate maize nitrogen content from UAV-acquired hyperspectral imagery. *https://doi.org/10.1117/12.2663817*, 12539:48–55, 6 2023a. ISSN 1996756X. doi: 10.1117/12.2663817. URL https://www.spiedigitallibrary.org/conference-proceedings-of-spie/12539/1253905/Combining-machine-learning-with-a-mechanistic-model-to-estimate-maize/10.1117/12.2663817.fullhttps://www.spiedigitallibrary.org/conference-proceedings-of-spie/12539/1253905/Combining-machine-learning-with-a-mechanistic-model-to-estimate-maize/10.1117/12.2663817.short. (pages 8, 19, 22, and 109)

Kai Li, Juanle Wang, Wenjing Cheng, Yi Wang, Yezhi Zhou, and Ochir Altansukh. Deep learning empowers the Google Earth Engine for automated water extraction

in the Lake Baikal Basin. *International Journal of Applied Earth Observation and Geoinformation*, 112:102928, 8 2022b. ISSN 1569-8432. doi: 10.1016/J.JAG.2022.102928. (page 20)

Yue Li, Yuxin Miao, Jing Zhang, Davide Cammarano, Songyang Li, Xiaojun Liu, Yongchao Tian, Yan Zhu, Weixing Cao, and Qiang Cao. Improving Estimation of Winter Wheat Nitrogen Status Using Random Forest by Integrating Multi-Source Data Across Different Agro-Ecological Zones. *Frontiers in Plant Science*, 13:890892, 6 2022c. ISSN 1664462X. doi: 10.3389/FPLS.2022.890892/BIBTEX. URL www.frontiersin.org. (page 23)

Zhenhai Li, Zhenhong Li, David Fairbairn, Na Li, Bo Xu, Haikuan Feng, and Guijun Yang. Multi-LUTs method for canopy nitrogen density estimation in winter wheat by field and UAV hyperspectral. *Computers and Electronics in Agriculture*, 162:174–182, 7 2019. ISSN 01681699. doi: 10.1016/j.compag.2019.04.005. URL www.elsevier.com/locate/compag. (page 38)

Zongpeng Li, Xinguo Zhou, Qian Cheng, Shuaipeng Fei, and Zhen Chen. A Machine-Learning Model Based on the Fusion of Spectral and Textural Features from UAV Multi-Sensors to Analyse the Total Nitrogen Content in Winter Wheat. *Remote Sensing 2023, Vol. 15, Page 2152*, 15(8):2152, 4 2023b. ISSN 2072-4292. doi: 10.3390/RS15082152. URL https://www.mdpi.com/2072-4292/15/8/2152/htmhttps://www.mdpi.com/2072-4292/15/8/2152. (pages 18, 109, and 111)

Jiaxing Liang, Wei Ren, Xiaoyang Liu, Hainie Zha, Xian Wu, Chunkang He, Junli Sun, Mimi Zhu, Guohua Mi, Fanjun Chen, Yuxin Miao, and Qingchun Pan. Improving Nitrogen Status Diagnosis and Recommendation of Maize Using UAV Remote Sensing Data. *Agronomy*, 13(8):1994, 8 2023. ISSN 20734395. doi: 10.3390/AGRONOMY13081994/S1. URL https://www.mdpi.com/2073-4395/13/8/1994/htmhttps://www.mdpi.com/2073-4395/13/8/1994. (pages 17, 103, and 109)

Zhenghao Liang, Xin Jin, Pengfei Zhai, Yan Zhao, Jinwen Cai, Shoupeng Li, Shuyun Yang, Changzhen Li, and Changjiang Li. Combination of organic fertilizer and slow-release fertilizer increases pineapple yields, agronomic efficiency and reduces greenhouse gas emissions under reduced fertilization conditions in tropical areas. *Journal of Cleaner Production*, 343:131054, 4 2022. ISSN 0959-6526. doi: 10.1016/J.JCLEPRO.2022.131054. (pages xxii, 2, 9, and 35)

Zhen Liao, Yu long Dai, Han Wang, Quirine M. Ketterings, Jun sheng Lu, Fu cang Zhang, Zhi jun Li, and Jun liang Fan. A double-layer model for improving the estimation of wheat canopy nitrogen content from unmanned aerial vehicle multispectral imagery. *Journal of Integrative Agriculture*, 22(7):2248–2270, 7 2023. ISSN 2095-3119. doi: 10.1016/J.JIA.2023.02.022. (pages xxiii, 9, and 34)

Huanhuan Liu, Yue Liu, Yu Chen, Mengen Fan, Yin Chen, Chengcheng Gang, Yongfa You, and Zhuonan Wang. Dynamics of global dryland vegetation were more sensitive to soil moisture: Evidence from multiple vegetation indices. *Agricultural and Forest Meteorology*, 331:109327, 3 2023a. ISSN 0168-1923. doi: 10.1016/J.AGRFORMET.2023.109327. (pages 5, 18, 19, 22, 41, 109, and 112)

Shishi Liu, Xiaohui Bai, Gege Zhu, Yu Zhang, Lantao Li, Tao Ren, and Jianwei Lu. Remote estimation of leaf nitrogen concentration in winter oilseed rape across growth stages and seasons by correcting for the canopy structural effect. *Remote Sensing of Environment*, 284:113348, 1 2023b. ISSN 0034-4257. doi: 10.1016/J.RSE.2022.113348. (page 19)

Tian Hu Liu, Xiang Ning Nie, Jin Meng Wu, Di Zhang, Wei Liu, Yi Feng Cheng, Yan Zheng, Jian Qiu, and Long Qi. Pineapple (Ananas comosus) fruit detection and localization in natural environment based on binocular stereo vision and improved YOLOv3 model. *Precision Agriculture*, 24(1):139–160, 2 2023c. ISSN 15731618. doi: 10.1007/S11119-022-09935-X/TABLES/5. URL https://link-springer-com.udea.lookproxy.com/article/10.1007/s11119-022-09935-x. (page 31)

Yang Liu, Yiguang Fan, Haikuan Feng, Riqiang Chen, Mingbo Bian, Yanpeng Ma, Jibo Yue, and Guijun Yang. Estimating potato above-ground biomass based on vegetation indices and texture features constructed from sensitive bands of UAV hyperspectral imagery. *Computers and Electronics in Agriculture*, 220:108918, 5 2024. ISSN 0168-1699. doi: 10.1016/J.COMPAG.2024.108918. (pages 24 and 112)

Alfonso Llanderal, Pedro García-Caparrós, José Pérez-Alonso, Juana Isabel Contreras, María Luz Segura, Juan Reca, and María Teresa Lao. Approach to petiole sap nutritional diagnosis method by empirical model based on climatic and growth parameters. *Agronomy*, 10(2), 2020. ISSN 20734395. doi: 10.3390/agronomy10020188. URL https://www.mdpi.com/2073-4395/10/2/188/htm. (pages 35 and 36)

Junjun Lu, Erfu Dai, Yuxin Miao, and Krzysztof Kusnierek. Improving active canopy sensor-based in-season rice nitrogen status diagnosis and recommendation using multi-source data fusion with machine learning. *Journal of Cleaner Production*, 380:134926, 12 2022a. ISSN 0959-6526. doi: 10.1016/J.JCLEPRO.2022.134926. (pages 19, 20, and 110)

Ning Lu, Yapeng Wu, Hengbiao Zheng, Xia Yao, Yan Zhu, Weixing Cao, and Tao Cheng. An assessment of multi-view spectral information from UAV-based color-infrared images for improved estimation of nitrogen nutrition status in winter wheat. *Precision Agriculture*, 23(5):1653–1674, 10 2022b. ISSN 15731618. doi: 10.1007/S11119-022-09901-7/METRICS. URL https://link.springer.com/article/10.1007/s11119-022-09901-7. (page 110)

Jan Lukáš, Pavel Hamouz, Jose Antonio Dominguez-Gómez, Dorijan Radočaj, Ante Šiljeg, Ivan Plaščak, Ivan Mari´c Mari´c, and Mladen Juriši´c Juriši´c. A Micro-Scale Approach for Cropland Suitability Assessment of Permanent Crops Using Machine Learning and a Low-Cost UAV. *Agronomy 2023, Vol. 13, Page 362*, 13(2):362, 1 2023. ISSN 2073-4395. doi: 10.3390/AGRONOMY13020362. URL https://www.mdpi.com/2073-4395/13/2/362/htmhttps://www.mdpi.com/2073-4395/13/2/362. (pages 22 and 111)

Lulu Ma, Xiangyu Chen, Qiang Zhang, Jiao Lin, Caixia Yin, Yiru Ma, Qiushuang Yao, Lei Feng, Ze Zhang, and Xin Lv. Estimation of Nitrogen Content Based on the Hyperspectral Vegetation Indexes of Interannual and Multi-Temporal in Cotton. *Agronomy 2022, Vol. 12, Page 1319*, 12(6):1319, 5 2022. ISSN 2073-4395. doi:

10.3390/AGRONOMY12061319. URL https://www.mdpi.com/2073-4395/12/6/1319/htmhttps://www.mdpi.com/2073-4395/12/6/1319. (page 110)

Victor Martins Maia, Rodinei Facco Pegoraro, Ignácio Aspiazú, Fernanda Soares Oliveira, and Danúbia Aparecida Costa Nobre. Diagnosis and management of nutrient constraints in pineapple. *Fruit Crops: Diagnosis and Management of Nutrient Constraints*, pages 739–760, 1 2020. doi: 10.1016/B978-0-12-818732-6.00050-2. (pages xxii and 2)

Parijata Majumdar, Sanjoy Mitra, and Diptendu Bhattacharya. IoT for Promoting Agriculture 4.0: a Review from the Perspective of Weather Monitoring, Yield Prediction, Security of WSN Protocols, and Hardware Cost Analysis. *Journal of Biosystems Engineering*, 46(4):440–461, 12 2021. ISSN 22341862. doi: 10.1007/S42853-021-00118-6/TABLES/16. URL https://aplicacionesbiblioteca.udea.edu.co:2430/article/10.1007/s42853-021-00118-6. (page 14)

Parijata Majumdar, Diptendu Bhattacharya, Sanjoy Mitra, and Bharat Bhushan. Application of Green IoT in Agriculture 4.0 and Beyond: Requirements, Challenges and Research Trends in the Era of 5G, LPWANs and Internet of UAV Things. *Wireless Personal Communications*, 131(3):1767–1816, 8 2023. ISSN 1572834X. doi: 10.1007/S11277-023-10521-1/FIGURES/26. URL https://link-springer-com.udea.lookproxy.com/article/10.1007/s11277-023-10521-1. (page 24)

C. Maraveas, D. Piromalis, K.G. Arvanitis, T. Bartzanas, and D. Loukatos. Applications of IoT for optimized greenhouse environment and resources management. *Computers and Electronics in Agriculture*, 198:106993, 7 2022. ISSN 0168-1699. doi: 10.1016/J.COMPAG.2022.106993. URL https://linkinghub.elsevier.com/retrieve/pii/S0168169922003106. (page 114)

Victor Martins, Rodinei Facco Pegoraro, Ignácio Aspiazú, Fernanda Soares Oliveira, and Danúbia Aparecida Costa Nobre. Diagnosis and management of nutrient constraints in pineapple. In Elsevier, editor, *Fruit Crops*, chapter 50, pages 739–760. Elsevier, Belo Horizonte, Brazil, primera edition, 1 2020. doi: 10.1016/b978-0-12-818732-6.00050-2. URL https://www.sciencedirect.com/science/article/pii/B9780128187326000502. (pages xii, 31, 32, 33, 34, and 35)

Senthilkumar Mathi, R Akshaya, and K Sreejith. An Internet of Things-based Efficient Solution for Smart Farming. *Procedia Computer Science*, 218:2806–2819, 1 2023. ISSN 1877-0509. doi: 10.1016/J.PROCS.2023.01.252. URL https://linkinghub.elsevier.com/retrieve/pii/S1877050923002521. (pages xxiii, 22, and 114)

Julio Mej and Jhon Guerrero Narvaez. Analysis of Normalized Vegetation Index in Castile Coffee Crops , Using Mosaics of Multispectral Images Acquired by Unmanned Aerial Vehicle (UAV). *Communications in Computer and Information Science. First International Conference, ICAT 2019*, pages 546–559, 2020. URL https://link.springer.com/chapter/10.1007/978-3-030-42520-3_43. (page 4)

Mello Prado. Nitrogen. In *Mineral nutrition of tropical plants*, volume 1, pages 69–98. Springer, Cham, Cham, 2021. doi: 10.1007/978-3-030-71262-4{_}4. URL https://link-springer-com.udea.lookproxy.com/chapter/10.1007/978-3-030-71262-4_4. (pages xxii and 72)

MicaSense. RedEdge Camera Radiometric Calibration Model – MicaSense Knowledge Base, 2020. URL https://support.micasense.com/hc/en-us/articles/115000351194-RedEdge-Camera-Radiometric-Calibration-Model. (pages 47 and 48)

MicaSense. Radiometric Calibration Model for MicaSense Sensors – MicaSense Knowledge Base, 2022. URL https://support.micasense.com/hc/en-us/articles/115000351194-RedEdge-Camera-Radiometric-Calibration-Model. (pages 76 and 77)

Saeid Minaei, Maryam Soltanikazemi, Hossein Shafizadeh-Moghadam, and Alireza Mahdavian. Field-scale estimation of sugarcane leaf nitrogen content using vegetation indices and spectral bands of Sentinel-2: Application of random forest and support vector regression. *Computers and Electronics in Agriculture*, 200:107130, 9 2022. ISSN 0168-1699. doi: 10.1016/J.COMPAG.2022.107130. (page 110)

Corpoica Minagricultura. PECTIA, Plan Estratégico de Ciencia, Tecnología e Innovación del Sector Agropecuario Colombiano, 2022. URL http://www.colombiacompetitiva.gov.co/sncei/Documents/pectia-terminado.pdf. (page 5)

Maimunah Mohd Ali, Norhashila Hashim, Siti Khairunniza Bejo, Mahirah Jahari, and Nurul Aqilah Shahabudin. Innovative non-destructive technologies for quality monitoring of pineapples: Recent advances and applications. *Trends in Food Science & Technology*, 133:176–188, 3 2023. ISSN 0924-2244. doi: 10.1016/J.TIFS.2023.02.005. URL https://linkinghub.elsevier.com/retrieve/pii/S0924224423000560. (page xxii)

A Mohsin, Abida Jabeen, Darakshan Majid, Farhana Mehraj Allai, A H Dar, B Gulzar, and H A Makroo. Pineapple. In Gulzar Ahmad Nayik and Amir Gull, editors, *Antioxidants in Fruits: Properties and Health Benefits*, pages 379–396. Springer Singapore, Singapore, 2020. ISBN 978-981-15-7285-2. doi: 10.1007/978-981-15-7285-2{_}19. URL https://doi.org/10.1007/978-981-15-7285-2_19. (pages xxii, 5, 32, 33, and 101)

David Montero, César Aybar, Miguel D. Mahecha, Francesco Martinuzzi, Maximilian Söchting, and Sebastian Wieneke. A standardized catalogue of spectral indices to advance the use of remote sensing in Earth system research. *Scientific Data 2023 10:1*, 10(1):1–20, 4 2023. ISSN 2052-4463. doi: 10.1038/s41597-023-02096-0. URL https://www.nature.com/articles/s41597-023-02096-0. (page 12)

Abdennabi Morchid, Rachid El Alami, Aeshah A. Raezah, and Yassine Sabbar. Applications of internet of things (IoT) and sensors technology to increase food security and agricultural Sustainability: Benefits and challenges. *Ain Shams Engineering Journal*, 15(3):102509, 3 2024a. ISSN 2090-4479. doi: 10.1016/J.ASEJ.2023.102509. (pages 24 and 25)

Abdennabi Morchid, Ishaq G. Muhammad Alblushi, Haris M. Khalid, Rachid El Alami, Surendar Rama Sitaramanan, and S. M. Muyeen. High-technology agriculture system to enhance food security: A concept of smart irrigation system using Internet of Things and cloud computing. *Journal of the Saudi Society of Agricultural Sciences*, 2 2024b. ISSN 1658-077X. doi: 10.1016/J.JSSAS.2024.02.001. (pages 24 and 114)

M Mouazen, Sizhe Xu, Xingang Xu, Clive Blacker, Rachel Gaulton, Qingzhen Zhu, Meng Yang, Guijun Yang, Jianmin Zhang, Yongan Yang, Min Yang, Hanyu Xue, Xiaodong Yang, and Liping Chen. Estimation of Leaf Nitrogen Content in Rice Using Vegetation Indices and Feature Variable Optimization with Information Fusion of Multiple-Sensor Images from UAV. *Remote Sensing 2023, Vol. 15, Page 854*, 15(3):854, 2 2023. ISSN 2072-4292. doi: 10.3390/RS15030854. URL https://www.mdpi.com/2072-4292/15/3/854/htmhttps://www.mdpi.com/2072-4292/15/3/854. (pages xxiii, 22, and 82)

Amarasingam Narmilan, Felipe Gonzalez, Arachchige Surantha Ashan Salgadoe, Unupen Widanelage Lahiru Madhushanka Kumarasiri, Hettiarachchige Asiri Sampageeth Weerasinghe, and Buddhika Rasanjana Kulasekara. Predicting Canopy Chlorophyll Content in Sugarcane Crops Using Machine Learning Algorithms and Spectral Vegetation Indices Derived from UAV Multispectral Imagery. *Remote Sensing 2022, Vol. 14, Page 1140*, 14(5):1140, 2 2022. ISSN 2072-4292. doi: 10.3390/RS14051140. URL https://www.mdpi.com/2072-4292/14/5/1140/htmhttps://www.mdpi.com/2072-4292/14/5/1140. (pages 22 and 111)

Manuela Zude-Sasse Nikos Tsoulias, Kowshik Kumar Saha. In-situ fruit analysis by means of LiDAR 3D point cloud of normalized difference vegetation index (NDVI). *Computers and Electronics in Agriculture*, 205:107611, 2 2023. ISSN 0168-1699. doi: 10.1016/J.COMPAG.2022.107611. (pages 22 and 112)

Angélica María Olaya, Alberto Díaz, Alejandro Fernández, and Alfredo Ayala. *Brechas tecnológicas de la cadena productiva de la piña en el Valle del Cauca y descripción del estado del arte*, volume 1. Centro Internacional de Agricultura Tropical (Ciat), Valle del Cauca, primera edición edition, 3 2022. ISBN 978-958-794-763-2. URL https://ladera.palmira.unal.edu.co/downloads/7_Pina_Brechas_Final_WEB.pdf. (pages 1 and 5)

F. S. Oliveira, V. M. Maia, M. P. dos Santos, R. F. Pegoraro, S. R. dos Santos, and M. K. Kondo. Yield and quality of pineapple fertigated with treated wastewater. *Fruits*, 77 (1), 2022. ISSN 1625967X. doi: 10.17660/TH2022/003. (page xxii)

Francisco M. Padilla, Michela Farneselli, Giorgio Gianquinto, Francesco Tei, and Rodney B. Thompson. Monitoring nitrogen status of vegetable crops and soils for optimal nitrogen management. *Agricultural Water Management*, 241:106356, 11 2020. ISSN 18732283. doi: 10.1016/j.agwat.2020.106356. URL https://www.sciencedirect.com/science/article/pii/S0378377420302225. (page 3)

Chanki Pandey, Prabira Kumar Sethy, Santi Kumari Behera, Jaya Vishwakarma, and Vishal Tande. Smart agriculture: Technological advancements on agriculture—A systematical review. In *Deep Learning for Sustainable Agriculture*, pages 1–56. Elsevier, 1 2022. doi: 10.1016/B978-0-323-85214-2.00002-1. URL https://linkinghub.elsevier.com/retrieve/pii/B9780323852142000021. (page 13)

Manish Patel, José Padarian, Andrew W. Western, Glenn J. Fitzgerald, Alex B. McBratney, Eileen M. Perry, Helen Suter, and Dongryeol Ryu. Retrieving canopy nitrogen concentration and aboveground biomass with deep learning for ryegrass and barley: Comparing models and determining waveband contribution. *Field Crops Research*, 294:108859, 4 2023. ISSN 0378-4290. doi: 10.1016/J.FCR.2023.108859. (page 23)

Manish Kumar Patel, Dongryeol Ryu, Andrew W. Western, Glenn J. Fitzgerald, Eileen M. Perry, Helen Suter, and Iain M. Young. A new multispectral index for canopy nitrogen concentration applicable across growth stages in ryegrass and barley. *Precision Agriculture*, 25(1):486–519, 2 2024. ISSN 15731618. doi: 10.1007/S11119-023-10081-1/FIGURES/8. URL https://link.springer.com/article/10.1007/s11119-023-10081-1. (pages 19 and 109)

Vivek Ramakant Pathmudi, Narendra Khatri, Sandeep Kumar, Antar Shaddad Hamed Abdul-Qawy, and Ajay Kumar Vyas. A systematic review of IoT technologies and their constituents for smart and sustainable agriculture applications. *Scientific African*, page e01577, 2 2023. ISSN 2468-2276. doi: 10.1016/J.SCIAF.2023.E01577. URL https://linkinghub.elsevier.com/retrieve/pii/S2468227623000364. (page xxii)

Suchitra M. Patil, Sunita Choudhary, Jana Kholová, Krithika Anbazhagan, Yogesh Parnandi, Priyanka Gattu, Srikanth Mallayee, Prasad Ksvv, V. Padma Kumar, P. Rajalakshmi, Magesh Chandramouli, and J. Adinarayana. UAV-based Digital Field Phenotyping for Crop Nitrogen Estimation using RGB Imagery. *2023 IEEE IAS Global Conference on Emerging Technologies, GlobConET 2023*, 2023. doi: 10.1109/GLOBCONET56651.2023.10150110. (pages 11, 19, 21, 42, and 109)

Sheng-zhao PEI, Hua-liang ZENG, Yu-long DAI, Wen-qiang BAI, and Jun-liang FAN. Nitrogen nutrition diagnosis for cotton under mulched drip irrigation using unmanned aerial vehicle multispectral images. *Journal of Integrative Agriculture*, 2 2023. ISSN 2095-3119. doi: 10.1016/J.JIA.2023.02.027. (pages 22 and 111)

Xuelian Peng, Dianyu Chen, Zhenjiang Zhou, Zhitao Zhang, Can Xu, Qing Zha, Fang Wang, and Xiaotao Hu. Prediction of the Nitrogen, Phosphorus and Potassium Contents in Grape Leaves at Different Growth Stages Based on UAV Multispectral Remote Sensing. *Remote Sensing 2022, Vol. 14, Page 2659*, 14(11):2659, 6 2022. ISSN 2072-4292. doi: 10.3390/RS14112659. URL https://www.mdpi.com/2072-4292/14/11/2659/htmhttps://www.mdpi.com/2072-4292/14/11/2659. (pages 21 and 110)

F. R.da S. Pereira, J. P. de Lima, R. G. Freitas, A. A. Dos Reis, L. R.do Amaral, G. K.D.A. Figueiredo, R. A.C. Lamparelli, and P. S.G. Magalhães. Nitrogen variability assessment of pasture fields under an integrated crop-livestock system using UAV, PlanetScope, and Sentinel-2 data. *Computers and Electronics in Agriculture*, 193: 106645, 2 2022. ISSN 0168-1699. doi: 10.1016/J.COMPAG.2021.106645. (pages 22 and 111)

Tinao Petso and Rodrigo S. Jamisola. A Review on Deep Learning on UAV Monitoring Systems for Agricultural Applications. *Studies in Computational Intelligence*, 1093: 335–368, 2023. ISSN 18609503. doi: 10.1007/978-3-031-28715-2{_}11/COVER. URL https://link.springer.com/chapter/10.1007/978-3-031-28715-2_11. (page 13)

Khongdet Phasinam, Thanwamas Kassanuk, Priyanka P. Shinde, Chetan M. Thakar, Dilip Kumar Sharma, Md Khaja Mohiddin, and Abdul Wahab Rahmani. Application of IoT and Cloud Computing in Automation of Agriculture Irrigation. *Journal of Food Quality*, 2022, 2022. ISSN 17454557. doi: 10.1155/2022/8285969. (pages 25 and 114)

Chander Prakash, Lakhwinder Pal Singh, Ajay Gupta, and Shiv Kumar Lohan. Advancements in smart farming: A comprehensive review of IoT, wireless communication, sensors, and hardware for agricultural automation. *Sensors and Actuators A: Physical*, 362:114605, 11 2023. ISSN 0924-4247. doi: 10.1016/J.SNA.2023.114605. (pages 14 and 26)

G. S. Prasanna Lakshmi, P. N. Asha, G. Sandhya, S. Vivek Sharma, S. Shilpashree, and S. G. Subramanya. An intelligent IOT sensor coupled precision irrigation model for agriculture. *Measurement: Sensors*, 25:100608, 2 2023. ISSN 2665-9174. doi: 10.1016/J.MEASEN.2022.100608. (pages 24 and 114)

Bayu Taruna Widjaja Putra, Hendra Cipta Wirayuda, Wahyu Nurkholis Hadi Syahputra, and Erwin Prastowo. Evaluating in-situ maize chlorophyll content using an external optical sensing system coupled with conventional statistics and deep neural networks. *Measurement*, 189:110482, 2 2022. ISSN 0263-2241. doi: 10.1016/J.MEASUREMENT.2021.110482. (pages 18 and 110)

Lang Qiao, Weijie Tang, Dehua Gao, Ruomei Zhao, Lulu An, Minzan Li, Hong Sun, and Di Song. UAV-based chlorophyll content estimation by evaluating vegetation index responses under different crop coverages. *Computers and Electronics in Agriculture*, 196:106775, 5 2022. ISSN 0168-1699. doi: 10.1016/J.COMPAG.2022.106775. URL https://www.sciencedirect.com/science/article/pii/S0168169922000928. (page 81)

Dorijan Radočaj, Ante Šiljeg, Rajko Marinović, and Mladen Jurišić. State of Major Vegetation Indices in Precision Agriculture Studies Indexed in Web of Science: A Review. *Agriculture 2023, Vol. 13, Page 707*, 13(3):707, 3 2023. ISSN 2077-0472. doi: 10.3390/AGRICULTURE13030707. URL https://www.mdpi.com/2077-0472/13/3/707/htmhttps://www.mdpi.com/2077-0472/13/3/707. (page 12)

Ricson L Ines, Precious Grace, B Daping, Zoila M Duque, and Romar P Regalario. Water Management of Organic-Based Pineapple in Upland Sloping Production Areas. *Agricultural Science*, 5(1):p1–p1, 4 2023. ISSN 2690-4799. doi: 10.30560/AS.V5N1P1. URL https://j.ideasspread.org/index.php/as/article/view/1166. (page 3)

Gilberto Rivera, Raúl Porras, Rogelio Florencia, and J. Patricia Sánchez-Solís. LiDAR applications in precision agriculture for cultivating crops: A review of recent advances. *Computers and Electronics in Agriculture*, 207:107737, 4 2023. ISSN 0168-1699. doi: 10.1016/J.COMPAG.2023.107737. URL https://www.sciencedirect.com/science/article/abs/pii/S0168169923001254. (page 11)

Edwin Blasnilo Rúa, Edwin Blasnilo Rúa, Andrea Isabel Barrera, and Benjamin Pinzón. Caracterización y diagnóstico de la cadena productiva de la piña en el departamento del Casanare. *Revista Estrategia Organizacional*, 5(0):29 – 47, 12 2016. ISSN 2339-3866. doi: 10.22490/25392786.2099. URL https://hemeroteca.unad.edu.co/index.php/revista-estrategica-organizacio/article/view/2099. (page 5)

Guojie Ruan, Urs Schmidhalter, Fei Yuan, Davide Cammarano, Xiaojun Liu, Yongchao Tian, Yan Zhu, Weixing Cao, and Qiang Cao. Exploring the transferability of wheat nitrogen status estimation with multisource data and Evolutionary Algorithm-Deep

Learning (EA-DL) framework. *European Journal of Agronomy*, 143:126727, 2 2023. ISSN 1161-0301. doi: 10.1016/J.EJA.2022.126727. (pages 9, 18, 19, 20, and 109)

Maneesha S. R, Sujeet Desai, S.Priya Devi, and Mathala J Gupta. Estimation of Crop Water Requirement of Pineapple (Ananas comosus (L.) Merr.) for Drip Fertigation. *International Journal of Bio-resource and Stress Management*, 13(Sep, 9):973–980, 9 2022. URL https://ojs.pphouse.org/index.php/IJBSM/article/view/4304. (page 32)

Tanzila Saba, Amjad Rehman, Khalid Haseeb, Saeed Ali Bahaj, and Jaime Lloret. Trust-based decentralized blockchain system with machine learning using Internet of agriculture things. *Computers and Electrical Engineering*, 108:108674, 5 2023. ISSN 0045-7906. doi: 10.1016/J.COMPELECENG.2023.108674. (pages 24 and 114)

Purificación Sáez-Plaza, María José Navas, Sławomir Wybraniec, Tadeusz Michałowski, and Agustín García Asuero. An Overview of the Kjeldahl Method of Nitrogen Determination. Part II. Sample Preparation, Working Scale, Instrumental Finish, and Quality Control. *http://dx.doi.org/10.1080/10408347.2012.751787*, 43(4):224–272, 10 2013. ISSN 10408347. doi: 10.1080/10408347.2012.751787. URL https://www.tandfonline.com/doi/abs/10.1080/10408347.2012.751787. (page 73)

Rabi N. Sahoo, R. G. Rejith, Shalini Gakhar, Rajeev Ranjan, Mahesh C. Meena, Abir Dey, Joydeep Mukherjee, Rajkumar Dhakar, Abhishek Meena, Anchal Daas, Subhash Babu, Pravin K. Upadhyay, Kapila Sekhawat, Sudhir Kumar, Mahesh Kumar, Viswanathan Chinnusamy, and Manoj Khanna. Drone remote sensing of wheat N using hyperspectral sensor and machine learning. *Precision Agriculture*, 25(2):704–728, 4 2023. ISSN 15731618. doi: 10.1007/S11119-023-10089-7/METRICS. URL https://link.springer.com/article/10.1007/s11119-023-10089-7. (pages 18 and 109)

D. R. K. Saikanth, Khushboo Gupta, Priya Srivastava, Manoher Saryam, K. Sudha Rani, Pooja Jena, and Sandeep Rout. Environmental Sustainability and Food Security of Traditional Agricultural Practices in India: A Review. *International Journal of Environment and Climate Change*, 13(8):1847–1856, 6 2023. ISSN 2581-8627. doi: 10.9734/IJECC/2023/V13I82138. URL https://journalijecc.com/index.php/IJECC/article/view/2138. (pages 5 and 11)

S. Sakthipriya and R. Naresh. Effective Energy Estimation Technique to classify the nitrogen and temperature for crop yield based Green house Application. *Sustainable Computing: Informatics and Systems*, page 100687, 2 2022. ISSN 2210-5379. doi: 10.1016/J.SUSCOM.2022.100687. URL https://linkinghub.elsevier.com/retrieve/pii/S2210537922000294. (page xxiii)

Itamar Salazar-Reque, Daniel Arteaga, Fabiola Mendoza, Maria Elena Rojas, Jonell Soto, Samuel Huaman, and Guillermo Kemper. Differentiating nutritional and water statuses in Hass avocado plantations through a temporal analysis of vegetation indices computed from aerial RGB images. *Computers and Electronics in Agriculture*, 213:108246, 10 2023. ISSN 0168-1699. doi: 10.1016/J.COMPAG.2023.108246. (pages 22, 24, and 112)

Adil K. Salman, Saad E. Aldulaimy, Huthaifa J. Mohammed, and Yaareb M. Abed. Performance of soil moisture sensors in gypsiferous and salt-affected soils. *Biosystems Engineering*, 209:200–209, 9 2021. ISSN 1537-5110. doi: 10.1016/J.BIOSYSTEMSENG.2021.07.006. (page 60)

Pritimoy Sanyal and Achyuth Sarkar. Application of Computer Science in Pineapple Cultivation and Diagnosis of its Diseases- A Systematic Study. *Proceedings of the 2021 IEEE 18th India Council International Conference, INDICON 2021*, 2021. doi: 10.1109/INDICON52576.2021.9691584. (page 33)

T. Saranya, C. Deisy, S. Sridevi, and Kalaiarasi Sonai Muthu Anbananthen. A comparative study of deep learning and Internet of Things for precision agriculture. *Engineering Applications of Artificial Intelligence*, 122:106034, 6 2023. ISSN 0952-1976. doi: 10.1016/J.ENGAPPAI.2023.106034. (page xxiii)

Abhinav Sharma, Arpit Jain, Prateek Gupta, and Vinay Chowdary. Machine Learning Applications for Precision Agriculture: A Comprehensive Review. *IEEE Access*, 9: 4843–4873, 2021. ISSN 21693536. doi: 10.1109/ACCESS.2020.3048415. (page 49)

Yuri Shendryk, Jeremy Sofonia, Robert Garrard, Yannik Rist, Danielle Skocaj, and Peter Thorburn. Fine-scale prediction of biomass and leaf nitrogen content in sugarcane using UAV LiDAR and multispectral imaging. *International Journal of Applied Earth Observation and Geoinformation*, 92:102177, 10 2020. ISSN 1872826X. doi: 10.1016/j.jag.2020.102177. URL https://aplicacionesbiblioteca.udea.edu.co:2062/science/article/pii/S0303243420303457. (pages xxiii, 40, 41, 52, 82, 88, and 103)

Meiyan Shu, Shuaipeng Fei, Bingyu Zhang, Xiaohong Yang, Yan Guo, Baoguo Li, and Yuntao Ma. Application of UAV Multisensor Data and Ensemble Approach for High-Throughput Estimation of Maize Phenotyping Traits. *Plant Phenomics*, 2022, 2022. ISSN 26436515. doi: 10.34133/2022/9802585. URL https://spj.science.org/doi/10.34133/2022/9802585. (pages 18, 21, 22, and 109)

Luís Silva, Luís Alcino Conceição, Fernando Cebola Lidon, and Benvindo Maçãs. Remote Monitoring of Crop Nitrogen Nutrition to Adjust Crop Models: A Review. *Agriculture 2023, Vol. 13, Page 835*, 13(4):835, 4 2023. ISSN 2077-0472. doi: 10.3390/AGRICULTURE13040835. URL https://www.mdpi.com/2077-0472/13/4/835/htmhttps://www.mdpi.com/2077-0472/13/4/835. (page 13)

Chiranjit Singha, Kishore Chandra Swain, Satiprasad Sahoo, and Ajit Govind. Prediction of soil nutrients through PLSR and SVMR models by VIs-NIR reflectance spectroscopy. *The Egyptian Journal of Remote Sensing and Space Sciences*, 26(4):901–918, 12 2023. ISSN 1110-9823. doi: 10.1016/J.EJRS.2023.10.005. (pages 18, 19, and 109)

Xiaoyu Song, Guijun Yang, Xingang Xu, Dongyan Zhang, Chenghai Yang, and Haikuan Feng. Winter Wheat Nitrogen Estimation Based on Ground-Level and UAV-Mounted Sensors. *Sensors 2022, Vol. 22, Page 549*, 22(2):549, 1 2022. ISSN 1424-8220. doi: 10.3390/S22020549. URL https://www.mdpi.com/1424-8220/22/2/549/htmhttps://www.mdpi.com/1424-8220/22/2/549. (pages 22, 23, and 111)

Yongchao Song, Jiping Bi, and Xuan Wang. Design and implementation of intelligent monitoring system for agricultural environment in IoT. *Internet of Things*, 25:101029, 4 2024. ISSN 2542-6605. doi: 10.1016/J.IOT.2023.101029. (page 114)

SPAD-502Plus. A lightweight handheld meter for measuring the chlorophyll content of leaves without causing damage to plants. SPAD-502Plus, 2021. (page 73)

Xi Su, Jiacheng Wang, Lu Ding, Jingshan Lu, Jiawen Zhang, Xia Yao, Tao Cheng, Yan Zhu, Weixing Cao, and Yongchao Tian. Grain yield prediction using multi-temporal UAV-based multispectral vegetation indices and endmember abundance in rice. *Field Crops Research*, 299:108992, 8 2023. ISSN 0378-4290. doi: 10.1016/J.FCR.2023.108992. (pages 22 and 111)

Ankita Aman Suparna Sinha. The Significance of 'D' Leaf in Pineapple. *Biomolecule Reports*, 2021. URL https://www.researchgate.net/publication/328939293_The_Significance_of_'D'_Leaf_in_Pineapple. (page 72)

Luís Guilherme Teixeira Crusiol, Marcos Rafael Nanni, Renato Herrig Furlanetto, Everson Cezar, and Guilherme Fernando Capristo Silva. Reflectance calibration of UAV-based visible and near-infrared digital images acquired under variant altitude and illumination conditions. *Remote Sensing Applications: Society and Environment*, 18:100312, 4 2020. ISSN 2352-9385. doi: 10.1016/J.RSASE.2020.100312. (page 42)

Jigme Thinley, Catherine Pickering, and Christopher Ndehedehe. Using vegetation and chlorophyll indices to model above ground biomass over time in an urban arboretum in subtropical queensland. *Remote Sensing Applications: Society and Environment*, 34:101202, 4 2024. ISSN 2352-9385. doi: 10.1016/J.RSASE.2024.101202. (pages 24 and 112)

Zezhong Tian, Yao Zhang, Haiyang Zhang, Zhenhai Li, Minzan Li, Jiangmei Wu, and Kaidi Liu. Winter wheat and soil total nitrogen integrated monitoring based on canopy hyperspectral feature selection and fusion. *Computers and Electronics in Agriculture*, 201:107285, 10 2022. ISSN 0168-1699. doi: 10.1016/J.COMPAG.2022.107285. (pages 21 and 110)

Yik-Tian Ting and Kah-Yoong Chan. Optimising performances of LoRa based IoT enabled wireless sensor network for smart agriculture. *Journal of Agriculture and Food Research*, 16:101093, 6 2024. ISSN 2666-1543. doi: 10.1016/J.JAFR.2024.101093. URL https://linkinghub.elsevier.com/retrieve/pii/S2666154324001303. (pages 25 and 114)

Nikos Tsoulias, Kowshik Kumar Saha, and Manuela Zude-Sasse. In-situ fruit analysis by means of LiDAR 3D point cloud of normalized difference vegetation index (NDVI). *Computers and Electronics in Agriculture*, 205:107611, 2 2023. ISSN 0168-1699. doi: 10.1016/J.COMPAG.2022.107611. (pages 39 and 81)

Anusha Vangala, Ashok Kumar Das, Vinay Chamola, Valery Korotaev, and Joel J.P.C. Rodrigues. Security in IoT-enabled smart agriculture: architecture, security solutions and challenges. *Cluster Computing 2022 26:2*, 26(2):879–902, 4 2022. ISSN 1573-7543. doi: 10.1007/S10586-022-03566-7. URL https://link-springer-com.udea.lookproxy.com/article/10.1007/s10586-022-03566-7. (page 114)

Kummari Venkatesh and K. Jairam Naik. An ensemble transfer learning for nutrient deficiency identification and yield-loss prediction in crop. *Multimedia Tools and Applications*, pages 1–27, 2 2024. ISSN 15737721. doi: 10.1007/S11042-024-18592-3/FIGURES/12. URL https://link-springer-com.udea.lookproxy.com/article/10.1007/s11042-024-18592-3. (pages 19 and 109)

Bhagyashree Verma, Rajendra Prasad, Prashant K. Srivastava, Suraj A. Yadav, Prachi Singh, and R. K. Singh. Investigation of optimal vegetation indices for retrieval of leaf chlorophyll and leaf area index using enhanced learning algorithms. *Computers and Electronics in Agriculture*, 192:106581, 1 2022. ISSN 0168-1699. doi: 10.1016/J.COMPAG.2021.106581. (page 81)

Veronika Vikuk, Andrea Spirkaneder, Patrick Noack, and Alexander Duemig. Validation of a sensor-system for real-time measurement of mineralized nitrogen in soils. *Smart Agricultural Technology*, 7:100390, 3 2024. ISSN 2772-3755. doi: 10.1016/J.ATECH.2023.100390. (page 35)

Manas Wakchaure, B.K. Patle, and A.K. Mahindrakar. Application of AI techniques and robotics in agriculture: A review. *Artificial Intelligence in the Life Sciences*, 3:100057, 12 2023. ISSN 2667-3185. doi: 10.1016/J.AILSCI.2023.100057. (page 13)

Niaz Wali. Pineapple (Ananas comosus). *Seyed Mohammad Nabavi y Ana Sanches Silva*, 2019. doi: 10.1016/B978-0-12-812491-8.00050-3. URL https://doi.org/10.1016/B978-0-12-812491-8.00050-3. (pages 32 and 33)

Dunliang Wang, Rui Li, Tao Liu, Shengping Liu, Chengming Sun, and Wenshan Guo. Combining vegetation, color, and texture indices with hyperspectral parameters using machine-learning methods to estimate nitrogen concentration in rice stems and leaves. *Field Crops Research*, 304:109175, 12 2023a. ISSN 0378-4290. doi: 10.1016/J.FCR.2023.109175. (page 112)

Dunliang Wang, Rui Li, Tao Liu, Shengping Liu, Chengming Sun, and Wenshan Guo. Combining vegetation, color, and texture indices with hyperspectral parameters using machine-learning methods to estimate nitrogen concentration in rice stems and leaves. *Field Crops Research*, 304:109175, 12 2023b. ISSN 0378-4290. doi: 10.1016/J.FCR.2023.109175. (pages 13, 17, 19, 20, 23, 103, 104, and 109)

Hannah Szu Han Wang and Yuan Yao. Machine learning for sustainable development and applications of biomass and biomass-derived carbonaceous materials in water and agricultural systems: A review. *Resources, Conservation and Recycling*, 190:106847, 3 2023. ISSN 0921-3449. doi: 10.1016/J.RESCONREC.2022.106847. URL https://www.sciencedirect.com/science/article/pii/S0921344922006796. (page 13)

Qi Wang, Xiaokai Chen, Huayi Meng, Huiling Miao, Shiyu Jiang, and Qingrui Chang. UAV Hyperspectral Data Combined with Machine Learning for Winter Wheat Canopy SPAD Values Estimation. *Remote Sensing 2023, Vol. 15, Page 4658*, 15(19):4658, 9 2023c. ISSN 2072-4292. doi: 10.3390/RS15194658. URL https://www.mdpi.com/2072-4292/15/19/4658/htmhttps://www.mdpi.com/2072-4292/15/19/4658. (page 22)

Qiang Wang, Álvaro Moreno-Martínez, Jordi Muñoz-Marí, Manuel Campos-Taberner, and Gustau Camps-Valls. Estimation of vegetation traits with kernel NDVI. *ISPRS Journal of Photogrammetry and Remote Sensing*, 195:408–417, 1 2023d. ISSN 0924-2716. doi: 10.1016/J.ISPRSJPRS.2022.12.019. (pages 36 and 112)

Wenhui Wang, Hengbiao Zheng, Yapeng Wu, Xia Yao, Yan Zhu, Weixing Cao, and Tao Cheng. An assessment of background removal approaches for improved estimation of rice leaf nitrogen concentration with unmanned aerial vehicle multispectral imagery at various observation times. *Field Crops Research*, 283:108543, 7 2022a. ISSN 03784290. doi: 10.1016/j.fcr.2022.108543. URL https://linkinghub.elsevier.com/retrieve/pii/S0378429022001149. (pages xxii and 110)

Xinbing Wang, Yuxin Miao, Rui Dong, and Krzysztof Kusnierek. Minimizing active canopy sensor differences in nitrogen status diagnosis and in-season nitrogen recommendation for maize with multi-source data fusion and machine learning. *Precision Agriculture*, 24(6):2549–2565, 12 2023e. ISSN 15731618. doi: 10.1007/S11119-023-10052-6/METRICS. URL https://link.springer.com/article/10.1007/s11119-023-10052-6. (pages 23 and 109)

Ying Wang, Wenjuan Shi, and Tianyang Wen. Prediction of winter wheat yield and dry matter in North China Plain using machine learning algorithms for optimal water and nitrogen application. *Agricultural Water Management*, 277:108140, 3 2023f. ISSN 0378-3774. doi: 10.1016/J.AGWAT.2023.108140. (page 24)

Zhonglin Wang, Junxu Chen, Jiawei Zhang, Xianming Tan, Muhammad Ali Raza, Jun Ma, Yan Zhu, Feng Yang, and Wenyu Yang. Assessing canopy nitrogen and carbon content in maize by canopy spectral reflectance and uninformative variable elimination. *The Crop Journal*, 10(5):1224–1238, 10 2022b. ISSN 2214-5141. doi: 10.1016/J.CJ.2021.12.005. (page 110)

Christopher Y.S. Wong. Plant optics: underlying mechanisms in remotely sensed signals for phenotyping applications. *AoB PLANTS*, 15(4):1–12, 7 2023. ISSN 20412851. doi: 10.1093/AOBPLA/PLAD039. URL https://dx.doi.org/10.1093/aobpla/plad039. (page 12)

Zhiyuan Yao, Huiling Hu, Yulong Li, Xiaoming Sun, Sina Adl, Xiaoguo Wang, Yingjie Zhang, and Bo Zhu. Soil micro-food webs at aggregate scale are associated with soil nitrogen supply and crop yield. *Geoderma*, 442:116801, 2 2024. ISSN 0016-7061. doi: 10.1016/J.GEODERMA.2024.116801. (page xxii)

Quan Yin, Yuting Zhang, Weilong Li, Jianjun Wang, Weiling Wang, Irshad Ahmad, Guisheng Zhou, and Zhongyang Huo. Estimation of Winter Wheat SPAD Values Based on UAV Multispectral Remote Sensing. *Remote Sensing 2023, Vol. 15, Page 3595*, 15(14):3595, 7 2023. ISSN 2072-4292. doi: 10.3390/RS15143595. URL https://www.mdpi.com/2072-4292/15/14/3595/htmhttps://www.mdpi.com/2072-4292/15/14/3595. (page 23)

Xin Zhang, Liangxiu Han, Tam Sobeih, Lewis Lappin, Mark A. Lee, Andew Howard, and Aron Kisdi. The Self-Supervised Spectral–Spatial Vision Transformer Network for Accurate Prediction of Wheat Nitrogen Status from UAV Imagery. *Remote*

Sensing 2022, Vol. 14, Page 1400, 14(6):1400, 3 2022a. ISSN 2072-4292. doi: 10.3390/RS14061400. URL https://www.mdpi.com/2072-4292/14/6/1400/htmhttps://www.mdpi.com/2072-4292/14/6/1400. (page 110)

Xuan Zhang, Hui Sun, Xingxing Qiao, Xiaobin Yan, Meichen Feng, Lujie Xiao, Xiaoyan Song, Meijun Zhang, Fahad Shafiq, Wude Yang, and Chao Wang. Hyperspectral estimation of canopy chlorophyll of winter wheat by using the optimized vegetation indices. *Computers and Electronics in Agriculture*, 193, 2 2022b. ISSN 01681699. doi: 10.1016/j.compag.2021.106654. URL https://www.sciencedirect.com/science/article/pii/S0168169921006712. (pages 110 and 112)

Y ; Zhang, J ; Xiao, K ; Yan, Hao Yang, Changping Huang, Dameng Yin, Xiuliang Jin, Zhenhai Li, Yali Zhang, Junqi Xiao, Kangting Yan, Xiaoyang Lu, Wanjian Li, Haoxin Tian, Linlin Wang, Jizhong Deng, and Yubin Lan. Advances and Developments in Monitoring and Inversion of the Biochemical Information of Crop Nutrients Based on Hyperspectral Technology. *Agronomy 2023, Vol. 13, Page 2163*, 13(8):2163, 8 2023. ISSN 2073-4395. doi: 10.3390/AGRONOMY13082163. URL https://www.mdpi.com/2073-4395/13/8/2163/htmhttps://www.mdpi.com/2073-4395/13/8/2163. (pages 21 and 36)

Jie Zheng, Xiaoyu Song, Guijun Yang, Xiaochu Du, Xin Mei, and Xiaodong Yang. Remote Sensing Monitoring of Rice and Wheat Canopy Nitrogen: A Review. *Remote Sensing 2022, Vol. 14, Page 5712*, 14(22):5712, 11 2022. ISSN 2072-4292. doi: 10.3390/RS14225712. URL https://www.mdpi.com/2072-4292/14/22/5712/htmhttps://www.mdpi.com/2072-4292/14/22/5712. (page 12)

Lili Zhou, Chenwei Nie, Tao Su, Xiaobin Xu, Yang Song, Dameng Yin, Shuaibing Liu, Yadong Liu, Yi Bai, Xiao Jia, and Xiuliang Jin. Evaluating the Canopy Chlorophyll Density of Maize at the Whole Growth Stage Based on Multi-Scale UAV Image Feature Fusion and Machine Learning Methods. *Agriculture (Switzerland)*, 13(4):895, 4 2023. ISSN 20770472. doi: 10.3390/AGRICULTURE13040895/S1. URL https://www.mdpi.com/2077-0472/13/4/895/htmhttps://www.mdpi.com/2077-0472/13/4/895. (pages 17, 18, 19, 23, and 109)

Xinbin Zhou, Gerard B.M. Heuvelink, Yusuke Kono, Tsutomu Matsui, and Takashi S.T. Tanaka. Using linear mixed-effects modeling to evaluate the impact of edaphic factors on spatial variation in winter wheat grain yield in Japanese consolidated paddy fields. *European Journal of Agronomy*, 133:126447, 2 2022. ISSN 1161-0301. doi: 10.1016/J.EJA.2021.126447. (page 11)

Cuicui Zhu, Jia Tian, Qingjiu Tian, Xiaoqiong Wang, and Qianjing Li. Using NDVI-NSSI feature space for simultaneous estimation of fractional cover of non-photosynthetic vegetation and photosynthetic vegetation. *International Journal of Applied Earth Observation and Geoinformation*, 118:103282, 4 2023. ISSN 1569-8432. doi: 10.1016/J.JAG.2023.103282. (pages 39, 41, and 112)

Wanxue Zhu, Ehsan Eyshi Rezaei, Hamideh Nouri, Zhigang Sun, Jing Li, Danyang Yu, and Stefan Siebert. UAV-based indicators of crop growth are robust for distinct water and nutrient management but vary between crop development phases. *Field Crops Research*, 284:108582, 8 2022. ISSN 0378-4290. doi: 10.1016/J.FCR.2022.108582. (pages 22 and 111)

Sándor Zsebő, László Bede, Gábor Kukorelli, István Mihály Kulmány, Gábor Milics, Dávid Stencinger, Gergely Teschner, Zoltán Varga, Viktória Vona, and Attila József Kovács. Yield Prediction Using NDVI Values from GreenSeeker and MicaSense Cameras at Different Stages of Winter Wheat Phenology. *Drones 2024, Vol. 8, Page 88*, 8(3):88, 3 2024. ISSN 2504-446X. doi: 10.3390/DRONES8030088. URL https://www.mdpi.com/2504-446X/8/3/88/htmhttps://www.mdpi.com/2504-446X/8/3/88. (page 23)